

Co-funded by the



(GRANT AGREEMENT: 661880)

DELIVERABLE D2.4, v2

Bacterial presence and activity in compacted bentonites

Editors: Trevor Taborowski, Andreas Bengtsson Alexandra Chukharkina, Anders Blom, and Karsten Pedersen, Microbial Analytics, Mölnlycke, Sweden.

Date of issue of this report: 25.04.2019 (Version 2)

Report number of pages: 96

Start date of project: 01.06.2015

This project has received funding from the Euratom research and training programme 2014-2018 under Grant Agreement no. 661880

Dissemination Level

PU	Public	P
PP	Restricted to other programme participants (including the Commission) Services)	
RE	Restricted to a group specified by the partners of the MIND project	
CO	Confidential, only for partners of the MIND project	

Contents

Contents	2
1 Introduction	11
1.1 Buffer material	11
1.2 Objectives of the MIND work package 2 and this report	11
1.3 Bacterial populations in bentonite clays.....	12
1.4 Methods for the detection of presence, numbers and activity of bacteria	12
1.5 This work.....	13
2 Elements, minerals and organic content of the studied clays	15
2.1 Mineral and element composition of the studied clays	15
2.2 Low-molecular weight organic matter in bentonite clays.....	18
2.2.1 Methods description	18
2.2.2 Specific results	19
2.3 The clay environment from a bacterial perspective	22
3 Cell separation from clay for visualization and nucleic acid analysis	24
3.1 Methods.....	24
3.1.1 Cell separation methods	25
3.1.2 Cultivation.....	25
3.1.3 Spiking of clay.....	25
3.1.4 Total number determination of cells with DAPI	25
3.1.5 Experiments 1, 2, 3 and 4 with Asha, Calcigel and MX-80	26
3.1.6 FEBEX clay experiments A and B.....	29
3.1.7 DNA extraction from bentonite clay	30
3.2 Results.....	31
3.2.1 Experiment 1	31
3.2.2 Experiment 2	32
3.2.3 Experiment 3	34
3.2.4 Experiment 4	34
3.2.5 FEBEX clay experiments.....	35
3.2.6 DNA extraction from bentonite.....	36

3.3	Development of a DNA extraction method.....	36
3.3.1	The extracted DNA was contaminated and had a low yield with method 1.....	36
3.3.2	The efficiency of the DNA extraction methods depends on the sample material....	37
3.4	Discussion	38
3.4.1	A possible method to extract bacterial cells from spiked and non-spiked bentonite clays.	38
3.4.2	The DNA yield of extracted bacteria from FEBEX clay was nominal.....	40
3.4.3	Evaluation of DNA yields	40
4	Metagenome versus 16S rDNA analysis of biofilm diversity.....	42
4.1	Methods.....	42
4.1.1	Sample description	42
4.1.2	Metagenomic sequencing methodology.....	42
4.2	Results and discussion	43
5	Presence and activity of sulphide- and acetate- producing bacteria in bentonite systems	44
5.1	Presence and activity of sulphide-producing bacteria.....	44
5.1.1	Methods	44
5.1.2	Clay density and cultivability of SPB.....	46
5.1.3	Clay density and activity of SPB.....	47
5.1.4	Clay pressure and activity of SPB	48
5.1.5	Lactate consumption and acetate production.....	49
5.2	Motivation for the follow up investigation presented next in this report	49
6	Mobility and reactivity of sulphide in bentonite clays.....	50
6.1.1	Calculation of the diffusion coefficient of $^{35}\text{S}^{2-}$ in Asha bentonite	51
6.2	Implications for engineered barriers	53
6.3	Motivation for the follow up investigation presented next in this report	53
7	Influence of bacteria and sulphide on bentonite clays	54
7.1	Experiments.....	54
7.2	Material and methods	54
7.2.1	Bentonite clays.....	54
7.2.2	Test cells	54

7.2.3	Influence of sulphide on bentonite clays during saturation.....	56
7.2.4	Influence of bacterial produced sulphide on the swelling pressure capacity of Asha	59
7.2.5	Analyses	61
7.2.6	Data processing, graphics and statistics	63
7.3	Results.....	63
7.3.1	Influence of sulphide on bentonite clays during saturation.....	63
7.3.2	Influence of bacterially produced sulphide on the swelling pressure capacity of Asha	67
7.4	Discussion	72
7.4.1	Influence of sulphide on the swelling pressure of bentonite clays	72
7.4.2	Influence of bacterial produced sulphide on the swelling pressure capacity of Asha	73
7.5	Data.....	75
8	Summary of factors influencing bacterial life in compacted bentonite	77
9	Acknowledgements	80
10	References	81
11	Appendix A.....	85
12	Appendix B.....	88

Figures

Figure 1-1. Examples of metabolites that can be used to detect appearance of metabolic activity are marked yellow, requirements for bacterial life are marked green, and possible constrains for bacterial life in compacted clays are marked blue.	13
Figure 1-2. Methods for quantification of bacteria in clays are marked green, appearance of bacteria in yellow and methods for identification are marked blue.	14
Figure 2-1. Appearance of a variety of bentonite clays (From Svensson et al. 2011).	15
Figure 3-1. Method scheme for all cell separation experiments.	25
Figure 3-2. Images of <i>P. fluorescens</i> extracted with buffer 2 from spiked bentonite clay powders. The left image shows extracted bacterial cells from spiked Asha bentonite clay powder, the middle image from spiked Calcigel bentonite clay powder and the right image from spiked MX-80 bentonite clay powder. All samples were stained with DAPI Vector shield mounting medium.	32
Figure 3-3 Images of <i>B. subtilis</i> extracted from spiked bentonite clay powders. The left image shows extracted bacterial cells from spiked Calcigel bentonite clay powder, the middle image	

from spiked MX-80 bentonite clay powder and the right image from spiked Asha bentonite clay powder. All samples were stained with DAPI Vector shield mounting medium.	33
Figure 3-4. Images of <i>B. subtilis</i> extracted from spiked bentonite clay powders after hydration and prolonged incubation in cell extraction buffer. The row A shows the extracted bacterial cells after hydration by incubation in cell extraction buffer with 0.5M NaCl for 16 h. The row B shows the corresponding images to each spiked bentonite clay powder after hydration by incubation in a NaCl-solution 0.9% for 16 h.	34
Figure 3-5. Images of <i>P. fluorescens</i> and <i>B. subtilis</i> extracted from spiked bentonite clay slurries. The row A shows the extracted bacterial cells with the cell extraction buffer and row B with sterile AGW.....	35
Figure 3-6. Images of extracted bacterial cells from non-spiked FEBEX clay sample B-C-60-18 after hydration. The clay was hydrated by incubation in 0.9% NaCl solution before cell extraction. The sample was stained with DAPI Vector shield mounting medium. Some of the cells have a blurred appearance due to that they are out of the focal plane of the microscope.	36
Figure 5-1. Left: A schematic cross section of a test cell. Right: An assembled test cell, spacers are not mounted.....	45
Figure 5-2. Surface radioactivity analysed on the copper disc of Rokle TC44 1750 (+) 78d (Bengtsson et al. 2017b).....	45
Figure 5-3. Number of cultivable cells (MPN) over wet density. Note that the y-axis is logarithmic. Control samples without bacterial addition are marked with filled symbols for each clay according to legend. Data collected from (Bengtsson et al. 2016; Bengtsson et al. 2017b; Bengtsson et al. 2017c; Bengtsson et al. 2017d; Bengtsson and Pedersen 2016; Bengtsson and Pedersen 2017).	46
Figure 5-4. Accumulated Cu_2^{35}S on copper discs over wet density for each tested clay according to legend. Vertical lines specify density intervals where sulphide-producing activity goes from positive to below detection. Data collected from (Bengtsson et al. 2016; Bengtsson et al. 2017b; Bengtsson et al. 2017c; Bengtsson et al. 2017d; Bengtsson and Pedersen 2016; Bengtsson and Pedersen 2017).	47
Figure 5-5. Amount of ^{35}S copper sulphide on copper discs versus swelling pressure. Data collected from (Bengtsson et al. 2016; Bengtsson et al. 2017b; Bengtsson et al. 2017c; Bengtsson et al. 2017d; Bengtsson and Pedersen 2016; Bengtsson and Pedersen 2017).	48
Figure 5-6. Produced acetate over wet density. The values in the graph have been subtracted with the amount of added lactate minus the amount of remaining lactate, meaning that the produced acetate in the graph is suggested to have originated from the analysed natural organic matter in the clays (see chapter 2.2). Data collected from Bengtsson et al (2017b; 2017).....	49
Figure 6-1. Transport of two different amounts of sulphide added to bentonite clays after 90 days of water saturation to 2000 kg m^{-3} wet density. There were significant amounts of S^0 in the black layers (see section 7 for details).	51
Figure 6-2. Asha 1750 kg m^{-3} diffusion plot with measured radioactivity over time. The linear fit is based on x-values in the day range 14 to 45: $^{35}\text{S} = -67.5 + 11.2 (\text{time})$	52
Figure 6-3. Asha 2000 kg m^{-3} diffusion plot with measured radioactivity over time. The linear fit is based on x-values in the day range from 23 to 45: $^{35}\text{S} = -44.2 + 2.69 (\text{time})$	52
Figure 7-1. Components of a test cell for the diffusion and mobility of sulphide in Asha.	56
Figure 7-2. Principal lay-out of the saturation system with mounted test cells used in preceding experiments with radiotracers, receiving the saturation salt solution from both top and bottom.	58

Figure 7-3 Influence of sulphide on bentonite clays during saturation: Schematic overview of samples and analyses.....	59
Figure 7-4. Influence of bacterial produced sulphide on the swelling pressure capacity of Asha: Schematic overview of samples and analyses.....	61
Figure 7-5. Experimental set up to drive off the H ₂ S gas for the sulphide analysis from bentonite clay samples.	62
Figure 7-6. Pressure registered by force transducers for compacted Asha bentonite clay with a wet density of 2000 kg m ⁻³ , during saturation with different sulphide concentrations.	64
Figure 7-7. Pressure registered by force transducers for compacted Calcigel bentonite clay with a wet density of 2000 kg m ⁻³ , during saturation with different sulphide concentrations.....	64
Figure 7-8. Pressure registered by force transducers for compacted MX-80 bentonite clay with a wet density of 2000 kg m ⁻³ , during saturation with different sulphide concentrations. The MX-80 control test cell experienced a sudden loss in pressure at start for unclear reasons, it was expected to reach >2000 kPa.....	65
Figure 7-9. The analysed sulphide concentrations (left figure) and the immobilised sulphide concentrations (right figure) for the three analysed positions of the saturated Asha bentonite clay core.	66
Figure 7-10. The analysed sulphur concentrations (left figure) and the analysed Fe ²⁺ concentrations (right figure) for the three analysed positions of the saturated Asha bentonite clay core.	66
Figure 7-11. The analysed sulphide concentrations (left figure) and the immobilised sulphide concentrations (right figure) for the three analysed positions of the saturated Calcigel bentonite clay core.	66
Figure 7-12. The analysed sulphur concentrations (left figure) and the analysed Fe ²⁺ concentrations (right figure) for the three analysed positions of the saturated Calcigel bentonite clay core.	67
Figure 7-13. The analysed sulphide concentrations (left figure) and the immobilised sulphide concentrations (right figure) for the three analysed positions of the saturated MX-80 bentonite clay core.	67
Figure 7-14. The analysed sulphur concentrations (left figure) and the analysed Fe ²⁺ concentrations (right figure) for the three analysed positions of the saturated MX-80 bentonite clay core.	67
Figure 7-15. Pressure curves for each test cell with Asha bentonite during the saturation time (0 – ~250 days). The key shows test cell number, bentonite density, addition of bacteria (+/-), AGW as saturation medium and addition of lactate (lac.).....	68
Figure 7-16. Most probable numbers of sulphide producing bacteria in pore water at three positions in bentonite cores of each test cell. The names indicate test cell number, bentonite density, addition of bacteria (+/-), AGW as saturation medium, addition of lactate (lac.) and position (P).	69
Figure 7-17. Concentration of sulphate in bentonite cores for each test cell. The names indicate test cell number, bentonite density, addition of bacteria (+/-), AGW as saturation medium and addition of lactate (lac.).....	70
Figure 7-18. Concentration of acetate at three positions in bentonite cores for each test cell. The names indicate test cell number, bentonite density, addition of bacteria (+/-), AGW as saturation medium and addition of lactate (lac.).....	70

Figure 7-19. Concentration of Fe ²⁺ at three positions in bentonite cores for each test cell. The names indicate test cell number, bentonite density, addition of bacteria (+/-), AGW as saturation medium and addition of lactate (lac.).....	71
Figure 7-20. Pictures of Asha clay cores from each test during sampling after incubation. The names indicate test cell number, bentonite density, addition of bacteria (+/-), AGW as saturation medium and addition of lactate (lac.).....	71
Figure 7-21. Added amounts of lactate to Rokle and Asha bentonite clays and the corresponding analysed amounts (Bengtsson et al. 2017b).	72
Figure 7-22. Added amounts of acetate to Rokle and Asha bentonite clays and the corresponding analysed amounts (Bengtsson et al. 2017b).	72
Figure 8-1. Variables influencing wet density, that upon water saturation give rise to suggested factors influencing bacterial viability, cultivability and activity (turquoise) except temperature, not coupled to wet density.....	78
Figure 8-2. Black colonies of iron sulphide produced by sulphide producing bacteria in Asha bentonite at 1750 kg/m ³ wet density and with addition of lactate and sulphide producing bacteria (From Figure 7-20).	79
Figure 8-3. Black colonies of iron sulphide produced by sulphide producing bacteria observed during sampling of test cell with GMZ bentonite (Bengtsson et al. 2017b).	79

Tables

Table 2-1. Average results from the XRD analyses of mineral compositions of the Volclay MX-80 (n=6), (Karnland 2010), Asha (n=>5) (Karnland 2010; Sandén et al. 2014), Calcigel (n=2) (Herbert and Moog 2002), Rokle (Karnland et al. 2006) and GMZ (Ye 2016) – = No data... 16	16
Table 2-2. The element composition of the bentonite materials expressed as weight percent of major element oxides of dry mass after leaching in 7 M HNO ₃ and analysis on ICP-SFMS; DM = dry mass.	16
Table 2-3. The element composition of the bentonite materials expressed as weight percent of major element oxides of dry mass after sintering and analysis on ICP-SFMS. LOI denotes the percent mass loss due to sintering (Loss on ignition); DM = dry mass.	17
Table 2-4. Output from gas chromatography mass spectroscopy analysis of organic compounds extracted from bentonite clays. CAS no., Chemical Abstract Service number.	20
Table 3-1. Buffers for cell extraction.	27
Table 3-2 TNC after cultivation	33
Table 3-3 TNC after cell extraction.	33
Table 3-4. NanoDrop results Method 1.....	37
Table 3-5. Picogreen results Method 1.....	37
Table 3-6. NanoDrop results Method 2.....	37
Table 3-7 Picogreen results Method 2.....	37
Table 3-8. Comparison of cell recovery for tested methods.	38
Table 4-1. The co-occurrence of genes in both metagenome and 16S rDNA libraries from ONK-PVA6 and ONK-KR15 biofilms presented as the percentage of all genes for phylogenetic groups of microorganisms that also were detected by the 16S rDNA analysis. Detailed numbers can be found in appendix A.....	43

Table 7-1. Salt solution for saturation of bentonite clays.	57
Table 7-2. Experimental parameters for each test cell.	59
Table 7-3 Buffer concentrations for experiment 6-9 and 11.	62
Table 7-4 Results of the sulphide analyses of the bentonite clay samples. P = position.	75
Table 7-5 Most probable numbers of SPB in pore water of Asha bentonite cores at three sample positions.	75
Table 7-6 Analysed concentration of sulphate, Fe ²⁺ , lactate and acetate at three positions in bentonite cores for each test cell.	76

Publishable Summary

The MIND project targets a number of high urgency and high importance topics identified in the Strategic Research Agenda, (SRA) (IGD-TP, 2011), focusing mainly on Key topic 2: Waste forms and their behaviour and Key topic 3: Technical feasibility and long-term performance of repository components. WP2 addresses SRA Key topic 3: Remaining key issues for the geological disposal of HLW (High Level Waste) concern the factors controlling sulphide production in the geosphere, including to what extent microorganisms can accelerate canister corrosion in the near-field either by hydrogen scavenging or by sulphide and/or acetate production. Further, it is important to identify conditions under which relevant bentonites inhibit bacterial activity, and to understand whether microorganisms can accelerate degradation of bentonite-based buffers and influence the long-term behaviour of plug systems and seals.

The work reported here aimed at 5 main objectives. 1) Analysis of the clay environment with respect to composition of minerals, elements and diversity of organic carbon. These characteristics may influence bacterial presence and activity differently in different clays. 2) Methods development regarding visualisation of bacteria in clays and analysis of diversity using nucleic acid sequencing methods. The methodological challenge was the extraction of cells and nucleic acids from the clay materials. The question if metagenome analysis reveal the same diversity as 16S rDNA gene sequencing does was also addressed. 3) Parallel with the work reported here, work with compacted bentonite specifically addressed the effect of wet density on sulphide producing activity. A new compilation of all data was done and interpreted. 4) The compacted clay work indicated that sulphide reacts with clays and is immobilised. Follow-up experiments with exposure of various bentonite clays to sulphide were performed to investigate if sulphide can degrade bentonite clays. 5) Previously, work with compacted bentonite was performed using radioactive sulphate ($^{35}\text{SO}_4$) which limited the possibility for downstream analysis. Next generation experimental configuration, without radioactivity, was developed and tested. This enabled investigation of bacterial presence, numbers and activity, swelling pressure effects and sulphide reactivity without the constraints imposed by the need to work with a radionuclide.

In the visualization and DNA extraction study bacteria were detached from clay particles by replacing the polyvalent cations with monovalent cations and increasing the electrostatic repulsion between the clay particles and the negatively charged bacteria with a buffer that was chosen to estimate the recovery rate from spiked bentonite clays. This procedure made it also possible to detach, extract and visualize bacterial cells from hydrated FEBEX clay. These bacteria had survived in the FEBEX for 18 years. Even if it was possible to detach and extract bacterial cells the recovery rate for bentonite clay spiked with bacteria was very low. One possibility is that a lot of bacterial cells remained attached to the clay particles and were centrifuged down in the low centrifugation step together with the clay. Another possible reason for the low recovery rate could be that the majority of bacterial cells died through the spiking and the dehydration caused by the freeze-drying step. Vegetative cells are sensitive to drying. Furthermore, it could be that the bacterial cells needed longer time than applied to be hydrated before cell extraction, because it is a critical step for the revival of cells after drying. Dehydrated bacterial cell walls are less permeable to water.

Metagenomic sequence data can be analysed with many different aspects. Here, we show that there was a relatively good overlap and occurrence of genes in the metagenome and 16S rDNA DNA libraries for Bacteria, but not for Archaea. The metagenome data suggests that only a

fraction of the population in the biofilms belonged to Archaea. Both methods showed the occurrence of sulphate-reducing bacteria (SRB).

The pore water composition will vary with the type of bentonite and the composition of the saturating groundwater. Various bentonite clays have small but significant amounts of natural and introduced (during mining) natural organic matter (NOM) that may be utilized by sulphide- and acetate-producing bacteria. Such NOM may also decrease or increase the mobility of radionuclides. There is a need in the long-term safety case for geological disposal radioactive wastes to explore if NOM in such buffers can promote activity of bacteria and influence radionuclide migration. A new method was been developed for the high-resolution determination and identification of low-molecular weight NOM in bentonite clays using solvent extraction and analysis by ion-trap mass spectrometry (MS) coupled with gas chromatography (GC). The studied bentonites varied in composition with respect to elements and minerals and the type and content of natural organic matter. The conditions for survival and activity of bacteria may, consequently, vary significantly between different bentonite types as inferred by the variation in the highest wet density at which sulphide production could be detected in compacted clays.

The swelling pressure in the bentonite originates from separating flocs in the bentonite. This means that a mechanical pressure arises between the separating flocs, approximately equal to the swelling pressure. Even in low-density bentonites (1500 kg m^{-3}), a pore size in the nm range would theoretically not allow for bacterial existence unless the bacteria could withstand the mechanical pressure from the separating flocs (0.09 MPa at 1500 kg m^{-3}). Prokaryotic cells can compensate for the mechanical pressure in compacted bentonite by turgor pressure. Published data on turgor pressure in prokaryotic cells mention pressures between 0.08 MPa and 2 MPa . An upper limit of 2 MPa turgor pressure would mean that cell integrity is possible, though limited, at bentonite swelling pressures below 2 MPa . Present results, reviewed and compiled here, suggest a limit at approximately 1 MPa . However, endospores can survive a much higher pressure.

Bacterial life, survival, presence, viability and activity were found to depend on several different variables in a buffer or backfill that relate to the water saturation and swelling of bentonites compacted to high density. Consequently, it was not density *per se* that controlled bacterial activity in the investigated compacted clays. Rather, other factors, that to some extent are related to the density and type of clay, controlled bacterial activity. Transport of nutrients to bacteria, as well as metabolic products such as sulphide from bacteria will be limited by diffusion due to the low porosity of buffers and backfill. Here, diffusion rates were determined in compacted clays using a radiotracer methodology. The results agreed well with previously published data.

Bacteria are very small and if there are pores or other inhomogeneities in buffer and backfill with lower than planned pressures, local bacterial activity will be possible. In addition, there will be interfaces between rock engineered disturbed zones and bentonite and between bentonite and canisters at which pressures may differ from the bulk of buffer and backfill. Sulphide-producing bacteria were found to form local colonies in some of the investigated compacted clays, likely in positions where impurities of the clay offer enough large pore space for bacterial life.

1 Introduction

The MIND project targets a number of high urgency and high importance topics identified in the Strategic Research Agenda, (SRA) (IGD-TP, 2011), focusing mainly on Key topic 2: Waste forms and their behaviour and Key topic 3: Technical feasibility and long-term performance of repository components. The Scientific Technical Work Programme of MIND was divided into two operative Work Packages (WPs):

WP1 addresses SRA Key topic 2: Remaining key issues for the geological disposal of ILW concerning the long-term behaviour, fate and consequences of organic materials in the waste along with H₂ generated by corrosion and radiolysis. The objectives of WP1 consequently are to reduce the uncertainty of safety-relevant microbial processes controlling radionuclide, chemical and gas release from long-lived intermediate level wastes (ILW) containing organics.

WP2 addresses SRA Key topic 3: Remaining key issues for the geological disposal of HLW (High Level Waste) concern the factors controlling sulphide production in the geosphere, including to what extent microorganisms can accelerate canister corrosion in the near-field either by hydrogen scavenging or by sulphide and/or acetate production. Further, it is important to identify conditions under which relevant bentonites inhibit bacterial activity, and to understand whether microorganisms can accelerate degradation of bentonite-based buffers and influence the long-term behaviour of plug systems and seals.

1.1 Buffer material

Bentonite clay will be used as a buffer material in engineered barrier systems (EBS) which will contain, protect and surround nuclear waste canisters in geological disposal concepts. The concepts rely on the swelling capabilities of the bentonite clay when it becomes water saturated as one of the main protective features. To reach desired swelling pressures of >5 MPa a clay dry density of >1600 kg m⁻³ is generally required. Depending on the mineralogy of the specific bentonite type and the groundwater composition, where salinity is an important factor, different swelling pressures are produced at the same wet density. A high density with a concomitant high swelling pressure is believed to have an inhibiting influence on bacterial activity of the natural bacterial populations in the bentonite clays, meaning that growth may be reduced and metabolic activity will cease, but present bacteria will not necessarily die. The dissimilatory reduction of sulphate, thiosulphate and sulphur to sulphide by sulphide-producing bacteria (SPB) is a main concern for the safety case of a geological disposal (SRA key topic 3) since sulphide is a corrosive agent for metal waste canisters.

1.2 Objectives of the MIND work package 2 and this report

The objectives of the MIND WP2 were to:

- Quantify the contribution of bacterially produced sulphide in buffers and in backfill and in the geosphere to the overall rate of sulfidic canister corrosion (Tasks 1 and 2).
- Gain systematic information on the effectiveness of specific bentonite buffers and their properties in inhibiting bacterial activity. (Task 3).
- Characterize the impact of bacterial activity of the long-term performance of bentonites and cementitious materials used in European geological disposal concepts, i.e. bacterial degradation of bentonites and cementitious materials. (Tasks 4 and 5).

The objectives of this report were mainly on tasks 3 and 4 and milestones 19, 25 and 28. Here we report results on these tasks and milestones produced in the laboratory of Microbial Analytics Sweden AB.

1.3 Bacterial populations in bentonite clays

Cultivable sulphide-producing bacteria have been detected in various types of commercially available bentonites including Asha, Calcigel and Wyoming MX-80 (Bengtsson and Pedersen 2017; Masurat et al. 2010a; Pedersen et al. 2000a; Svensson et al. 2011) and MIND D2.6. Cultivable sulphide-producing bacteria have also been found in a full-scale demonstration repositories in Switzerland and Sweden (Arlinger et al. 2013b; Bengtsson et al. 2017d), in various pilot and full-scale tests of bentonite and copper canister performance (Johansson et al. 2017; Karnland et al. 2009; Lydmark and Pedersen 2011; Smart et al. 2014) and in the Boom Clay formation (Bengtsson and Pedersen 2016). Analysis of DNA sequences in libraries of DNA extracted from various bentonites generally shows a large diversity of bacteria including SPB, and there is commonly a large proportion of spore forming bacteria, a survival form well adapted to dry clays (Chi Fru and Athar 2008; Lopez-Fernandez et al. 2015) and MIND D2.7.

There is, consequently, overwhelming evidence that SPB and many other types of bacteria, e.g. acetogenic bacteria, are present in commercial bentonite clays. They may originate from the mining sites or from industrial processing of the clays because such processing open-up for introduction of bacteria from air, and all surfaces and materials that comes in contact with the clay on its way from the mines to the user. The bacteria likely survive in the dry clays as spores, or as completely desiccated cells. Bentonite or rather montmorillonite, has a verified high affinity for water and the cell membrane of bacterial cells is water permeable. If a bacterial cell is surrounded by bentonite, it is possible that the water affinity of montmorillonite will extract water from the cell, leaving it in a desiccated state. The phenomenon of drying cells for prolonged storage is well known and commonly used in microbiology (Gherna 1994). Slow desiccation can yield higher viability and heat resistance, after prolonged storage, than can fast desiccation (Laroche and Gervais 2003; Potts 1994) for both spores and vegetative cells (Fine and Gervais 2005). Bacteria consequently have several mechanisms to survive prolonged periods of exposure to heat and desiccation. When water saturation of the clay starts, spores and desiccated cells can be activated and start to metabolize.

1.4 Methods for the detection of presence, numbers and activity of bacteria

Bacterial activity is generally measured by the turn-over of one or several metabolic products such as acetate or in the case of SPB, the production of sulphide (Figure 1-1). Bacterial viability (or presence) on the other hand does not imply that the bacteria must be active *in vivo* or *in situ*, it only states that they are able to become activated when a suitable environment presents itself (Figure 1-2). Dormant bacteria can, for instance, survive for millions of years in subseafloor sediments (Preisler et al. 2007). Analyses such as most probable number (MPN) is an example of methods that measure bacterial viability. To keep consensus of the terminology used to describe bacterial metabolic status some definitions follows here with the words and meanings used in this report.

1. Activity: bacteria are active and have an ongoing metabolism (Figure 1-1).
2. Presence: bacteria exists in the sample or at the sampled site and they are present as viable cells (Figure 1-2).

3. Viability: bacteria are alive and active or exists as dormant cells which have the power to become active when presented with a favourable environment (Figure 1-2).
4. Cultivability: bacteria can be cultivated in tubes with liquid media or on agar plates (Figure 1-2).

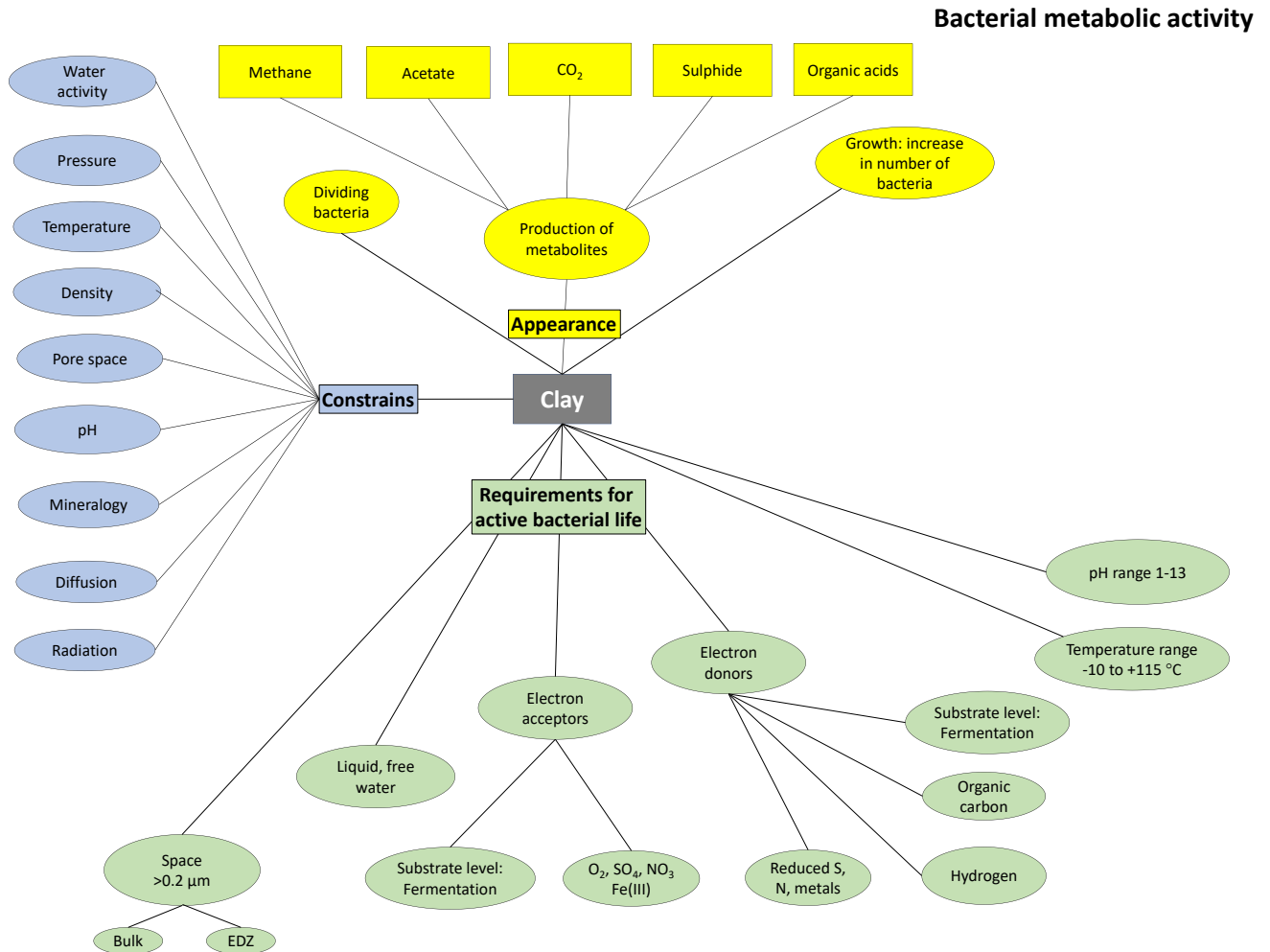


Figure 1-1. Examples of metabolites that can be used to detect appearance of metabolic activity are marked yellow, requirements for bacterial life are marked green, and possible constrains for bacterial life in compacted clays are marked blue.

1.5 This work

This work aimed at the following objectives:

- A. Analysis of the clay environment with respect to composition of minerals, elements and diversity of organic carbon. These characteristics (constrains and requirements in Figure 1-1) may influence bacterial presence and activity differently in different clays (Task 3).
- B. Methods development regarding visualisation of bacteria in clays and analysis of diversity using nucleic acid sequencing methods (Identification and quantification in Figure 1-2). The methodological challenge is the extraction of cells and nucleic acids from the clay materials. Does metagenome analysis reveal same diversity as does 16S rDNA gene sequencing? (Mainly milestones and background information to the WP2 tasks).

- C. Parallel with the work reported here, work with compacted bentonite was funded by SKB, specifically addressing the effect of wet density on sulphide producing activity (Appearance in Figure 1-1). A new compilation of all data was done and interpreted (external parallel research).
- D. The compacted clay work indicated that sulphide reacts with clays and is immobilised. Follow-up experiments with exposure of various bentonite clays to sulphide were performed to investigate if sulphide can degrade bentonite clays (Task 4).
- E. Previously, work with compacted bentonite was performed using radioactive sulphate ($^{35}\text{SO}_4$) which limited the possibility for downstream analysis. Next generation experimental configuration, without radioactivity, was developed and tested. This enabled investigation of bacterial presence, numbers and activity, swelling pressure effects and sulphide reactivity without the constraints imposed by the need to work with a radionuclide (Figure 1-1) (Task 3 and 4).

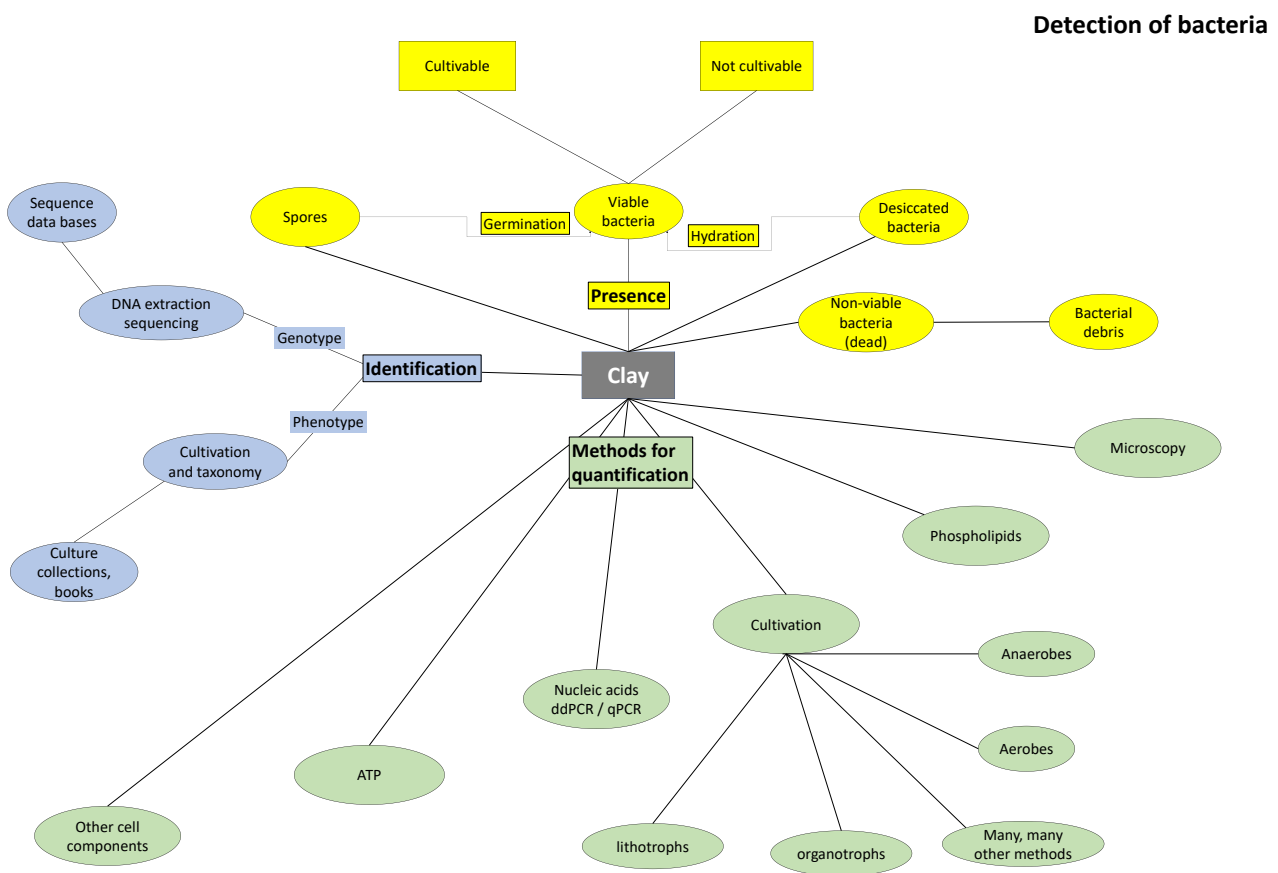


Figure 1-2. Methods for quantification of bacteria in clays are marked green, appearance of bacteria in yellow and methods for identification are marked blue.

2 Elements, minerals and organic content of the studied clays

Bentonite clays differ in appearance just by the look of them (Figure 2-1). They are mined around the world and will, therefore have varying compositions of elements, minerals and organic compounds. These differences will constitute varying conditions for bacterial life in bentonite buffer and backfill. Therefore, clays included in this report were characterised to enable evaluation of the possible influence of clay characteristics on bacterial presence and activity in our investigations.

2.1 Mineral and element composition of the studied clays

Six different bentonites were analysed in this MIND work: Wyoming Volclay MX-80 (USA), Asha (India), Calcigel (Germany), GMZ (Gaomiaozhi, China), Rokle (Czech Republic) and FEBEX clay (Switzerland). In addition Boom Clay (Belgium) has been included as a reference to a non-swelling clay (Bengtsson and Pedersen 2016).

The mineral composition was analysed by other laboratories previously (Table 2-1). All bentonite clays had a high content of montmorillonite and minor amounts of various other clay minerals. Volclay MX-80 and Asha had most montmorillonite followed by Rokle, GMZ and Calcigel. FEBEX is reported to have >88% montmorillonite (Bengtsson et al. 2017d).

In this MIND work, the element composition was analysed with inductively coupled plasma sector field mass spectrometry (ICP-SFMS) after two different treatments. First, the clays were leached with 7 M HNO₃ and the leachates were analysed with ICP-SFMS (ALS Scandinavica, Luleå, Sweden). Second the clays were sintered (1000 °C) and thereafter dissolved in diluted nitric acid (ALS Scandinavica, Luleå, Sweden). The leaching method shows elements that potentially can be leached to the pore water while the sinter method report the total amount of elements. However, the diversity of analysed elements was larger for the leching method compared to the sinter method. The Asha and Rokle bentonites contained more heavy elements such as Cd, Co, Cr, Cu and V than the other clays (Table 2-2). The Asha and Rokle bentonites also contained much more iron (analysed as Fe₂O₃) compared with the other clays (Table 2-3).



Figure 2-1. Appearance of a variety of bentonite clays (From Svensson et al. 2011).

Table 2-1. Average results from the XRD analyses of mineral compositions of the Volclay MX-80 (n=6), (Karnland 2010), Asha (n=>5) (Karnland 2010; Sandén et al. 2014), Calcigel (n=2) (Herbert and Moog 2002), Rokle (Karnland et al. 2006) and GMZ (Ye 2016) – = No data

Component	Asha	Volclay MX-80	Rokle	GMZ	Calcigel
Montmorillonite	82	81	69.4	75.4	66
Muscovite	1.9	3.4	2.8	–	14
Plagioclase	0.82	3.5	0.2	–	3
Pyrite	0.66	0.6	1.1	–	0
Quartz	1.2	3.0	2.5	11.7	8.2
Other	13.4	8.5	24	12.9	8.8

Table 2-2. The element composition of the bentonite materials expressed as weight percent of major element oxides of dry mass after leaching in 7 M HNO₃ and analysis on ICP-SFMS; DM = dry mass.

Element	Unit	Clay						
		Asha	Volclay MX-80	Rokle	GMZ	Calcigel	FEBEX	Boom Clay
DM	%	91.5	91.7	84.2	91.8	91.2	83.4	97.2
As	mg/kg DM	<3	8.46	<3	4.00	4.88	5.00	9.18
Ba	mg/kg DM	54.5	34.3	122	60.9	93.2	31.2	44.8
Be	mg/kg DM	0.56	1.53	1.38	6.64	1.99	1.96	0.718
Cd	mg/kg DM	0.211	0.27	<0.1	<0.1	0.118	<0.1	<0.1
Co	mg/kg DM	50.3	1.34	31.3	0.756	7.18	1.10	9.73
Cr	mg/kg DM	71.4	0.26	52.8	1.82	12.8	2.04	32.8
Cu	mg/kg DM	114	3.10	68.8	6.79	9.58	4.57	22.0
Fe	mg/kg DM	42500	4520	51400	4070	12400	2310	17600
Hg	mg/kg DM	<1	<1	<1	<1	<1	<1	<1
Mn	mg/kg DM	725	102	694	28.7	647	235	74.3
Ni	mg/kg DM	57.4	3.16	49.1	1.48	16.3	3.70	34
P	mg/kg DM	281	160	1400	125	218	128	178
Pb	mg/kg DM	1.33	43.3	3.73	3.05	24.3	14.2	19.0
Sr	mg/kg DM	220	203	94.0	307	41.5	148	62.5
V	mg/kg DM	60.9	0.403	23.7	1.10	2.83	1.19	20.8
Zn	mg/kg DM	139	80.3	61.6	4.87	51.7	7.99	67.2

Table 2-3. The element composition of the bentonite materials expressed as weight percent of major element oxides of dry mass after sintering and analysis on ICP-SFMS. LOI denotes the percent mass loss due to sintering (Loss on ignition); DM = dry mass.

Element	Unit	Clay				
		Asha	Volclay MX-80	Rokle	GMZ	Calcigel
DM	%	91.4	91.9	83.9	91.8	91.3
SiO ₂	% DM	45.5	61.2	45.3	64.9	56.6
Al ₂ O ₃	% DM	16.9	18.4	13.6	13.4	17.8
CaO	% DM	2.85	1.15	2.10	0.841	1.69
Fe ₂ O ₃	% DM	13.0	4.15	13.4	3.31	6.11
K ₂ O	% DM	0.128	0.599	0.584	0.605	1.55
MgO	% DM	2.34	2.02	3.40	2.90	2.92
MnO	% DM	0.112	0.0146	0.0921	0.0368	0.0850
Na ₂ O	% DM	1.30	1.56	1.21	1.50	0.251
P ₂ O ₅	% DM	0.0954	0.0541	0.364	0.0370	0.0531
TiO ₂	% DM	1.03	0.148	2.69	0.124	0.402
Sum	% DM	83.3	89.3	82.7	87.7	87.5
LOI 1000°C	% DM	9.5	5.9	9.1	4.6	7.0
Ba	mg/kg DM	95.5	273	234	251	312
Be	mg/kg DM	<0.5	1.51	2.03	6.41	3.21
Co	mg/kg DM	74.2	<5	53.6	<5	10.1
Cr	mg/kg DM	239	<10	333	18.7	41.6
Mo	mg/kg DM	<5	<5	<5	<5	<5
Nb	mg/kg DM	10.9	28.1	80.6	53.1	20.7
Ni	mg/kg DM	111	<10	165	<10	39.3
Sc	mg/kg DM	48.1	4.59	23.4	8.35	16.1
Sr	mg/kg DM	244	254	163	348	79.7
V	mg/kg DM	203	9.10	196	15.8	47.1
W	mg/kg DM	0.416	0.421	1.27	1.94	1.44
Y	mg/kg DM	81	39.4	23.3	48.6	41.8
Zr	mg/kg DM	92.5	199	298	96.9	234

2.2 Low-molecular weight organic matter in bentonite clays

Various bentonite clays have small but significant amounts of natural and introduced (during mining) natural organic matter (OM) than may be utilized by sulphide- and acetate-producing bacteria. Such OM may also decrease or increase the mobility of radionuclides. There is a need in the long-term safety case for geological disposal radioactive wastes to explore if OM in such buffers can promote activity of bacteria and influence radionuclide migration (Marshall et al. 2015; Marshall 2014). A new method was developed here for the high-resolution determination and identification of low-molecular weight OM in bentonite clays using solvent extraction and analysis by ion-trap mass spectrometry (MS) coupled with gas chromatography (GC).

There is considerable lack of knowledge on the exact nature of OM in bentonite clays (Marshall 2014). Current analysis methods have focused on determination of the total organic content and not on speciation. Furthermore, the analysis methods used for determination of total OM involve heating steps that could possibly affect detection of additional low-molecular OM that could be lost by evaporation.

This work presents a new high-resolution analysis of extractable OM from bentonite. The method has been tested on six different clays and the results show that a considerable amount of total OM exists as relatively low-molecular molecules containing functional groups as carboxylic acids, ketones, aldehydes and alcohols, among others. This kind of OM is easily accessible as carbon source for microbiological growth and earlier presumptions that the OM would be present as hardly-digested larger molecules and even graphite carbon will have to be reconsidered. More tests on the clays are needed for a certain evaluation of the fraction of OM that is easily accessible versus determinations of total OM. The main goal has been to set up a useful analytical method for this kind of analysis.

The method development has involved selection of extraction solvent to improve recovery and induce swelling of the clay, extraction conditions necessary for effective extraction, methods for pre-treating of the clay and concentration of the extract that not causes loss of OM, optimisation of the actual injection on the GC to avoid thermal decomposition of larger molecules and methods for evaluating obtained data. The last step involving the actual identification of different substances is carried out using spectral deconvolution using the AMDIS software (NIST institute, USA) and library search against a large, validated spectral library with more than 400 000 different substances (NIST 14, NIST institute, USA).

With an existing high-resolution method for identification of OM accessible for microorganisms it is possible to evaluate different bentonite clays as a possible carbon source for bacterial growth. The results (see 2.2.2) indicate that differences between the composition of OM in the clays exist, that some clays are contaminated by substances originating from the excavation as explosives and hydraulic fluids and finally that the heating of clay necessary for some methods determining total OM by for instance combustion could result in loss of low-molecular OM from the dry clay.

2.2.1 Methods description

Clay samples were analysed granulated in dry condition. On dry samples, there was no risk that the extraction would be affected by non-miscible water-solvent phase formation. The extraction was performed using a Soxhlet extractor (Jensen 2007) and ethyl acetate as solvent. The choice of ethyl acetate (Rathburn, Genetec, Gothenburg, Sweden) as solvent was made on the presumption that the clay samples contained both polar and non-polar organic compounds and that the

extraction from the dry samples was most efficient using a solvent that has affinity for both polar and non-polar molecules.

The mass of each sample used for the extraction was 35 g. The sample was placed into a cellulose thimble (Hahnemühle Dassel, Germany) and extracted using 80 mL ethyl acetate for 4 hours. The number of repeated extraction cycles was approximately 16. The collected extracts were evaporated using N₂ to a final volume of 2 mL. The extract was collected in 2 mL glass vials intended for analysis of trace organics equipped with a PTFE-lined red rubber seal (Genetec, Gothenburg, Sweden). As a correction for possible present impurities in solvents and timbles as well as for possible contamination from sample handling, blank samples were prepared. These were in the form of empty Soxhlet timbles extracted using exactly the same procedure as for the clay samples. Also repeated injections of the pure solvent were made.

The samples were analysed on GC-MS (Gas Chromatography - Mass Spectrometry). The instrument used was an Agilent 7090B chromatograph (Agilent, California, USA) connected to an Agilent 240 Ion-Trap (Agilent, Palo Alto, USA) operating in internal ionization mode. The gas chromatograph was equipped with a programmed-temperature vaporization injector (MMI, Gerstel, Mülheim, Germany) and the separating column used was a VF-5ms, 30m × 0.25mm × 0.25 μm (Agilent, Middelburg, the Netherlands). The injector was operated in the temperature range of 60-350 °C and the chromatograph oven was programmed in the range of 35-340 °C using helium as a carrier gas. Acquisition in the ion-trap was in the range 38-400 atomic mass units (amu). The samples were analysed in numerical order with blank samples between every clay sample. Analysis of all samples and corresponding blanks was made as one full sequence run overnight.

For evaluation the chromatogram from a blank sample, prepared as described above, peaks present in the clay samples only but absent in the blank sample were taken under account. Then the whole sample chromatogram was evaluated using library search of the obtained component spectra in the NIST 14 mass spectral library. In some cases, inexact matching compounds are given.

2.2.2 Specific results

The analysis showed a large diversity of organic compounds in the clays (Table 2-4). Rokle and GMZ had the largest diversity follow by FEBEX, Asha, Volclay MX-80 and Calcigel.

In all samples, straight and branched alkanes were found. Carboxylic acids (fatty acids) of the corresponding alkanes were also detected, but at significantly lower levels than the alkanes. A foul odour was detected from the extract of the MX-80 clay.

Apart from the substances found in all samples there were individual differences between the clays as well. The following groups of substances were characteristic. Calcigel: Traces of borneol-related derivatives, a rigid cyclic compound. FEBEX: Derivatives of sugar (ribose)-related compounds as well as succinates, aromatic alcohols and larger cyclic and branched ketones and carboxylic acids. MX-80: Alcohols and aldehydes of lower molecular weight, derivatives of pyrrole (probably causing the odour) as well as sterols and larger polyaromatic substances (PAH). The analysis is not quantitative, but when comparing the total signal in the chromatograms the general trend in total amount of organic matter was the same as a trend in colour of the extract. Lowest amount (analysed as peak area) in the clear Asha extract and highest in the brownish MX-80 extract.

The origin of these compounds is likely a combination of compounds presents before mining and compounds introduced during mining and processing. Alkanes were found in all clays and likely originate from diesel fuel. TNT was found in GMZ and could have been introduced during blasting. The borneol-related derivatives may have been present before mining and could originate from ancient forests.

Table 2-4. Output from gas chromatography mass spectroscopy analysis of organic compounds extracted from bentonite clays. CAS no., Chemical Abstract Service number.

Organic Compound	CAS no.
Asha	
alkanes	
alkenes	
phthalates	
Hexanoic acid	142-62-1
Benzyl alcohol	100-51-6
Cyclododecanol	1502-05-2
Nonanoic acid	112-05-0
[2-(2-Butoxyethoxy)ethyl] acetate	124-17-4
Hexadecanoic acid	57-10-3
Octadecanoic acid	57-11-4
Volclay MX-80	
alkanes	
alkenes	
phthalates	
sterols	
Hexanoic acid	142-62-1
Octanal	124-13-0
2-Nonen-1-ol	2104-79-6
3-Ethyl-4-methylpyrrole-2,5-dione	20189-42-8
Fluorene	86-73-7
Benzo(a)pyrene	192-97-2
Rokle	
alkanes	
alkenes	
alcohols	
aldehydes	
carboxyl acid esters	
phthalates	
Styrene	100-42-5
Hexanoic acid	142-62-1
4-Chlorophenyl benzoate	2005-08-05
Naphthalene	91-20-3
1,2-Benzisothiazole	272-16-2
2-methylnaphthalene	91-57-6

1-methylnaphthalene	90-12-0
Triacetin	102-76-1
Vanillin	121-33-5
Methylnaphthalene derivative	
Nonanoic acid	112-05-0
Decanoic acid	334-48-5
t-Butylhydroquinone	1948-33-0
Undecanoic acid	112-37-8
Benzophenone	119-61-9
2(3H)-Benzothiazolone	934-34-9
Tridecanoic acid	638-53-9
Phenanthrene	85-01-8
Tetradecanoic acid	544-63-8
Phenanthrene	85-01-8
6,10,14-Trimethylpentadecan-2-one	502-69-2
phenanthrene derivatives	
Butyl citrate	77-94-1
Dehydroabiatic acid	1740-19-8

GMZ

alkanes	
alkenes	
chloroalkanes	
aldehydes	
Phenol derivatives	
carboxylic acids	
carboxyl acid esters	
phthalates	
n-Propyl acetate	109-60-4
Furfural	1998-01-01
2-n-Butylacrolein	1070-66-2
1-Hexanol	111-27-3
2-Heptanone	110-43-0
Cyclohexanone	108-94-1
2-chloro-3-methyl-1-phenylbutan-1-one	78706-77-1
Phenol	108-95-2
Heptanoic acid	111-14-8
Hexyl acetate	142-92-7
2-Nonen-1-ol	31502-14-4
(+)-2-Bornanone	464-49-3
endo-Borneol	507-70-0
toluic acid ester	
.alpha.-Terpineol	98-55-5
2,3,4-Trifluorobenzoic acid, tridec-2-ynyl ester	-
Vanillin	121-33-5
2,6-Di-tert-butyl-p-benzoquinone	719-22-2

TNT	118-96-7
Bayer 28,589	728-40-5
7,9-Di-tert-butyl-1-oxaspiro(4,5)deca-6,9-diene-2,8-dione	82304-66-3
Cholestane	481-21-0

FEBEX

alkanes	
alkenes	
phthalates	
cyclic compounds including different alkyl groups	
Hexanoic acid	142-62-1
Benzyl alcohol	100-51-6
Heptanoic acid	111-14-8
Decamethylcyclopentasiloxane	541-02-6
Cyclohexanol, 2,3-dimethyl-	1502-24-5
Nonanoic acid	112-05-0
Decanoic acid	334-48-5
Vanillin	121-33-5
Cyclododecane	294-62-2
Dodecanoic acid	143-07-7
Benzophenone	119-61-9
Succinic acid, 2-(2-chlorophenoxy)ethyl ethyl ester	-
Tridecanoic acid	638-53-9
Hexadecanoic acid	112-80-1
Octadecanoic acid	57-11-4

Calcigel

alkanes	
alkenes	
Hexanoic acid	142-62-1
(+)-2-Bornanone	464-49-3
Nonanoic acid	112-05-0
2,2-Dimethoxy-2-phenylacetophenone	24650-42-8
7,9-Di-tert-butyl-1-oxaspiro(4,5)deca-6,9-diene-2,8-dione	82304-66-3
2-Ethylhexyl hydrogen adipate	4337-65-9
4-Methyl-2-pentadecyl-1,3-dioxane	54950-57-1

2.3 The clay environment from a bacterial perspective

The mineral/element composition of the clays is multifaceted and it is not possible to deduce any direct effects on bacteria. Many of the elements are essential for life such as Co, Mo, P, Ni and V while Cd, Cr and Pb are toxic. However, the toxic elements are bound in various minerals and may not be present as ions in toxic concentrations.

The organic carbon diversity varies significantly between the clays. Many of them can be utilised by bacteria as sources of carbon and energy while other are typical metabolic products expelled by bacteria. Such expelled compounds can often be used by other bacteria in “food chains”.

In summary, when bacterial life in buffer and backfill is under investigation, it appears very important that relevant clays intended for use are investigated in safety analysis. The conditions for bacterial life differ significantly over clay types. Additional clays should be studied as well for general understanding of similarities and differences between clays.

3 Cell separation from clay for visualization and nucleic acid analysis

The adhesion of bacterial cells to soil particles surfaces involves a variety of mechanisms which operate simultaneously. Bacterial cells, clay minerals and humic acid particles are usually negatively charged, resulting in repulsion at large distance. As stated in the colloid stability theory, the interaction between negatively charged particles is a function of ionic strength. In particular, this means the concentration of divalent or polyvalent cations (Lindahl and Bakken 1995). Hence the majority of indigenous soil bacteria are efficiently adsorbed to clay surfaces when the concentration of divalent cations is high. Therefore, the target is the electrostatic forces between bacteria and soil colloids (Marshall 1976). The colloid stability theory only includes electrostatic and van der Waals forces. However, there are other mechanisms in action, which result in binding energies over a wide range of energy levels. Those bonds are not necessarily broken by regulating the ionic strength (Lindahl and Bakken 1995).

Experiments at Microbial Analytics Sweden AB trying to directly extract DNA from bentonite with commercially available kits resulted in no measurable yield of DNA. Therefore, an indirect DNA extraction method and another direct DNA extraction method was developed to analyse the bacterial community of bentonite clay.

The general idea for the indirect DNA extraction method is to replace the polyvalent cations with monovalent cations. This should lead to increased electrostatic repulsion between the clay particles and the negatively charged soil bacteria. Additionally, detergents dissolve extracellular polymeric substances that are involved in adhesion of bacterial cells to soil particles. Application of a physical force disperses the soil and enhances desorption of bacterial cells.

Two different methods for the direct DNA extraction were tried out and aimed to increase the yield of DNA. The methods were tested with biofilms of SPB and *Gallionella sp.* The first steps in both methods are almost identical. The sample is suspended in a buffer and the bacterial cells are lysed with the help of the enzymes lysozyme and proteinase K and afterwards further lysed by SDS. In the first method, modified from Gabor et al. (2003), the buffer to suspend the sample contains cetyltrimethyl ammonium bromide (CTAB), which removes membrane lipids and promotes cell lysis.

In one of the developed methods the DNA is then extracted and purified with the classic phenol:chloroform extraction method. Subsequently the DNA is precipitated with the alcohol precipitation. In the other method, after the cell lysis the SDS is precipitated with potassium acetate (modified from Selenska and Klingmüller 1991). Then the DNA is precipitated with polyethylene glycol 6000 (PEG600) in presence of a high salt concentration.

The aim of this study was to establish a cell separating method and a DNA extraction method. The cell separation method would enable subsequent DNA extraction. Both methods would make it possible to use downstream analyses.

3.1 Methods

This section is divided in cell separation experiments and DNA extraction experiments. Figure 3-1 shows an overall scheme of the cell separation method procedure.

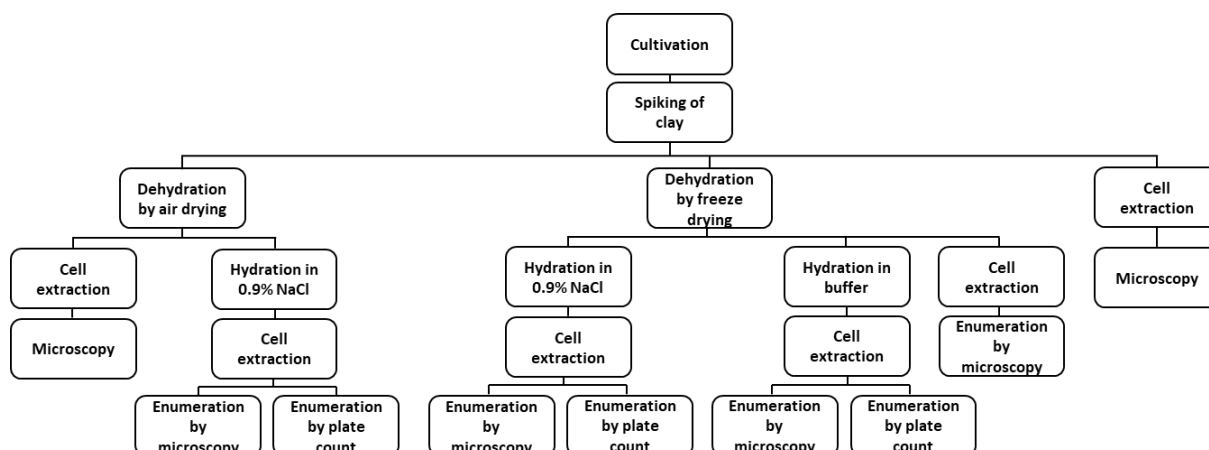


Figure 3-1. Method scheme for all cell separation experiments.

3.1.1 Cell separation methods

The listed methods below were used in all cell separation experiments. Methods that were specific for the single experiments are listed under respective experiment.

3.1.2 Cultivation

The bacteria *Bacillus subtilis* from Culture Collection of the University of Göteborg (CCUG), Gothenburg, Sweden, no. 48815A and *Pseudomonas fluorescens* (CCUG no. 32456A) were cultivated in nutrient broth (Scharlau, Barcelona, Spain) for 16 h at 30 °C and 140 rpm.

3.1.3 Spiking of clay

After cultivation, the total number of cells (TNC) was estimated with acridine orange to be able to calculate the amounts of bacteria per gram of bentonite clay. In this report different spiking methods were used (see respective experiment). The bentonite powders used in this study were MX-80, Asha and Calcigel (provided by SKB, Äspö Hard Rock Laboratory, Sweden).

3.1.4 Total number determination of cells with DAPI

After cell extraction a dilution series was made from the obtained sample and analysed. A reasonable dilution was chosen to be able to count bacterial cells. 1 mL of the sample was filtered on to a polycarbonate filter (GVS Life Science, Sanford, ME, USA). A small drop (circa 10 µL) of DAPI with Vector shield mounting medium (Vector Laboratories, Burlingame, CA, USA) was added on a glass slide and the polycarbonate filter was put on top. Another drop (circa 25 µL) of DAPI was added directly on the polycarbonate filter and covered with a cover slide. The mounted slide was incubated in the dark for 20 – 30 minutes. Afterwards the bacterial cells were counted with a Zeiss Axio Scope.A1 microscope (Carl Zeiss AB, Stockholm, Sweden) under UV-light.

For the counting procedure 30 images were taken with an AxioCam 506 mono camera (Carl Zeiss AB, Stockholm, Sweden) and the Zen lite program. An image had an area of 0.0125 mm² and all bacterial cells were counted in the image. To obtain a good statistical calculation at least 600 bacterial cells on 15 pictures were needed. If there were less than 600 bacterial cells, 30 images were analysed. It was important to count systematically so that the counted images spread across the polycarbonate filter and the same image is not counted twice. If the density per image was ≥ 100 bacterial cells, the sample was further diluted.

3.1.5 Experiments 1, 2, 3 and 4 with Asha, Calcigel and MX-80

Experiment 1

Spiking and dehydration by air drying

In the first experiment 40 g of bentonite clay powder (Asha, Calcigel, MX-80) was dissolved in 740 mL of sterile Analytical grade water (AGW) in a large glass Petri dish inside a fume hood. The formation of lumps was avoided by constant stirring on a magnetic stirrer (Fisher Scientific GTF, Lund, Sweden) while the bentonite clay powder was slowly added. Then 60 mL of a *P. fluorescens* culture, with known TNC, was added to the dissolved bentonite clay. The mixture was further stirred for a good distribution of the bacteria. Afterwards the spiked bentonite slurry was air dried. The fume hood window was locked in position and a standard ventilator was placed in front of the Petri dishes to dry the slurry. After the complete evaporation of the water the dried spiked bentonite clay was scraped from the Petri dishes with a sterile spoon and transferred to a mortar. The spiked bentonite clay was then grinded to a fine powder and diluted with bentonite clay powder 1:10. The spiked bentonite clay powder was stored at 4 °C until cell extraction.

Cell extraction procedure

Three different buffers were tested to estimate which was the most suitable for cell extraction of bacteria from spiked bentonite clays. Each buffer (Figure 3-1) contained a detergent which dissolved extracellular polymeric substances and dispersed the clay particles. A chelating agent in the buffers replaced the polyvalent cations with monovalent cations and increased electrostatic repulsion between the clay particles and the negatively charged soil bacteria (van Elsas et al. 2006).

Fifty mL of each buffer was stirred on a magnetic stirrer and MgCl₂ was added to a final concentration of 0.5 M for buffer 1 and 2. In case of buffer 2, 1 g of Chelex100 (SIGMA-ALDRICH Chemie GmbH, Schnelldorf, Germany) was subsequently added. 5 g of each spiked bentonite clay powder (Asha, Calcigel, MX-80) was slowly added to each buffer. The homogenized slurries were transferred to a 50 mL Falcon tube and centrifuged at 1000 × g for 15 minutes at 10 °C, to collect coarse particles. Afterwards the supernatant, circa 45 mL, was transferred into a new 50 mL Falcon tube and centrifuged at 4565 × g for 1 hour at 10 °C, to collect the bacterial cells and remaining clay particles. The supernatant, circa 45 mL, was discarded and the pellet was resuspended in 3 mL of sterile phosphate-buffered saline (PBS). Carefully 1 mL Nycodenz 80% (w/v) (SIGMA-ALDRICH Chemie GmbH, Schnelldorf, Germany) was placed beneath the sample and centrifuged at 4565 × g for 30 minutes at 10 °C. Nycodenz separates according to buoyant density. Bacteria have a lower buoyant density than most soil particles (Bakken and Lindahl 1995). The remaining clay particles formed a pellet on the bottom while the detached bacteria remained in the supernatant and interphase. The 3 mL supernatant and interphase were transferred into a new 15 mL Falcon tube. Then 1 mL of this sample was filtered and stained as described in the first paragraph of 3.1.4. The stained filters of the different buffers were analysed qualitative.

Table 3-1. Buffers for cell extraction.

Buffer	Components	Reference
1	Tris-HCl 0.1 M; pH 8 Sodium EDTA 0.1 M SDS 0.1% (w/v) CTAB 1% (w/v) 0.5M MgCl ₂	(Gabor et al. 2003)
2	sodium deoxycholate 0.1% (w/v) polyethylene glycol 6000 2.5% (w/v) 0.5M MgCl ₂ Chelex100 1g per 5 g sample	Gabor et al. 2003)
3	Tris-HCl 0.05 M; pH 8.0 NaCl 0.2 M Sodium pyrophosphate 0.05 M Tween 80 0.01% (w/v)	(Malave-Orengo et al. 2010)

Experiment 2

Spiking and dehydration by freeze-drying

In the second experiment 100 mL of a *B. subtilis* culture, with a known TNC, was mixed with 50 g (MX-80 and Calcigel) or 100 g (Asha) bentonite clay powder. The formation of lumps was avoided by constant stirring on a magnetic stirrer while the bentonite clay powder was slowly added. If needed sterile filtered AGW was added to dissolve the bentonite clay completely. The spiked bentonite clay slurry was stirred for at least 30 minutes. Afterwards it was incubated at 4 °C for 2 h. This incubation step allowed the bacteria to adhere to the bentonite clay particles. Before freeze-drying the spiked bentonite clay was transferred into a specific vessel (AB Ninolab, Upplands Väsby, Sweden) for freeze-drying. Then the slurry was frozen solid at -21 °C and subsequently freeze dried with a Labconco Freeze dry system/Freezone 4.5 (AB Ninolab, Upplands Väsby, Sweden). The spiked bentonite clay powder was stored at 4 °C until cell extraction.

Cell extraction procedure to estimate the recovery rate

The buffer 2 (now called cell extraction buffer) from experiment 1 was used for further cell extractions and quantitative estimation of extracted bacteria in these experiments. The procedure of cell extraction was the same as described in Experiment 1. However, NaCl at a final concentration of 0.2 M was used instead of MgCl₂. The TNCs were estimated as described in 3.1.4.

At a later point of this experiment a hydration step before cell extraction of the spiked bentonite clay powder was included. The spiked bentonite clay powders were each incubated for 16 h in cell extraction buffer and a sterile NaCl-solution 0.9% (w/v).

Recovery rate calculation

After the estimation of the TNC after cell extraction (TNC_{a.e.}) the recovery rate was calculated. First the TNC_{a.e.} was multiplied by the total volume of the sample and then divided by the amount

of spiked bentonite powder, used for the cell extraction, to be able to compare it to the TNC before cell extraction ($TNC_{b.e.}$). The recovery rate was calculated as:

$$\text{Recovery rate} = \frac{TNC_{a.e.} \times 100\%}{TNC_{b.e.}}$$

Plate count

From the obtained sample a dilution series was made and analysed by plate count to estimate the number of viable bacterial cells. 0.1 mL of each dilution was spread out on three nutrient agar (NA) plates using a sterile bacterial spreader. The NA plates were incubated for 24 h at 30 °C and subsequently analysed. Plates with more than 200 colonies or fewer than 30 colonies were regarded as statistically not acceptable. The following formula was used to estimate the number of bacteria:

$$B = \frac{N}{d}$$

B = number of bacteria

N = average number of colonies counted on three plates

d = dilution factor.

Experiment 3

Spiking and dehydration by air drying

In the third experiment 50 g of bentonite clay powder (Calcigel) was dissolved in 70 mL of a sterile NaCl-solution 0.9 % (w/v) in a large glass Petri dish inside a fume hood. The formation of lumps was avoided by constant stirring on a magnetic stirrer while the bentonite clay powder was slowly added. Then 15 mL of each bacterial culture (*P. fluorescens* and *B. subtilis*), with known TNC, were added to the dissolved bentonite clay. The spiked bentonite clay slurry was stirred for at least 30 minutes. Afterwards it was incubated at 4 °C for 12 h.

Then the spiked bentonite clay slurry was air dried. The fume hood window was fixed in an open position and a standard ventilator was placed in front of the glass Petri dish to dry the slurry. After the complete evaporation of the water the dried spiked bentonite clay was scraped from the Petri dishes with a sterile spoon and transferred to a sterile beaker and stored at 4 °C until cell extraction.

Hydration before cell extraction

The spiked bentonite clay powder was incubated for 24 h in a sterile NaCl-solution 0.9% (w/v) at 4 °C and constant shaking at 200 rpm. Afterwards the hydrated spiked clay was centrifuged at $10\,000 \times g$ for 30 minutes and the supernatant was discarded.

Cell extraction procedure

In the third experiment the cell extraction procedure was applied as described in Experiment 1. However, the same clay sample was extracted twice to increase the recovery rate. The NaCl was this time directly added to the cell extraction buffer. The obtained samples were filtered and stained as described in the first paragraph of 3.1.4.

Plate count

Plate count was used as described in Experiment 2.

Experiment 4

Spiking of clay

30 g of powdered bentonite added (Calcigel, Asha and MX-80) were spiked with 25 mL of a *P. fluorescens* and a *B. subtilis* culture (50 mL in total), with known TNC. Additionally, 20 mL of sterile NaCl-solution 0.9% (w/v) were added and the slurries were stirred for at least 30 min. The spiked bentonite clay slurries were incubated for 24 h at 4 °C for adhesion of the bacteria to the clay particles. Then the spiked bentonite clay slurries were stored at 4 °C until cell extraction.

Cell extraction procedure

In the fourth experiment the cell extraction procedure was applied as described in experiment 1. As a control one of each spiked clay slurry sample was treated with sterile AGW. NaCl was not directly added to the buffer. Instead it was added after the spiked clay slurries were dissolved in the cell extraction buffer. The final concentration was 0.2 M for Asha and Calcigel and 0.4 M for MX-80. The obtained samples were filtered and stained as described in the first paragraph of 3.1.4.

3.1.6 FEBEX clay experiments A and B

Hydration of FEBEX clay before cell extraction

Experiment A

50 g of FEBEX clay of the core sample B-C-60-18 was dissolved in 200 mL sterile AGW for 16 h to hydrate the bacteria and make the cell walls more permeable for staining. The liquid supernatant was discarded after hydration.

Experiment B

50 g of FEBEX clay of the core sample B-C-60-18 was dissolved in 50 mL sterile 0.9% NaCl-solution 0.9% (w/v) for 24 h. After the hydration the FEBEX clay was filled into 50 mL Falcon tube and centrifuged 10000 × g for 30 minutes. The supernatant was discarded afterwards.

Cell extraction

Experiment A

The cell extraction procedure was applied as described in experiment 1. For the cell extraction 20 g of the hydrated FEBEX clay was used and dissolved in 200 mL of cell extraction buffer. The FEBEX-clay was added under constant stirring. The obtained samples were filtered and stained as described in the first paragraph of 3.1.4.

Experiment B

The cell extraction procedure was applied as described in experiment 1. For the cell extraction the 50 g hydrated FEBEX clay was used and dissolved in 200 mL of cell extraction buffer which additionally contained 0.2 M NaCl. The FEBEX-clay was extracted twice and the supernatants were pooled. The high-speed centrifugation step was carried out with a fixed angle rotor at 10000 × g for 30 minutes. The pellet fraction was resuspended in a total volume of 5 mL PBS. 2 mL of Nycodenz 80%[□] (w/v) were used for the buoyant density centrifugation step. The obtained samples were filtered and stained as described in the first paragraph of 3.1.4.

Enumeration with ATP analysis

The ATP biomass kit HS for total ATP in living cells was used (No. 266-311, BioThema AB, Handen, Sweden) to analyse ATP in samples of Experiment A & B. This analysis kit was developed based on the results of Lundin *et al.* (1986) and Lundin (2000). The method was performed as described in Eydal and Pedersen (2007).

DNA extraction and quantification

Total genomic DNA from the bacterial cells was extracted according to the manufacturers protocol using the MO BIO PowerWater DNA isolation kit (MO BIO Laboratories, Carlsbad, CA, USA). The extracted DNA was stored at $-20\text{ }^{\circ}\text{C}$.

The double-stranded (ds) DNA concentration was measured fluorometrically using the Stratagene MX3005p fluorometer with MXPro software (Agilent Technologies, Santa Clara, CA, USA) and the Quant-it Picogreen reagent kit (cat. no. P7589; Molecular Probes), according to the manufacturer's specifications.

Droplet digital PCR (ddPCR)

The extracted DNA was quantified with droplet digital polymerase chain reaction (ddPCR) (Yang *et al.* 2014). This is a new technology and enables the precise quantification of target nucleic acids in a sample. The prepared sample with Master Mix, primers and DNA is loaded in a droplet generator cartridge. The generated droplets are transferred to a 96-well plate, foil sealed, and amplified by PCR. After amplification each droplet was analysed by a plate reader to determine the fraction of PCR-positive droplets in the original sample. These data are then analyzed using Poisson statistics to determine the target DNA template concentration in the original sample. Sulphate-reducing bacteria (SRB) were detected with the primers apsAF304 and apsAR416 which are specific for the functional gene for the adenosine-5'-phosphosulfate (APS) reductase.

3.1.7 DNA extraction from bentonite clay

DNA extraction from bentonite clay with commercial kits were carried out before developing lab-specific methods. Sample materials of full compacted bentonite from mini-canisters 4 and 5 (from the MINICAN project, Johansson *et al.* 2017)) were used for the DNA extractions. Total genomic DNA from the bentonite clay was extracted according to the manufacturer's protocol using the MO BIO PowerMax Soil DNA isolation kit (MO BIO Laboratories, Carlsbad, CA, USA). 2 g of clay sample was dissolved in 15 mL Powerbead Solution and vortexed for 15 minutes. In total 50 g bentonite was used. Then the beads and Solution C1 (1.2 mL) were added and vortexed for 5 minutes. For 4 DNA extractions one Spin Filter was used. All samples from the same clay sample were pooled. The DNA was subsequently concentrated via vacuum centrifugation at $37\text{ }^{\circ}\text{C}$. The dsDNA concentration was quantified as described above.

Development of a DNA extraction method

Method 1 (modified after Gabor *et al.* 2003)

Biofilm samples of *Gallionella sp.* and sulphate-reducing-bacteria (SRB) were centrifuged at $10\ 000 \times g$ for 10 minutes and the supernatant was discarded. These two samples and 10 g of FEBEX clay were each mixed with the lysis buffer (0.1 M Tris-HCl, 0.1M sodium EDTA, 1.5 M NaCl, CTAB 1 % (w/v), pH 8).

Afterwards 1 mL (FEBEX clay) or 500 μL (*Gallionella sp.* and SRB) of Lysozyme (50 mg mL⁻¹) and 200 μL (FEBEX clay) or 100 μL (*Gallionella sp.* and SRB) of Proteinase K (10 mg mL⁻¹) were

added. The samples were incubated at 37 °C for 1 h. Subsequently 4 mL 20% SDS (end concentration 2%) were added and the samples were incubated at 70 °C for 2 h under shaking. Then the samples were centrifuged at 6000 × g for 10 minutes. The supernatants were transferred into new tubes. Afterwards the DNA was extracted. 1 volume (vol) of a phenol:chloroform:isoamylalcohol (25:24:1) was added, centrifuged at 6000 × g for 2 minutes and the upper phase was transferred. 1 vol of chloroform:isoamylalcohol (24:1) was added afterwards, centrifuged at 6000 × g for 2 minutes and the upper phase was transferred. To precipitate the DNA 1/10 vol of sodium acetate (3 M, pH 5.2) and 2.5 vol of 99% ethanol were added and mixed and incubated overnight at 4 °C. Then the samples were centrifuged at 10 000 × g for 5 min. The pellets were washed with 500 µL 70% ethanol and air dried. Finally, the pellets were suspended in 50 µL DNase/RNase free water and transferred into a new 1.5 mL Eppendorf tube.

Method 2 (modified from Selenska and Klingmüller 1991)

The biofilm samples *Gallionella sp.* and SRB were centrifuged at 10 000 × g for 10 minutes and the supernatant was discarded. These two samples and 10 g of FEBEX clay were each mixed with the buffer (0.12 M Na₂HPO₄, pH 8).

The cell lysis was performed as described in Method 1. Then the samples were centrifuged at 8 000 × g for 15 minutes. The supernatants were transferred into new tubes. 1 vol of potassium acetate (1.5 M, pH 5,2) was added to precipitate the SDS. The samples were centrifuged at 10000 × g for 10 minutes and the supernatants were transferred into new tubes. Then 0.167 vol of NaCl (3 M) and 0.4 vol of PEG6000 50% (w/v) were added to precipitate the DNA at 4 °C overnight. The samples were centrifuged at 4565 × g for 30 min and the supernatants were discarded. The pellets were washed with 500 µL 70% ethanol and air dried. Finally, the pellets were suspended in 100 µL DNase/RNase free water and transferred into a new 1.5 mL Eppendorf tube.

DNA quantification

The quality of the extracted DNA was evaluated with NanoDrop by measuring the A260/280 and A230/260 values.

The dsDNA concentration was quantified as described above (DNA extraction and quantification). The extracted DNA was stored at -20 °C and subsequently used for sequencing.

ddPCR

The extracted DNA were analysed with ddPCR (0) SRB were detected with the primers apsAF304 and apsAR416 which are specific for the functional gene for the adenosine-5'-phosphosulfate (APS) reductase. *Gallionella* were detected with primers GAL319f and GAL516r which were designed for the specific sequence of the 16S rDNA of *Gallionella* (Hallbeck and Pedersen 2014).

3.2 Results

3.2.1 Experiment 1

Buffer 2 extracted bacteria from spiked bentonite clay powders

In experiment 1 three different buffers were used to extract bacterial cells from spiked bentonite clay powders (Table 3-1). The buffer 2 showed the best results to extract bacteria from spiked bentonite clay powders (Figure 3-2). This buffer was chosen for further cell extraction experiments.



Figure 3-2. Images of P. fluorescens extracted with buffer 2 from spiked bentonite clay powders. The left image shows extracted bacterial cells from spiked Asha bentonite clay powder, the middle image from spiked Calcigel bentonite clay powder and the right image from spiked MX-80 bentonite clay powder. All samples were stained with DAPI Vector shield mounting medium.

3.2.2 Experiment 2

The recovery rate for cell extraction from spiked bentonite clay powders was very low

In experiment 2 the cell extraction buffer was used to estimate the recovery rate for the extraction of bacterial cells from spiked bentonite clay powders. Figure 3-3 shows extracted *B. subtilis* from spiked and dehydrated bentonite clay powders. The 10^{-1} dilution was used for the calculation of the TNC_{a.e.}, because the bacterial cell density was the most suitable to estimate the TNC. The amount of extracted bacterial cells for Calcigel was 6.2×10^4 cells g^{-1} and for MX-80 5.4×10^4 cell g^{-1} (Table 3-3). The calculated recovery rate for Calcigel was 0.25% and for MX-80 0.22% (Table 3-3). The cell extraction for spiked Asha resulted in no visible *B. subtilis* cells (Figure 3-3, right image).

Calculation example for Calcigel

$$TNC_{b.e.} = 7.4 \times 10^8 \text{ cells } g^{-1}$$

$$TNC_{a.e.} = 3.1 \times 10^6 \text{ cells } mL^{-1}$$

Amount of bentonite clay powder = 5 g

1. TNC_{a.e.} in cells g^{-1}

$$\frac{3.1 \times 10^6 \text{ cells } mL^{-1} \times 3 \text{ mL}}{5 \text{ g}} = 1.86 \times 10^6 \text{ cells } g^{-1}$$

2. Recovery rate

$$\frac{1.86 \times 10^6 \text{ cells } g^{-1} \times 100\%}{7.4 \times 10^8 \text{ cells } g^{-1}} = 0.25\%$$

Table 3-2 TNC after cultivation

Bacteria	TNC (cells mL ⁻¹)	Standard deviation (cells mL ⁻¹)	Date
<i>B. subtilis</i>	3.7×10^8	1.3×10^7	2016-03-10
<i>B. subtilis</i>	3.3×10^8	2.2×10^7	2016-04-01

Table 3-3 TNC after cell extraction.

Bentonit clay powder	Amount of bentonit clay powder (g)	TNC _{a.e.} (cells mL ⁻¹)	Standard deviation	cells g ⁻¹	Recovery rate (%)
Calcigel	5	3.1×10^6	1.6×10^5	1.86×10^6	0.25
MX-80	5	2.7×10^6	2.8×10^5	1.62×10^6	0.22



Figure 3-3 Images of *B. subtilis* extracted from spiked bentonite clay powders. The left image shows extracted bacterial cells from spiked Calcigel bentonite clay powder, the middle image from spiked MX-80 bentonite clay powder and the right image from spiked Asha bentonite clay powder. All samples were stained with DAPI Vector shield mounting medium.

Hydration in NaCl-solution or prolonged incubation in the cell extraction buffer had no effect and no growth on NA-plates occurred

In Experiment 2 it was investigated if hydration with a NaCl-solution 0.9% (w/v) or a prolonged incubation time, in the cell extraction buffer, influences the recovery rate. Each spiked bentonite clay powder was incubated for 16 h. The amount of extracted bacterial cells decreased strongly for all three spiked bentonite powders (Figure 3-4). Only spiked Calcigel showed after hydration by incubation in a NaCl-solution 0.9% more bacterial cells in comparison to the cell extraction buffer, were almost no bacterial cells were visible (Figure 3-4). However, the amount of bacterial cells for spiked Calcigel (Figure 3-4 Calcigel B) was less than in Figure 3-3 (left image). In addition, 0.1 mL of all samples were spread out on NA-plates and incubated for 24 h at 30 °C. No growth occurred on any of the NA-plates.

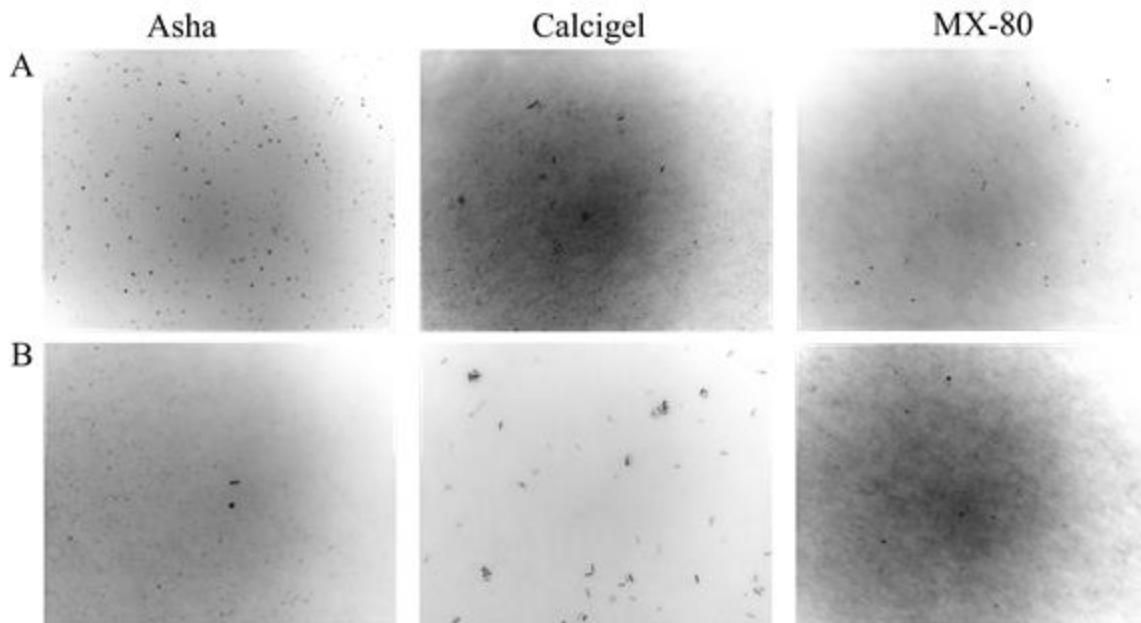


Figure 3-4. Images of B. subtilis extracted from spiked bentonite clay powders after hydration and prolonged incubation in cell extraction buffer. The row A shows the extracted bacterial cells after hydration by incubation in cell extraction buffer with 0.5M NaCl for 16 h. The row B shows the corresponding images to each spiked bentonite clay powder after hydration by incubation in a NaCl-solution 0.9% for 16 h.

3.2.3 Experiment 3

No bacterial cells could be extracted from spiked Calcigel

In the third experiment Calcigel bentonite clay powder was spiked with *P. fluorescens* and *B. subtilis*, with a known TNC. It was not possible to extract cells from the spiked and air dried Calcigel bentonite clay.

3.2.4 Experiment 4

AGW extracted P. fluorescens and B. subtilis from spiked bentonite slurries

In the fourth experiment spiked clay slurries were used and no dehydration was done. Bacterial cells could be extracted from the spiked bentonite clay slurries with the cell extraction buffer as well with sterile AGW.

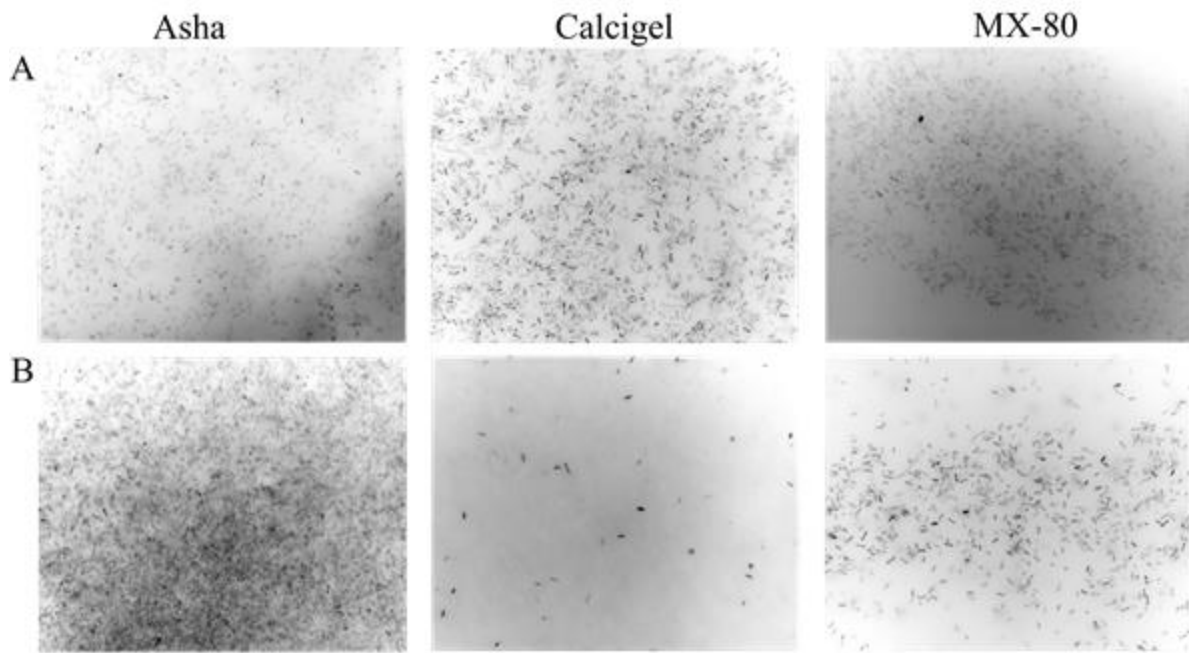


*Figure 3-5. Images of *P. fluorescens* and *B. subtilis* extracted from spiked bentonite clay slurries. The row A shows the extracted bacterial cells with the cell extraction buffer and row B with sterile AGW.*

3.2.5 FEBEX clay experiments

It was possible to extract cells from non-spiked hydrated FEBEX clay

In Experiment A FEBEX clay of the core B-C-60-18 was hydrated by incubation in sterile AGW for 16 h (Bengtsson et al. 2017d). Figure 3-6 shows that it was possible to extract bacterial cells from non-spiked FEBEX clay with the developed method. For Experiment A 29300 amol ATP mL⁻¹ (SD ±2480 amol ATP mL⁻¹) were measured for this extraction.

In Experiment B FEBEX clay of the core B-C-60-18 was hydrated longer and in sterile NaCl-solution 0.9%. The extraction procedure was also performed twice. For Experiment B 147 000 amol ATP mL⁻¹ (SD ±15700 amol ATP mL⁻¹) were measured. Subsequently the total genomic DNA was extracted with the MO BIO PowerWater DNA isolation kit. The dsDNA concentrations were measured fluorometrically using the Stratagene MX3005p fluorometer with MXPro software and the Quant-it Picogreen reagent kit. The total dsDNA concentration was 0.34 ng µL⁻¹. Furthermore, the extracted DNA was quantified with ddPCR for SRB's with primers specific for the *apsA* gene. In the 100 µL eluate 155 SRB-related cells were identified by ddPCR. This gives a MPN number of 3 SRB-related cells g⁻¹.



Figure 3-6. Images of extracted bacterial cells from non-spiked FEBEX clay sample B-C-60-18 after hydration. The clay was hydrated by incubation in 0.9% NaCl solution before cell extraction. The sample was stained with DAPI Vector shield mounting medium. Some of the cells have a blurred appearance due to that they are out of the focal plane of the microscope.

3.2.6 DNA extraction from bentonite

DNA could not be extracted with the MO BIO PowerMax kit from bentonite clay

Experiments were performed to directly extract DNA from bentonite clay before developing a cell extraction method. Sample materials of full compacted bentonite from canister sampling 4 and 5 (MINICAN project) were used for the DNA extractions. The DNA concentration quantification with the Quant-iT dsDNA High-Sensitivity kit and the qPCR Mx3005P resulted in no measurable DNA yield.

3.3 Development of a DNA extraction method

3.3.1 The extracted DNA was contaminated and had a low yield with method 1

In the first method the DNA was extracted after cell lysis with a phenol:chloroform:isoamylalcohol mixture. The samples were analysed with NanoDrop for contamination. The 260/280 values for all samples were below 1.8 and the 260/230 values were below 1 (Table 3-4).

Subsequently the dsDNA concentrations were measured fluorometrically using the Stratagene MX3005p fluorometer with MXPro software and the Quant-it Picogreen reagent kit. The highest dsDNA yield was achieved for the SRB sample with $1.98 \text{ ng } \mu\text{l}^{-1}$. The yield for *Gallionella sp.* was $0.95 \text{ ng } \mu\text{l}^{-1}$ and for FEBEX clay $0.18 \text{ ng } \mu\text{l}^{-1}$ (Table 3-5).

Table 3-4. NanoDrop results Method 1.

Sample	ng μl^{-1}	260/280	260/230
<i>Gallionella sp.</i>	18.0	1.28	0.65
SRB	53.0	1.41	0.93
FEBEX	9.58	1.33	0.80

Table 3-5. Picogreen results Method 1.

Sample	ng μl^{-1}
<i>Gallionella sp.</i>	0.95
SRB	1.98
FEBEX clay	0.18

Increases DNA yield for SRB and FEBEX with Method 2

In the second Method the SDS was precipitated with potassium acetate after cell lysis. The 260/280 value for the FEBEX clay sample was below 1.8 and for *Gallionella sp.* and SRB over 1.8. The 260/230 values were below 1 for all samples (Table 3-6).

The highest dsDNA yield was again achieved for the SRB sample with 12.69 ng μl^{-1} . The DNA yield for *Gallionella sp.* was 0.26 ng μl^{-1} and for FEBEX clay 0.75 ng μl^{-1} (Table 3-7).

Table 3-6. NanoDrop results Method 2

Sample	ng μl^{-1}	260/280	260/230
<i>Gallionella sp.</i>	7.13	2.09	0.23
SRB	5.32	6.03	0.71
FEBEX	2.52	0.94	0.35

Table 3-7 Picogreen results Method 2

Sample	ng μl^{-1}
<i>Gallionella sp.</i>	0.26
SRB	12.6
FEBEX clay	0.75

3.3.2 The efficiency of the DNA extraction methods depends on the sample material

The extracted DNA samples were also quantified with ddPCR. The biofilm samples of SRB and FEBEX for SRB with primers specific for the *apsA* gene and the biofilm sample *Gallionella sp.* for

Gallionella with primer pair GAL which were designed for the specific sequence of the 16S rDNA of *Gallionella ferruginea*. The DNA extraction method 1 resulted in more cells for the sample FEBEX (12 cells cm^{-2}) and *Gallionella sp.* ($27300 \text{ cells g}^{-1}$) in comparison with method 2. However, method 2 resulted in more cell cm^{-2} for the sample SRB ($26200 \text{ cell cm}^{-2}$) compared to method 1 (Table 3-8).

Table 3-8. Comparison of cell recovery for tested methods.

Sample	Target	Sample area (cm^2) (biofilm)	Sample weight (g)	Volume eluate (μL)	Cells cm^{-2}	Cells g^{-1}
FEBEX method 1	SRB	-	10	50	-	12
FEBEX method 2	SRB	-	10	100	-	4
SRB method 1	SRB	5.63	-	50	18	-
SRB method 2	SRB	5.63	-	100	26200	-
<i>Gallionella sp.</i> method 1	<i>Gallionella</i>	5.63	-	50	27300	-
<i>Gallionella sp.</i> method 2	<i>Gallionella</i>	5.63	-	100	8730	-

3.4 Discussion

3.4.1 A possible method to extract bacterial cells from spiked and non-spiked bentonite clays.

Bacteria are generally reversibly bound to soil particles. The target to disrupt the bond between bacteria and soil colloids is the electrostatic forces (Jacobsen and Rasmussen 1992). In the first experiment bacterial cells were extracted from spiked and dehydrated bentonite powders with buffer 2 (cell extraction buffer) (Figure 3-2). This buffer was also used to estimate the recovery rate. The cell extraction buffer consists of sodium deoxycholate and PEG 6000. Sodium deoxycholate is a mild detergent, which dissolved extracellular polymeric substances and dispersed the clay particles. PEG 6000 was used to precipitate the bacterial cells. The chelating agent Chelex100 replaces the polyvalent cations with monovalent cations and increases the electrostatic repulsion between the clay particles and the negatively charged bacteria (Gabor et al. 2003; van Elsas et al. 2006). Through low speed centrifugation the coarse particles were separated from the detached bacteria. Additionally, buoyant density centrifugation with Nycodenz enabled separation of the remaining clay particles from the bacteria (Lindahl and Bakken 1995).

In the experiment 2 $1.86 \times 10^6 \text{ cells g}^{-1}$ were extracted from spiked and dehydrated Calcigel and $1.62 \times 10^6 \text{ cell g}^{-1}$ from MX-80. It was not possible to extract bacterial cells from spiked and dehydrated Asha in this experiment (Table 3-3). However, the calculated recovery rate for Calcigel and MX-80 was very low. One possible explanation is that many bacterial cells remained attached to the clay particles. Those bacterial cells were then centrifuged to the bottom in the low centrifugation step, together with the clay particles. This could result in a bias when non-spiked

clay samples are analysed for their bacterial community, because only abundant microbes would be detached. Another possible reason for the low recovery rate could be that a vast number of bacterial cells died through the spiking and dehydration steps. Vegetative cells of *B. subtilis* are sensitive to drying (Fine and Gervais 2005). Usually protective agents like non-fat milk solids, serum, trehalose, glycerol, betaine, adonitol, sucrose, glucose, lactose or polymers are used to protect the cells (Morgan et al. 2006). In this study no protective agent was used for the dehydration at freeze-drying, which might have endangered the survival of the bacterial cells. In case of Asha it seems that all bacterial cells had died off during the dehydration in the second experiment. Furthermore, the freeze-drying process for spiked Asha took 72 h compared to 24 h for spiked MX-80 and Calcigel. This extended dehydration by freeze-drying possibly killed all bacterial cells. Another consideration is that the bacterial cells need to be hydrated before cell extraction. It is a critical step for the revival of cells after preservation by freeze-drying (Morgan et al. 2006). Bacterial cell walls are less permeable in a dehydrated state hence it is possible that DAPI could not stain all extracted bacterial cells. This would give a false number when the cell number was estimated with DAPI staining. *B. subtilis* is a rod-shaped bacterium, however in Figure 3-3 some bacterial cells appear more coccoid than rod-shaped. This indicates that the bacterial cells are dehydrated and as mentioned are more difficult to stain. Therefore, a hydration step before cell extraction was included.

The hydration in NaCl-solution 0.9% or prolonged incubation in the cell extraction buffer in experiment 2 showed no increase of extracted bacterial cells. In contrast the number of bacterial cells decreased severely. This cell extraction took place about two weeks later. After dehydration the spiked bentonite clay powders were stored at 4 °C and it seems that also the storage led to a loss of bacterial cells. At last plate counting was used to examine the cell number with another method. However, no growth on any NA-plates occurred, which also supports the conclusion that the cells died during dehydration with freeze-drying and the subsequent storage.

As a consequence of experiment 2 the spiked bentonite slurries were again dehydrated by air drying in experiment 3. Freeze-drying seems to be unfavourable for the estimation of the recovery rate. It was thought that air drying may reduce the stress on the bacterial cells and increase viability. However, no cells could be extracted from the new batch of spiked and air-dried bentonite clays. Due to complication with dehydration of the bentonite clays, this approach was discarded. Instead it was tried to extract bacterial cells from clay slurries and calculate the recovery rate.

In experiment 4 cell extraction was carried out with bentonite slurries, to reduce the complication that occurred with dehydration of the spiked bentonite clay. The bentonite clay slurries were incubated at 4 °C to enable adhesion of the bacteria to the clay particles. Sterile deionised water was used as a control, because it was thought that the amounts of extracted bacteria should be negligible than compared to the extraction buffer. However, deionised water seemed to have the same extraction efficiency as the extraction buffer (Figure 3-5). A possible reason could be that the bacteria did not adhere to the clay particles. Therefore, sterile deionised water had the same effect as the extraction buffer.

In conclusion the extraction of bacterial cells from spiked bentonite clays faces several complications. If the spiked bentonite clay slurries are dehydrated the bacterial cells are exposed to stress which reduces the viability in a great extent. This complicates the estimation of a recovery rate for a chosen extraction buffer, because the number of bacteria that survived the dehydration process cannot be estimated. Consequently, the calculated recovery rates are

probably underestimations because the initial number of viable cells per g spiked bentonite clay was overestimated. The use of bentonite clay slurries instead was confronted with the problem that the bacteria seemed not to adhere to the clay particles and even deionised water was able to “extract” the bacteria. However, this is probably not the case for bacteria which occur naturally in clay. This could be tested with the FEBEX clay which was in a prototype repository for 18 years.

3.4.2 The DNA yield of extracted bacteria from FEBEX clay was nominal

FEBEX is a full-scale engineered barrier system (EBS) experiment of a typical High Level Waste (HLW) or Spent Fuel (SF) disposal concept (Bengtsson et al. 2017d). It provides a unique opportunity for characterization of bacterial processes in an engineered barrier and its components. For 18 years a canister to be used for radioactive waste in the future underwent heat by heating elements inside the steel canisters and the bentonite buffer has been slowly hydrating with natural occurring water. The method described for spiked bentonite clays was performed on clay of the core B-C-60 18. It was possible to extract bacterial cells and $14\ 7000\ \text{amol ATP mL}^{-1}$ (SD $\pm 15700\ \text{amol ATP mL}^{-1}$) was measured for the sample in experiment B. The total dsDNA concentration was low ($0.34\ \mu\text{g }\mu\text{L}^{-1}$). It is possible that cell lysis with the MO BIO DNA extraction kit was not sufficient enough for the different occurring bacteria. A laboratory-developed protocol at Micans for cell lysis could be applied to increase the yield of DNA. After the DNA extraction the cells g^{-1} were estimated via ddPCR. For the analysis the gene *apx4* was chosen as a target for the identification of SRB. The ddPCR result showed that 3 cells g^{-1} were present. The MPN trough cultivation showed 4–46 SRB cells ggw^{-1} (Bengtsson et al. 2017d).

3.4.3 Evaluation of DNA yields

Before the cell extraction experiments, direct DNA extractions were done with the MO BIO PowerMax kit. In another attempt no measurable DNA could be directly extracted from sample materials of fully compacted bentonite from the Mini canister sampling 4 and 5 (MINICAN project). Therefore, it was tried to establish a different direct DNA extraction method. Two methods were used to increase the DNA yield and be able to analyse the bacterial communities of bentonite clays. In both methods the bacterial cells were lysed with lysozyme, Proteinase K and SDS. In the first method the DNA was afterwards extracted and purified with the phenol:chloroform extraction method. Then the DNA was precipitated with alcohol. In the second method the SDS was precipitated with potassium acetate after cell lysis and then the DNA was precipitated with PEG6000 in presents of a high salt concentration.

The first method achieved only for the SRB sample a DNA concentration over $1\ \text{ng }\mu\text{L}^{-1}$ (Table 3-5). The 260/280 values for all samples were below 1.8 (Table 3-4) which indicated that no protein, phenol or other as contaminants were present. A ratio of ~ 1.8 is generally accepted as “pure” for DNA. The 260/230 values were also below 1 (Table 3-4) and indicated that contaminants like EDTA, carbohydrates and phenol were present. Expected 260/230 values are commonly in the range of 2.0-2.2.

The second method resulted in a high DNA yield of $12.69\ \text{ng }\mu\text{L}^{-1}$ for the SRB sample (Table 3-7). However, the 260/280 and 260/230 values indicated contaminations for all samples (Table 3-6). The presence of contaminants like proteins, phenol or carbohydrates seem to be a problem with either method. Although the second method gave a higher yield for the SRB sample, both methods failed a yield of $\geq 1\ \text{ng }\mu\text{L}^{-1}$ for *Gallionella sp.* And the FEBEX clay.

The first method could be improved by precipitation of the DNA before the extraction with phenol:chloroform:isoamylalcohol. Otherwise large volumes of phenol:chloroform:isoamylalcohol are needed for the DNA extraction. This makes the method expensive and probably leaves a higher risk of phenol contamination. The second method would need an additional purification step after DNA precipitation to reduce contaminants. Furthermore, the precipitation could be done with anion exchange columns after cell lysis to purify the extracted DNA from contaminants.

After the DNA extraction the cell numbers per g clay or cm² biofilm were estimated via ddPCR. The ddPCR result showed that the DNA extraction method 1 was more efficient for the samples FEBEX and *Gallionella sp.* in comparison to method 2. However, method 2 resulted in more cell cm⁻² for the sample SRB compared to method 1. The efficiency seems to be dependent on the sample material and sample location, since bacteria are not evenly distributed in environmental samples and are motile. This complicates the comparison of different DNA extraction methods that are evaluated on environmental samples.

4 Metagenome versus 16S rDNA analysis of biofilm diversity

Biofilm samples from two boreholes in the ONKALO underground research laboratory Finland, ONK-PVA6 and ONK-KR15 were sent for metagenomics sequencing. These samples were previously sequenced and 16S rRNA gene amplicon libraries were constructed by using primers that span the v6 hypervariable regions of Bacteria and Archaea (Pedersen et al. 2014). The results revealed communities of microorganisms with representation of sulphate-reducing (*Desulfobacula*) sulphur-reducing (*Desulfuromonas*), di-sulphide-, sulphur- and thiosulphate-disproportionating (*Desulfurivibrio*, *Desulfocapsa*), sulphur-oxidizing (Thermoplasmatales) and anaerobic CH₄ oxidizing (Methanosarcinales-ANME-2) microorganisms (Pedersen et al. 2017c). The purpose of metagenome sequencing was to investigate if metagenome sequencing and 16S rDNA sequencing return similar diversity information.

4.1 Methods

4.1.1 Sample description

Two identical flow cell field circulation systems comprising four flow cells each, a micropump, two pressure meters, a flow meter, and a 4-L expansion vessel were prepared for the experiments (Pedersen et al. 2014). Groundwater from boreholes in the ONKALO tunnel, ONK-PVA6 and ONK-KR15, was pumped under in situ pressure from the respective aquifer isolated by the packer systems to the flow cells and then back to the aquifer via two parallel, 1/8-inch polyetheretherketone (PEEK) thermoplastic tubes of high-pressure liquid chromatography quality. In short, a metal-free packer system isolated an aquifer in the ONK-PVA6 borehole located 32.7–32.9 m from the tunnel rock face at a depth of 327 m; the transmissivity of the aquifer was $1.07 \times 10^{-9} \text{ m}^2 \text{ s}^{-1}$. A similar metal-free packer system isolated an aquifer in the ONK-KR15 borehole located 75.0–75.2 m from the tunnel rock face at a depth of 399 m; the transmissivity of the aquifer was $7.6 \times 10^{-9} \text{ m}^2 \text{ s}^{-1}$. Details can be found in the report by Edlund et al. (2016), the samples were collected during SURE phase 3.

4.1.2 Metagenomic sequencing methodology

Metagenomic shotgun sequencing of the DNA from the biofilms were executed with NextSeq at Marine Biology Laboratory (MBL) at Woods Hole, USA. Picogreen (Invitrogen) was used to quantitate the genomic DNA samples. DNA was sheared using a Covaris and libraries were constructed with the Nugen Ovation Ultralow Library protocol. The aim was an insert size of 225-250 base pairs to enable read merging. Amplified libraries were visualized on an Agilent DNA1000 chip or Caliper HiSens Bioanalyzer assay, pooled at equimolar concentrations based on these results, and size selected using a Sage PippinPrep 2% cassette. The library pool was quantified using a Kapa Biosystems qPCR library quantification protocol, then sequenced on the Illumina NextSeq in a 2x150 paired-end sequencing run using dedicated read indexing. The samples were demultiplexed with bcl2fastq. There were about 108 GB of Data in zip format for the three samples. Sixteen metagenomic libraries were pooled onto a full NextSeq500 high throughput flowcell. Theoretical NextSeq yield was 400 clusters (800 reads; 400 paired end reads). The header in FASTAQ was @NB500928:49:HC2K7BGXY:1:11101:9511:1057 1:N:0:CTCGTA "NB500928" is the Nextseq. The header included the index, it is the last field, CTCGTA in the above example. The adapters were trimmed by the Illumina program. There were no in-house modifications for shotgun sequencing. The sequencing primers were standard

Illumina primers that came with the sequencing kit. Raw shotgun sequencing reads were trimmed and subjected to de novo and mapped to scaffolds that were binned by GC content, read coverage and phylogenetic profile within the binning interface of ggkbase (<http://ggkbase.berkeley.edu/>).

4.2 Results and discussion

Genes that could be assigned to a specific phylogenetic level, i.e. class, order, family or genus, in the metagenome and the 16S rDNA libraries were compared and co-occurrence were registered (Table 4-1). The proportion of genes belonging to Bacteria showed good match between the two libraries for both sampled biofilms. From 35% to 55% of the genes co-occurred. The remaining proportion did not, which suggests that the two methods do not overlap fully. Both methods indicate that the proportions of SRB were relatively small which is in agreement with data reported previously by Pedersen et al. (2017c). For archaea, there were large differences which can be explained by the different methodologies. The 16S rDNA method utilizes a primer pair that are specific for Archaea (Av6) while the shogun method does not distinguish between Bacteria or Archaea. Sequencing methods are not reliable quantitative tools, but the occurrence of various genes in sequence libraries should to some extent reflect the occurrence in the analysed samples. Genes belonging to Archaea were represented by only a fraction of a percent in the metagenome. This suggests that there were very few Archaea in the sampled biofilms. The 16S rDNA library for the Archaea selective primers was, as expected, totally dominated by Archaea related genes.

Metagenomic sequence data can be analysed with many different aspects. Here, we show that there was a relatively good overlap and occurrence of genes in the metagenome and 16S rDNA DNA libraries for Bacteria, but not for Archaea. The metagenome data suggests that only a fraction of the population in the biofilms belonged to Archaea. Both methods agreed on the occurrence of SRB.

Table 4-1. The co-occurrence of genes in both metagenome and 16S rDNA libraries from ONK-PVA6 and ONK-KR15 biofilms presented as the percentage of all genes for phylogenetic groups of microorganisms that also were detected by the 16S rDNA analysis. Detailed numbers can be found in appendix A.

Phylogenetic group	ONK-PV6		ONK-KR15	
	Metagenome	16S rDNA (bv6/av6)	Metagenome	16S rDNA (bv6/av6)
Total Bacteria %	35.0	40.3	47.1	55.1
Total SRB %	2.25	2.72	2.12	11.0
Total Archaea %	0.34	82.4	0.18	65.6

5 Presence and activity of sulphide- and acetate-producing bacteria in bentonite systems

The clays analysed and discussed in this report have been investigated previously. This chapter compiles and summarizes previously performed work with test cells and compacted bentonite in figures that have not been published until now. Six different commercially available bentonites of interest for geological disposal concepts have been studied. Sulphide producing activity was first studied using Wyoming Volclay MX-80 (Masurat et al. 2010b; Pedersen 2010; Pedersen et al. 2000b). Thereafter Wyoming Volclay MX-80 (USA), Ashapura (India) and Calcigel (Germany) was investigated (Bengtsson and Pedersen 2017). The clays GMZ (Gaomiaozi, China) and Rokle (Czech Republic) were also investigated (Bengtsson et al. 2017b) as was FEBEX clay (Switzerland) (Bengtsson et al. 2017d) and in addition Boom Clay (Belgium) has been studied as a reference to a non-swelling clay (Bengtsson and Pedersen 2016). Finally, to fully understand the mobility and reactivity of sulphide in bentonite clays, investigations were done using suspensions of bentonite clays and sulphide (Pedersen et al. 2017b).

5.1 Presence and activity of sulphide-producing bacteria

5.1.1 Methods

Test cells

The methods and equipment have been described in detail previously (Bengtsson and Pedersen 2016; Bengtsson and Pedersen 2017) and are only briefly summarized here. Cylindrical test cells made of titanium were used in the experiments (Figure 5-1). The cells were filled with the respective bentonite clay powder with addition of a bacterial cocktail consisting of three different species of SPB, except control cells that were filled with clay without added SPB. The bentonite clay powders were compacted to a specific volume and then water saturated with a salt solution. A copper disc that simulated a copper canister was installed in the clay core bottom when the clay cores had reached the planned wet densities and were fully water saturated. On the opposite clay core side to the copper disc, $^{35}\text{SO}_4^{2-}$ together with lactate, which is a preferred carbon and energy source for SPB, were added. This radioactive substance was used as a tracer for bacterial reduction of sulphur in sulphate to sulphide. The radioactivity of Cu_2^{35}S that had formed on the copper discs was located and quantified using electronic autoradiography (See example in Figure 5-2). Samples were taken from different layers of the bentonite core and analysed for distribution of ^{35}S , of sulphate, acetate, lactate and most probable number of cultivable SPB.

Favourable growth conditions were obtained by the addition of lactate which is a preferred carbon and energy source for most SPB. Lactate is metabolically oxidized to acetate by many sulphate-reducing bacteria upon growth. Hence, the experimental design offers two different methods of analysing bacterial activity; the accumulation of Cu_2^{35}S on the copper discs and the production of acetate, where the accumulation of Cu_2^{35}S is specific to SPB and the production of acetate could be performed both by SPB and other natural types of bacteria in the clays. Since acetate was analysed on several different positions throughout the clay cores it also gave an understanding on where the bacterial activity took place. In addition, sulphide is generally believed to diffuse through bentonite like a regular ion but it has recently been shown that sulphide is partly immobilized in bentonite (see chapter 0) (Pedersen et al. 2017d). If immobilization occurred, the observed levels of Cu_2^{35}S accumulation might not be in direct correlation to the level of SPB activity since sulphide produced in the middle of the clay core

possibly never reached the copper discs. Besides being a great complement to the Cu_2^{35}S analysis where bacterial activity can be discovered even if it is masked by the sulphide immobilization effect, the analysis of produced acetate also showed if bacteria could use the found organic carbon sources (see chapter 2.2) in the clays other than the added lactate.

Test cells experiments have not been performed with the FEBEX bentonite. However, clay samples have been analysed for viability at different densities and water content levels after 18 years of incubation in a heated full-scale simulation of a geological disposal concept in granitic bedrock (Bengtsson et al. 2017d).

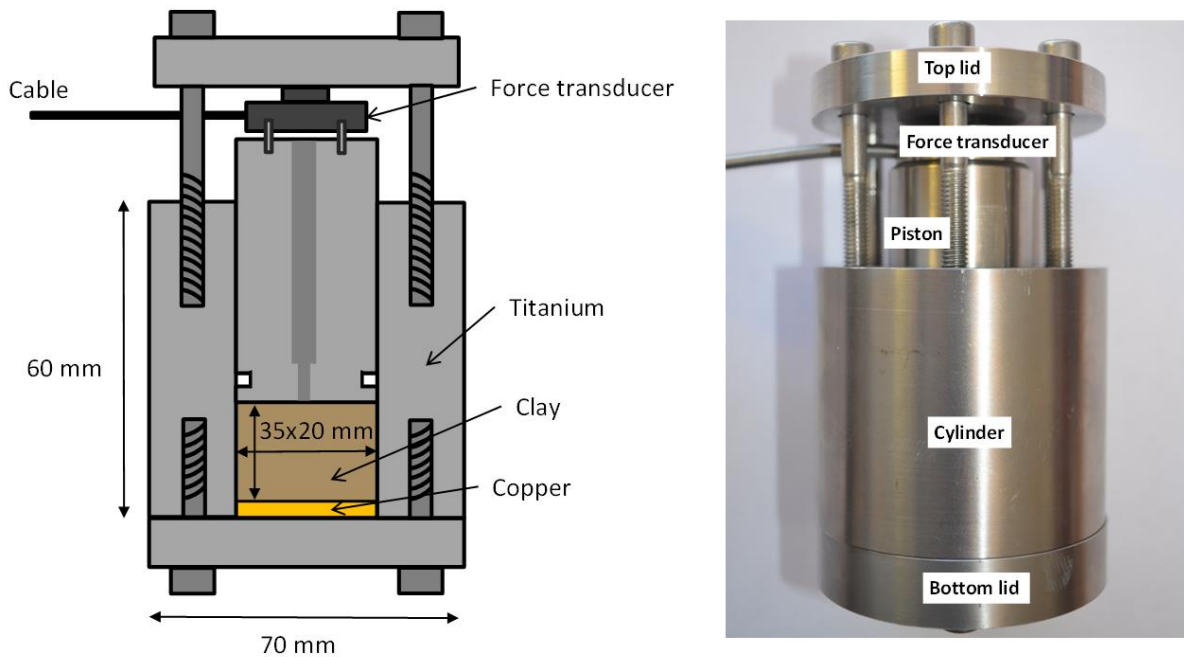


Figure 5-1. Left: A schematic cross section of a test cell. Right: An assembled test cell, spacers are not mounted.

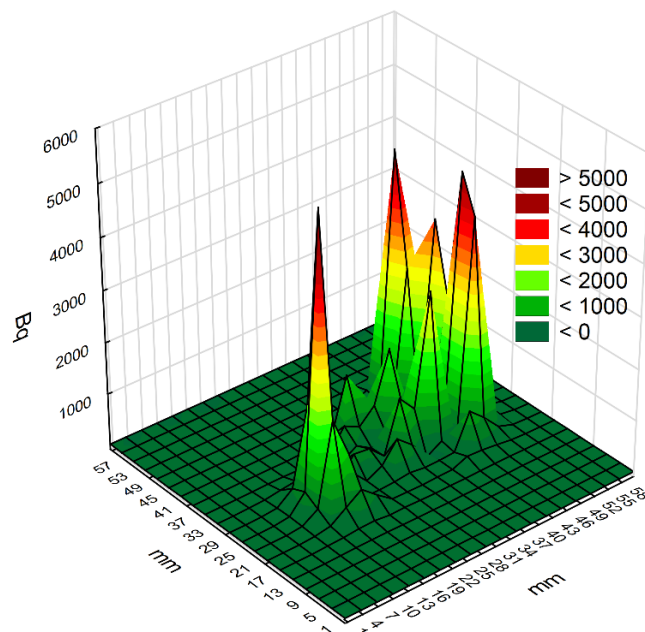


Figure 5-2. Surface radioactivity analysed on the copper disc of Rokle TC44 1750 (+) 78d (Bengtsson et al. 2017b).

5.1.2 Clay density and cultivability of SPB

As shown in Figure 5-3, the overall cultivability of SPB cultivated from clay samples decreased over wet density. The far highest numbers reported as number per litre of pore water ($>300 \times 10^6$ MPN L⁻¹) were found below 1850 kg m⁻³ for samples of Asha and GMZ, both with and without initial bacterial addition. In addition, above 1850 kg m⁻³ there was predominantly samples with bacterial addition that could be cultivated. This may indicate that the inherent, cultivable SPB populations in the tested bentonites were inactivated during the experiment in wet densities over 1850 kg m⁻³, although with some exceptions (Figure 5-3).

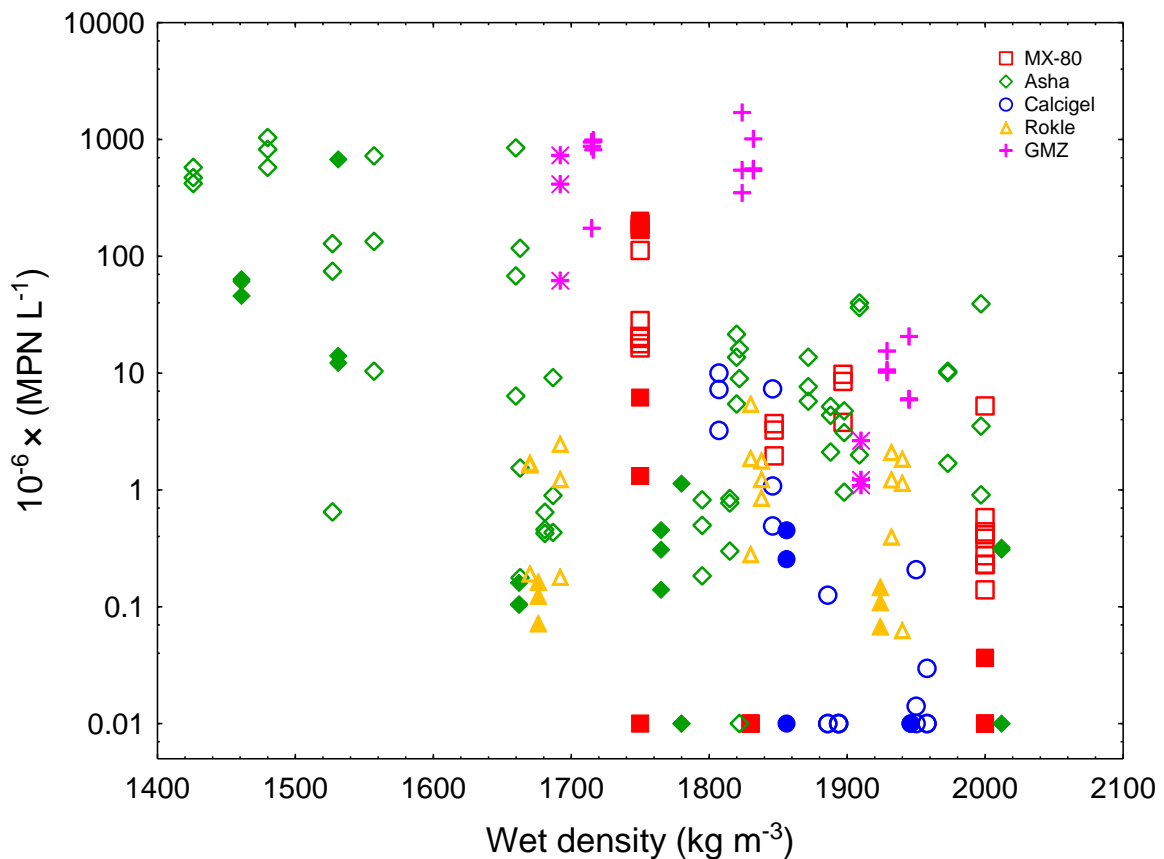


Figure 5-3. Number of cultivable cells (MPN) over wet density. Note that the y-axis is logarithmic. Control samples without bacterial addition are marked with filled symbols for each clay according to legend. Data collected from (Bengtsson et al. 2016; Bengtsson et al. 2017b; Bengtsson et al. 2017c; Bengtsson et al. 2017d; Bengtsson and Pedersen 2016; Bengtsson and Pedersen 2017).

5.1.3 Clay density and activity of SPB

The different analysed clays had varying mineralogy with a large difference in content of toxic trace metals and iron for Asha and Rokle compared to the other clays (Table 2-2, Table 2-3). Figure 5-4 shows that the intervals where the measurable accumulation of Cu_2^{35}S for each clay changes from significant to below detection. For GMZ and Boom Clay the threshold densities are yet to be determined. Rokle has the lowest threshold density. The density threshold of Rokle, Asha, Volclay MX-80 and Calcigel all fell approximately in the order of iron and heavy metal contents from the lowest to the highest values of Fe_2O_3 (Table 2-2, Table 2-3). For GMZ and Boom Clay, no cut-off density within the tested densities could be found. It is therefore concluded that density alone does not control bacterial activity in clays.

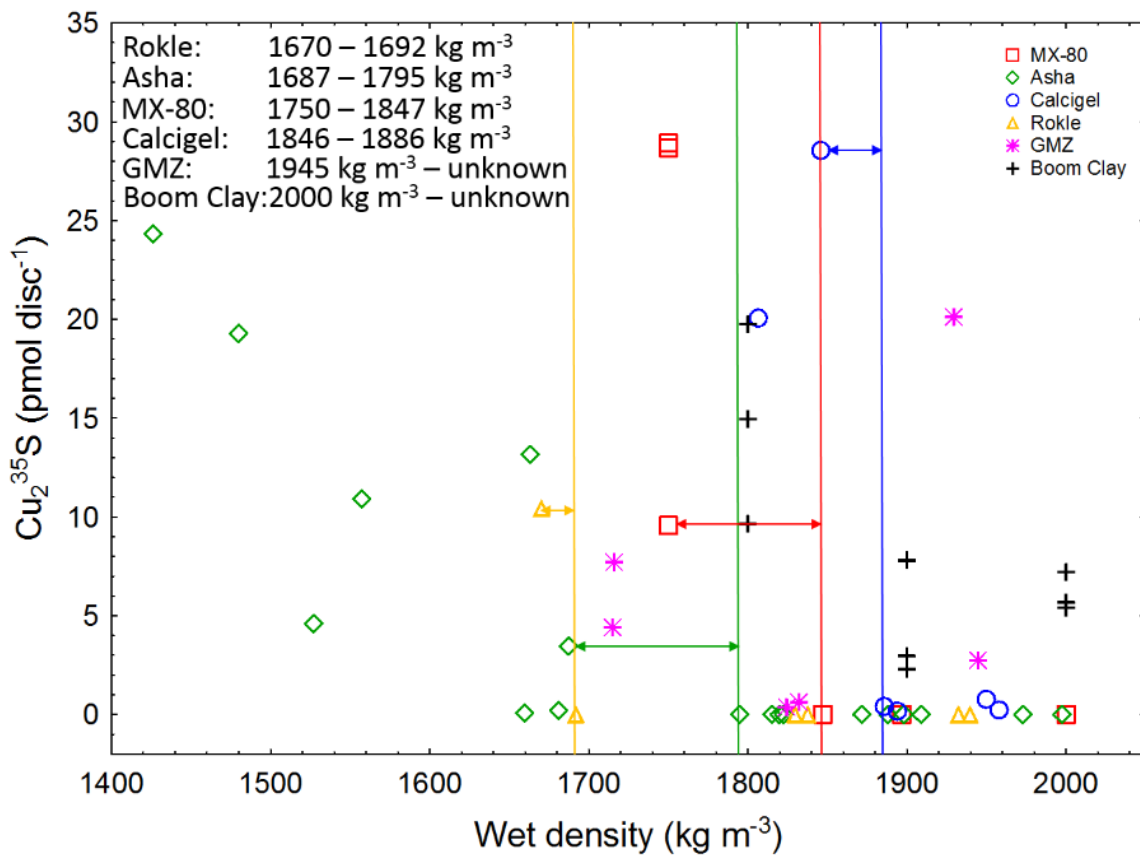


Figure 5-4. Accumulated Cu_2^{35}S on copper discs over wet density for each tested clay according to legend. Vertical lines specify density intervals where sulphide-producing activity goes from positive to below detection. Data collected from (Bengtsson et al. 2016; Bengtsson et al. 2017b; Bengtsson et al. 2017c; Bengtsson et al. 2017d; Bengtsson and Pedersen 2016; Bengtsson and Pedersen 2017).

5.1.4 Clay pressure and activity of SPB

When plotting sulphide production analysed as copper sulphide on the discs versus measured pressure, there was a limit for the bentonite clays at approximately 1000 kPa above which Cu_2^{35}S could not be detected, or, was very close to the detection limit Figure 5-5. The non-swelling BOOM clay still had some active sulphide producing bacteria at 2500 kPa.

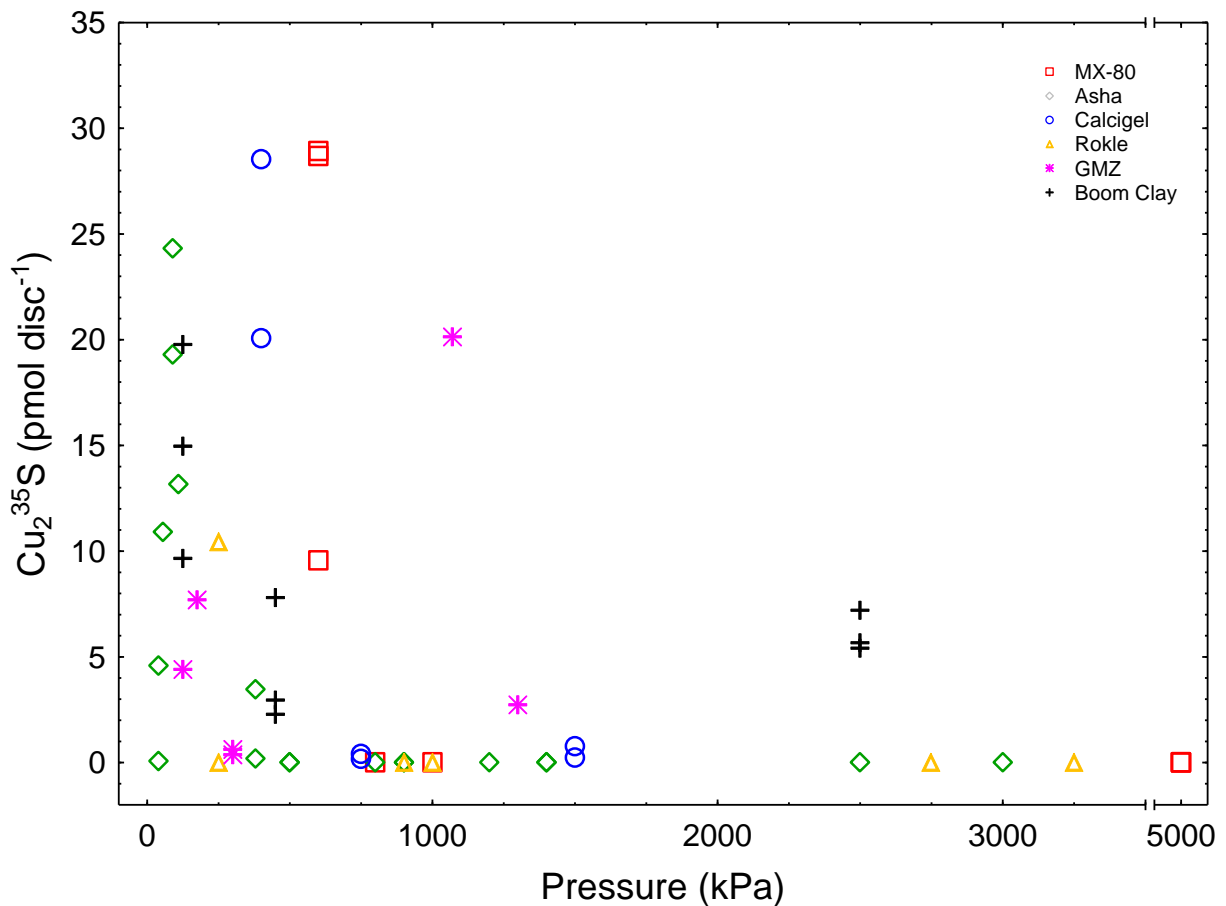


Figure 5-5. Amount of ^{35}S copper sulphide on copper discs versus swelling pressure. Data collected from (Bengtsson et al. 2016; Bengtsson et al. 2017b; Bengtsson et al. 2017c; Bengtsson et al. 2017d; Bengtsson and Pedersen 2016; Bengtsson and Pedersen 2017).

5.1.5 Lactate consumption and acetate production

The methodology of analysing acetate and lactate was introduced on experiments with Rokle, Asha and GMZ. Detailed experimental lay-out are described in papers and reports by Bengtsson et al (2017b; 2017). There was generally more acetate produced than what could be explained by the observed consumption of lactate. There must, consequently, have been other sources of organic carbon available for the excess production of acetate. The organic matter found in the clays (see chapter 2.2) is the most plausible source. A verification experiment showed that the applied methods for lactate and acetate analyses were indeed precise and accurate (Figure 7-21 and Figure 7-22).

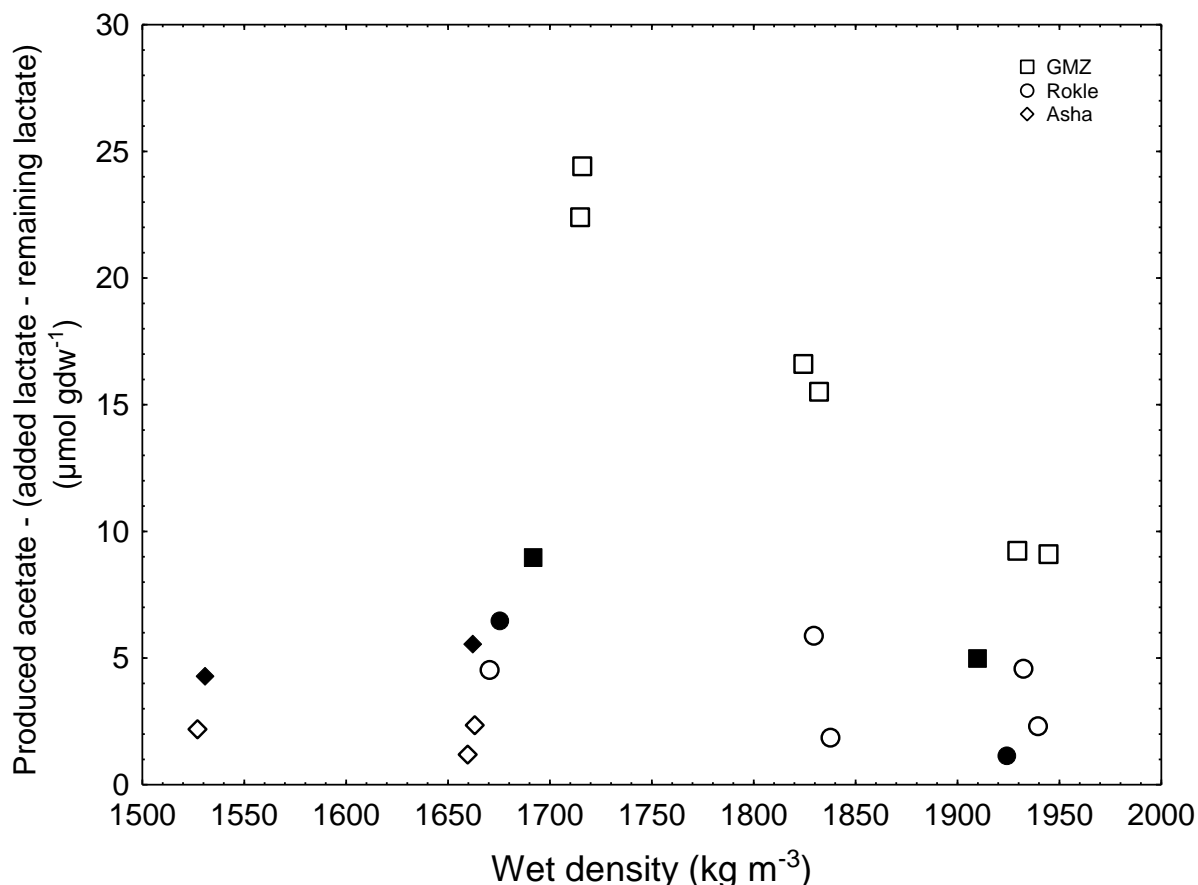


Figure 5-6. Produced acetate over wet density. The values in the graph have been subtracted with the amount of added lactate minus the amount of remaining lactate, meaning that the produced acetate in the graph is suggested to have originated from the analysed natural organic matter in the clays (see chapter 2.2). Data collected from Bengtsson et al (2017b; 2017).

5.2 Motivation for the follow up investigation presented next in this report

Comparisons between observed Cu₂S and consumed sulphate indicated that more sulphide was produced than registered by the copper discs. It appeared as if sulphide was immobilised in the clay. This was supported by the previous observation of black stained, very radioactive positions on top of the clay plugs (Pedersen 2010). It was, therefore, decided to test the effect from sulphide on bentonite clays to verify that bentonite clays immobilise sulphide. In addition, new methods were needed to evaluate reactivity of sulphide in bentonite clays.

6 Mobility and reactivity of sulphide in bentonite clays

The possibility that bacterial processes that may degrade buffers one way or another has been addressed in MIND in Task 4. Several different groups of bacteria produce H₂S in their dissimilatory metabolism. It was, consequently, important to investigate the effect of sulphide on bentonite clays. If sulphide reacts with ferric iron in the clay, it may have implications to the stability of the montmorillonite and the transport properties of sulphide through bentonite buffers and back-fill. The reduction of ferric iron by sulphide from SPB was recently demonstrated for freshwater sediments (Hansel et al. 2015). The authors showed that sulphide was oxidized to sulphur concomitant with the reduction of a range of different ferric iron oxides to ferrous iron. They suggested that this was an abiotic oxidation-reduction process. A similar process may occur in bentonites, where sulphide reduces ferric iron (Fe³⁺) to ferrous iron (Fe²⁺) concomitant with the oxidation of sulphide to elemental sulphur (Eq 1). The ferrous iron could react with free sulphide and form iron(II) sulphide FeS (Eq 2). The generalised sum of these processes is given in Eq 3.



The dissociation constant for HS⁻/H₂S is 10^{-6.98} (Richard and Luther 2007). The pH of groundwater in repository environments, and in clay pore water is buffered above 7, which means that sulphide mainly will be present as HS⁻ when pH approaches 8 or higher.

In a published study (Pedersen et al. 2017b), produced within the MIND project, the effect of sulphide on bentonites were investigated. Sulphide was found to reduce ferric iron in bentonites denoted Asha, MX-80 and Calcigel under the formation of elemental sulphur, ferrous iron and iron sulphide. The published paper is enclosed in Appendix B. These reactions rendered an immobilisation capacity of the clays that was 40 μmole sulphide (g clay)⁻¹ or more, depending on the load of sulphide, and type of clay. In addition, using a diffusion method developed for Boom clay (Bengtsson and Pedersen 2016), the effective diffusion coefficients for sulphide (³⁵S⁻²) in Asha bentonite, compacted to saturated wet densities of 1750 kg m⁻³ and 2000 kg m⁻³, were determined to be 2.74×10⁻¹¹ m² s⁻¹ and 6.60×10⁻¹² m² s⁻¹, respectively (Figure 6-2 and Figure 6-3). In opposite, when the diffusion experiment was repeated with Calcigel, the added ³⁵S⁻² did not come through the clay. Likely, Calcigel immobilised all added ³⁵S⁻². In tests with addition of sulphide on Volclay MX80, Asha and Calcigel clays, blackening due to FeS formation clearly demonstrated how the sulphide moved in a front until exhausted. The immobilisation effect is visual in Figure 6-1.

Data for diffusion of sulphide in compacted, water saturated bentonites in the literature is limited. D_e for sulphide in 1750 kg m⁻³ wet density bentonite is estimated to be in the order of 7 × 10⁻¹² m² s⁻¹ (King et al. 2011). Eriksen and Jacobsson (1982) found D_e in the order of 9 × 10⁻¹² m² s⁻¹ for MX-80 at 2100 kg m⁻³ wet density. Further data showed D_e was estimated to be to be 1.26 × 10⁻¹¹ m² s⁻¹ at 1745 kg m⁻³ wet density and 2.19 × 10⁻¹² m² s⁻¹ at 2004 kg m⁻³ wet density for MX-80 (Lee et al.). Previously, D_e for H³⁵S⁻ in compacted Wyoming MX-80 bentonite was calculated from experiments studying the activity of sulphate-reducing bacteria in bentonite (Pedersen, 2010). The D_e in Wyoming MX-80 at a wet density of 2000 kg m⁻³ was calculated to be 2 × 10⁻¹² m² s⁻¹ and 1.2 × 10⁻¹¹ m² s⁻¹ at 1750 kg m⁻³ wet density. The difference between the

calculated values may be due to experimental conditions. Although Asha and MX-80 are different in their chemical composition, D_e decreases in a similar way with increasing of wet density.

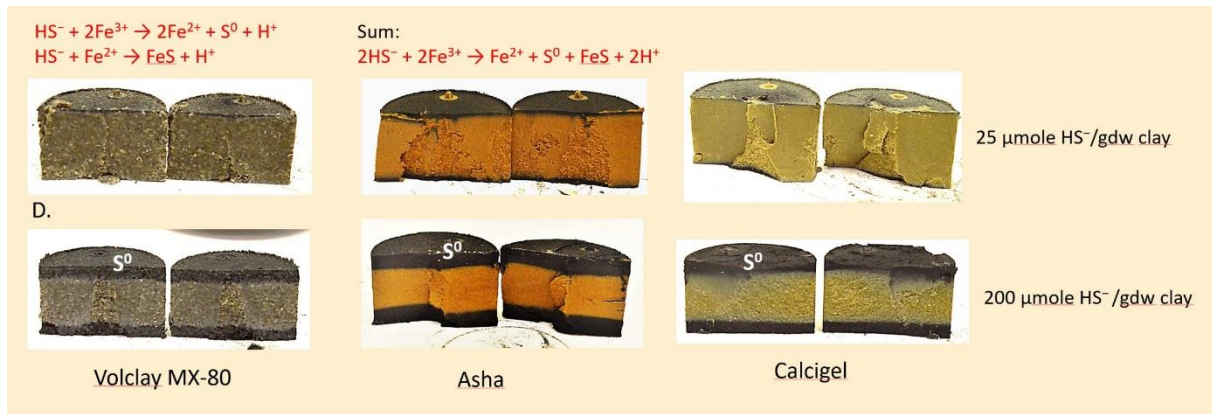


Figure 6-1. Transport of two different amounts of sulphide added to bentonite clays after 90 days of water saturation to 2000 kg m^{-3} wet density. There were significant amounts of S^0 in the black layers (see section 7 for details).

6.1.1 Calculation of the diffusion coefficient of $^{35}\text{S}^{2-}$ in Asha bentonite

The concentration of ^{35}S began to increase after 3 days on the receiving side for the wet density of 1750 kg m^{-3} . The increase halted after day 6 but increased again after day 14 in concentration and was linear until the end of the experiment after 45 days (Figure 6-2). The wet density of 2000 kg m^{-3} showed a similar pattern. Figure 6-3 shows that the ^{35}S concentration increased from day 4 until day 10 and then stayed constant. After 20 days the concentrations increased linearly for the rest of the experimental time. Linear regressions of the measurements of activity yield rates of increase of ^{35}S activity in the receiving reservoir gave 0.1292 Bq s^{-1} and 0.0311 Bq s^{-1} for the wet densities 1750 kg m^{-3} and 2000 kg m^{-3} , respectively.

Assuming this corresponds to the (quasi-) steady-state flux m' of ^{35}S activity through the clay cores, the effective diffusion coefficients can be calculated from Fick's law (Eq. 1)

$$m' = D_e \cdot A \cdot (C_1 - C_0) / d \quad (1)$$

with D_e the effective diffusion coefficient ($\text{m}^2 \text{ s}^{-1}$), $A = 0.01752 \cdot \pi = 9.62 \times 10^{-4} \text{ m}^2$, the cross-sectional area of the clay core, $C_1 = 9.79 \times 10^{10} \text{ Bq m}^{-3}$, the concentration of H^{35}S^- in the donor reservoir, which can be considered as (quasi-) constant as the flux that leaves this reservoir was very small compared to the inventory in the reservoir, $C_0 \cong 0 \text{ Bq m}^{-3}$, the concentration in the receiving reservoir, which can be considered approximately equal to zero as it remained very small compared to C_1 and $d = 0.02 \text{ m}$ the thickness of the clay core. This calculation yielded the effective HS^- diffusion coefficients $2.74 \times 10^{-11} \text{ m}^2 \text{ s}^{-1}$ for the wet density 1750 kg m^{-3} and $6.60 \times 10^{-12} \text{ m}^2 \text{ s}^{-1}$ for the wet density 2000 kg m^{-3} .

The same experiment was done for Calcigel however the concentrations stayed very low and constant for 34 days and the experiment was discontinued (data not shown).

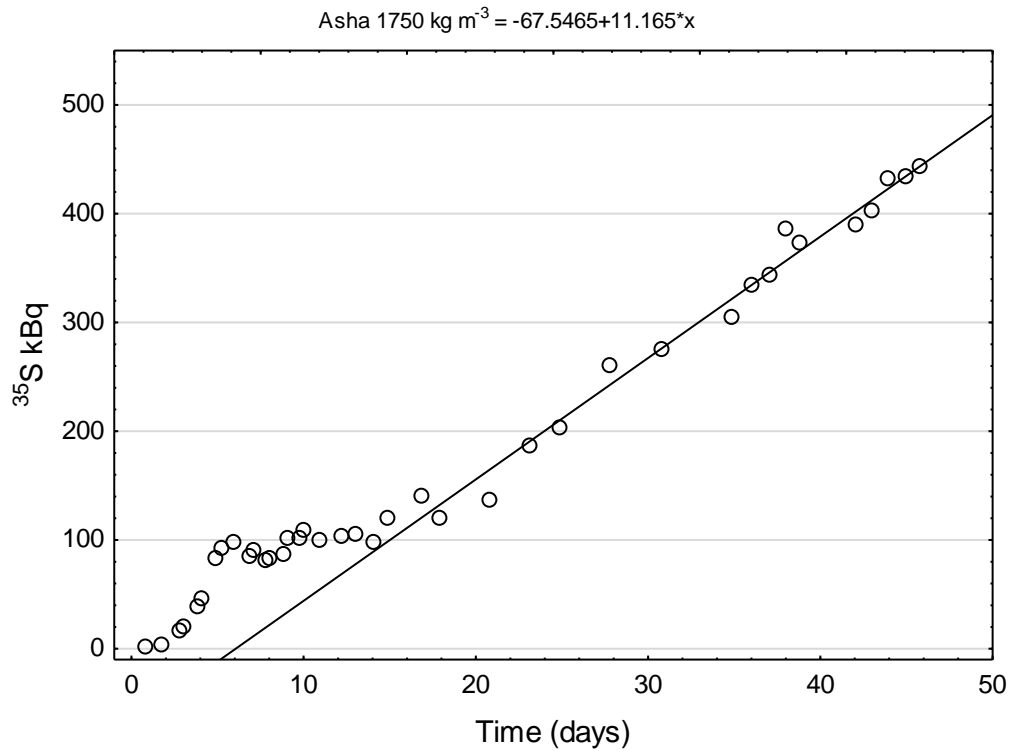


Figure 6-2. Asha 1750 kg m⁻³ diffusion plot with measured radioactivity over time. The linear fit is based on x-values in the day range 14 to 45: $^{35}\text{S} = -67.5 + 11.2 (\text{time})$.

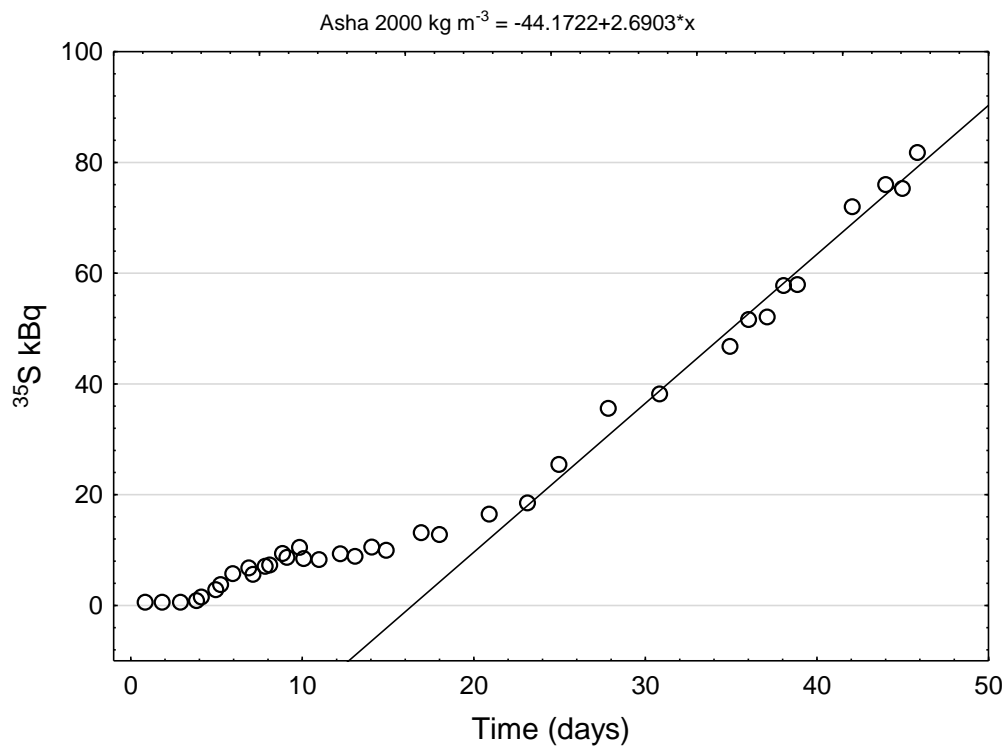


Figure 6-3. Asha 2000 kg m⁻³ diffusion plot with measured radioactivity over time. The linear fit is based on x-values in the day range from 23 to 45: $^{35}\text{S} = -44.2 + 2.69 (\text{time})$.

6.2 Implications for engineered barriers

Sulphide may originate from metabolic activity of SPB in the geosphere, buffers, backfill and in organic wastes. All three investigated clays immobilised significant amounts of the added Na_2S up to at most $90 \mu\text{mole H}_2\text{S (g clay)}^{-1}$ at the highest load of Na_2S . This immobilisation effect can reduce the mass of sulphide that reacts with metal canisters over repository life times which may influence the longevity of metal canisters. There was a clear retardation in transport of sulphide also at a low load of $\leq 0.45 \mu\text{mole H}_2\text{S (g clay)}^{-1}$ in the diffusion experiment which suggests that the immobilisation capacity of the clays spans over a large range of sulphide amounts. This immobilisation capacity does not include the immobilisation of sulphide as FeS . The immobilisation capacity may, therefore, be larger than indicated above, in buffers with pH above 7. Sulphide will, consequently, not initially migrate as a non-reactive monovalent anion (HS^-) in engineered clay barriers. The transport of sulphide in bentonite buffers should be modelled as reactive until all ferric iron available to react with sulphide is reduced to ferrous iron. Further, the oxidation of sulphide to sulphur in bentonite EBS will create a concentration gradient of sulphide in groundwater adjacent to the barrier. This oxidation will induce a diffusive transport of sulphide towards the clay until reactive ferric iron is depleted and available ferrous iron has formed FeS . Thereafter, the bentonite will act only as a diffusion barrier and the metal canisters will be the only sink for sulphide.

The processes demonstrated by Pedersen et al., (2017b) will, consequently, cause an S immobilisation effect that can reduce the mass of sulphide that reacts with metal canisters over repository life times that may influence the longevity of metal canisters. However, the immobilisation of sulphide by bentonites in EBS will retard the transport of sulphide towards metal canisters, but reduction of structural ferric iron may be problematic due to the destabilizing effect of ferrous iron on dioctahedral smectites (Bradbury et al. 2014; Lantenois et al. 2005; Soltermann 2014). The sulphide concentrations applied in this work were higher than what is generally found in geological environments intended for radioactive waste repositories and is, therefore, not fully realistic. The incorporation of SPB in experiments with clays as done elsewhere (Bengtsson and Pedersen 2016; Bengtsson and Pedersen 2017; Liu et al. 2012; Stone et al. 2016), can provide more realistic experimental conditions for detailed analysis of the influence of sulphide from SPB on the stability of bentonite in engineered barriers.

6.3 Motivation for the follow up investigation presented next in this report

Here, sulphide was added in fixed amounts to suspensions of bentonite clays. In reality, bentonite will occur as compacted to high densities. Sulphide may then either enter from the surrounding geological matrix (in groundwater) or, sulphide may be produced in the buffer at local positions or evenly throughout the buffer. Next step investigated addition of sulphide to compacted clay and production of sulphide by SPB in the clay matrix. Further, because of literature results then has shown Fe^{2+} to destabilised montmorillonite, effects on swelling pressure from added sulphide and sulphide from active SPB in the clay matrix.

7 Influence of bacteria and sulphide on bentonite clays

7.1 Experiments

This work investigated the influence of various sulphide concentrations on the swelling pressure of compacted bentonite clay and the influence of bacterial produced sulphide on the swelling pressure. It also investigated cultivability of SPB in compacted bentonite clay samples. Radiotracer detection was replaced with non-radioactive procedures, mainly developed as described by Pedersen et al., (2017b).

Influence of sulphide on the swelling pressure of bentonite clays

In this experiment the effect of sulphide on the swelling pressure capacity of the bentonite clays Asha, MX-80 and Calcigel was analysed. The bentonite clays were compacted and saturated to a wet density of 2000 kg m^{-3} with three different sulphide concentrations. The swelling pressures were registered over a 96-day period with force transducers (Figure 5-1). Afterwards the bentonite clays were analysed for sulphide, ferrous iron and elemental sulphur to investigate the reactivity of sulphide with ferric iron to ferrous iron and the concomitant reduction of sulphide to elemental sulphur in the bentonite clays.

Influence of bacterially produced sulphide on the swelling pressure capacity of Asha

In this experiment the effect of activity of SPB on swelling pressure of the bentonite clay Asha was analysed over a long (260 days) incubation time. Asha was compacted and saturated to a wet density of 1750 kg m^{-3} and 2000 kg m^{-3} under various conditions. In some test cells the carbon source lactate was used to induce bacterial sulphide-producing activity. The bacterial survival in the bentonite was analysed through the most probable number (MPN) approach. Furthermore, to investigate bacterial activity in Asha the sulphate, lactate and acetate concentrations were analysed. Finally, after the incubation time the bentonite clays were analysed for sulphide, ferrous iron and sulphur. The analysis helped to investigate the reactivity of bacterially produced sulphide with ferric iron and the concomitant reduction of sulphide to elemental sulphur in Asha.

7.2 Material and methods

7.2.1 Bentonite clays

In this work the bentonite clays Asha, MX-80 and Calcigel which are rich in montmorillonite were used (Table 2-1). MX-80 and Asha are sodium bentonites while Calcigel is a calcium bentonite which is reflected in the amounts of CaO and Na₂O (Table 2-2 and Table 2-3). Furthermore, Asha contains nearly three times more iron than the other two clays. Calcigel has a smaller amount of montmorillonite and contains no sulphate. All three contain carbon but Calcigel contains three times less organic carbon.

7.2.2 Test cells

Identical test cells were used to create saturated bentonite cores with densities of 1750 kg m^{-3} and/or 2000 kg m^{-3} . A test cell consisted of a titanium cylinder with lid on top and water saturation lid on the bottom, both attached by six Allen screws for each lid. The water saturation bottom lid had a 2 mm inlet hole which allowed water to enter the test cell and reach the bentonite. A piston operated inside the cylinder. The piston had a longitudinal inside hole to get water inflow from both top and bottom. When the piston was at its most extended position, a $35 \times 20 \text{ mm}$ confined cavity was produced inside the cylinder. This cavity was filled with the

respective bentonite powder. By using spacers on the screws running through the top lid the volume inside the test cell was kept constant. The pressure created by the swelling bentonite pushed the piston upwards and by doing so a force transducer mounted between the piston and top lid was compressed. The amount of compression, which stood in direct correlation to the bentonite swelling pressure, was recorded by a data collection system connected to a computer (see section 0). To stop the bentonite from swelling into the inlet holes, and also to get an evenly distributed inlet flow, a 40 µm pore size titanium filter (34.8 × 2.0 mm) (GKN sinter metals, Germany, item no 3A7400) was mounted with two Phillips screws on the inside of the water saturation lid and piston.

Force transducer and data collection

The force transducers used to register the swelling pressure from the bentonites were purchased from Stig Wahlström Automatik, Stockholm, Sweden and had a load range from 0 to 907 kg (AL131DL, Honeywell model 53). The force transducers were connected to a data collection system consisting of transducer amplifiers for strain gage (Stig Wahlström Automatik, model DR7DC), a programmable logic controller (model Direct Logic 06) and a PC with a custom built software (CRS Reactor Engineering, Stenkullen, Sweden) for calibration and monitoring of the force transducer signals. The readings from the transducers were calibrated from 0 to 5 MPa against two externally calibrated manometers (S-11, 0–6 MPa, 4-20 mV G1 / 2; WIKA – AB Svenska IndustriInstrument, Göteborg, Sweden).

Compaction of bentonite

The day before compaction of the bentonites the water content was determined. 3 × 1 g of each bentonite powder batch was heated at 105 °C for 20 h in aluminium bowls. The average of the weight difference before and after heating for the three replicates was thus equal to the initial water content of each bentonite powder batch. The amount of bentonite (m_{solids}) needed to obtain the planned wet density for each test cell was calculated using the following equation (from Karnland 2010).

$$m_{\text{solids}} = V_{\text{total}} \times \rho_m - m_{\text{max water}}$$

Where ρ_m is the saturated density, m_{solids} is the mass of the solids, $m_{\text{max water}}$ is the maximum possible mass of water, and V_{total} is the total volume of all components (solids and water). Grain densities were obtained from Karnland (2006). The analysed dry and wet densities agreed with calculated values ($\pm 1\%$).

Each test cell was assembled with a water saturation lid and a titanium filter and placed on an analytical scale where the calculated amounts of bentonite powder (m_{solids}) was weighed in. A water saturation piston was inserted in each test cell cylinder and in those cases where the bentonite powder volume was larger than the test cell volume (V_{total}) the bentonite powder was compacted with a workshop press ($<25 \text{ kg cm}^{-2}$) (Biltema, Göteborg, Sweden, cat no.15-846).



Figure 7-1. Components of a test cell for the diffusion and mobility of sulphide in Asha.

Water saturation of bentonite

After the water content determination of the bentonite clay the test cells were assembled with the top plate, force transducers, water saturation piston and the bottom lid and then mounted on a custom-built water saturation system (Figure 7-2). The system was alternately evacuated to < 10 Pa total pressure and filled with N_2 to remove all oxygen (O_2). When the system was anaerobic it was left evacuated and sterile anaerobic Analytical grade water (AGW), with or without sulphide and salts, was added to the system with 200 kPa total pressure. The AGW was delivered to the test cells by a pressure transmitting device consisting of a steel cylinder with a piston made of poly-ether-ether-ketone (PEEK). The piston was pressurized with nitrogen gas on the outer side of the piston. The inner side of the piston was filled with AGW under anaerobic conditions. All tubes and the pressure transmitter were sterilized in an autoclave at $121^\circ C$ for 20 minutes before use. The water saturation ended when the swelling pressure stabilized.

7.2.3 Influence of sulphide on bentonite clays during saturation

In this experiment the effect of sulphide on the swelling pressure capacity of the bentonite clays Asha, MX-80 and Calcigel at a wet density of 2000 kg m^{-3} was investigated. Four identical test cells were assembled for each bentonite as described in 7.2.2 and the load was registered. Each bentonite was compacted as described in 7.2.2. One test cell of each bentonite clay was used as a control and saturated with a salt solution (Table 7-1). The remaining three test cells of each bentonite clay were saturated with the salt solution containing sulphide. Three concentrations were chosen as described next to investigate the effect of sulphide on the swelling pressure.

Production of saturation solution

The saturation solution (Table 7-1) was produced anaerobe with an 80/20 % mixture of nitrogen (N₂) and carbon dioxide (CO₂). The pH of the saturation solution was adjusted to pH 7.2. Before the Na₂S crystals were added, 0.25 L of the saturation solution was transferred into an infusion flask as a control saturation solution. Additionally, 50 g L⁻¹ NaCl was added to this control saturation solution.

Afterwards 19 g L⁻¹ of Na₂S was added to the remaining 0.75 L of the saturation solution. The final sulphide concentration in the bentonite clays was ~20 μmol g⁻¹. A sample was taken and the sulphide concentration and pH were measured. The pH needed to be lowered with 0.072 L, 1.2 M HCl to pH 6.9. Afterwards 0.25 L was transferred in to an infusion flask. Then 75 g L⁻¹ Na₂S was added to the remaining saturation solution (0.5 L). The final sulphide concentration in the bentonite clays was respectively ~50 μmol g⁻¹. The concentration and pH were controlled as before and 0.14 L, 1.2 M HCl was added to lower the pH to 7.4. Afterwards 0.25 L was transferred in to an infusion flask. At last 15 g L⁻¹ Na₂S was added to the remaining saturation solution (0.25 L). The final sulphide concentration in the bentonite clays was respectively ~120 μmol g⁻¹. The concentration and pH were controlled as before and 0.078 L, 2.77 M HCl was added to set the pH to 7.3. Then 0.25 L were transferred in to an infusion flask. The saturation solutions were transferred into steel cylinder inside an anaerobic box with an atmosphere consisting of 97 % N₂ and 3 % H₂, O₂ < 1 ppm (COY Laboratory Products, Grass Lake, MI, USA).

Table 7-1. Salt solution for saturation of bentonite clays.

Addition	Amount
Analytical grade water (mL)	1000
NaCl (g L ⁻¹)	7.0
CaCl ₂ × 2H ₂ O (g L ⁻¹)	1.0
KCl (g L ⁻¹)	0.67
NH ₄ Cl (g L ⁻¹)	1.0
KH ₂ PO ₄ (g L ⁻¹)	0.15
MgCl ₂ × 6H ₂ O (g L ⁻¹)	0.5
NaHCO ₃ -lösning (mL L ⁻¹)	60
Na ₂ S (g L ⁻¹)	See 0

Saturation of bentonite

After compaction of the bentonite the test cells were assembled and mounted on a custom-built saturation system (Figure 7-2). The system was evacuated to < 10 Pa total pressure and filled with N₂ to remove all oxygen (O₂). When the system was anaerobic it was left evacuated. The saturation solutions were delivered to the test cells by a pressure transmitting device consisting of a steel cylinder with a piston made of poly-ether-ether-ketone (PEEK). The piston was pressurized with N₂ gas on the outer side of the piston. All tubes and the pressure transmitter were sterilized in an autoclave at 121 °C for 20 minutes before use. The pressures created by the swelling bentonites were monitored and the test cells were kept unaltered until the end of the experiment. Water could move freely in and out of the bentonite during the saturation.



Figure 7-2. Principal lay-out of the saturation system with mounted test cells used in preceding experiments with radiotracers, receiving the saturation salt solution from both top and bottom.

Sampling of bentonite clays from the test cells

The test cells saturated with $\sim 50 \mu\text{mol}$ sulphide g^{-1} clay were sampled. For the estimation of sulphide, samples were taken for two series in duplicates from three different positions, in total 12 samples. For the ferrous iron content duplicates were taken from three different positions. For the estimation of ferrous iron samples were taken in duplicates from three different positions, in total 6 samples.

Test cell preparations

The pressure logging in the force transducer software was stopped and the test cells were decoupled from the saturation system. Then the force transducer and the spacers were removed and the screws on the top lid were exchanged through shorter screws. Then the whole test cell was transferred in to an anaerobic box with an atmosphere consisting of 97 % N_2 and 3 % H_2 , $\text{O}_2 < 1$ ppm (COY Laboratory Products, Grass Lake, MI, USA). The top lid was then attached again, however with shorter screws to be able to push the piston all the way to the bottom. Afterwards the water saturation lid was removed, and the piston was pressed up by turning the screws. The appearance of the bentonite clays core was photo documented.

Samples for the water content and pore water analyses

For the estimation of the pore water the test cell without saturation lid was weighed with the saturated bentonite clay and without it. For the estimation of the water content three 50 mL Falcon tubes were weighed. 1 g from each position was transferred to the three Falcon tubes. Then the Falcon tubes were weighed again with the samples.

Samples for sulphide, ferrous iron and sulphur analyses

Samples for all analyses were taken from three positions. The first position was the bottom of the test cell (water saturation bottom lid), the second and third positions were 7 mm and 14 mm measured from the bottom towards the top of the saturated clay core. Figure 7-3 shows an overview of sampling and analyses handling. The samples (1 g wet weight each) were transferred to 50 mL serum bottles.

Afterwards 18 mL deoxygenated AGW was added to each sample and sealed with a blue rubber plug. The samples shook overnight in the anaerobe box. Next day the samples were taken out of the anaerobic box and 2 mL of a citric acid/Na₂HPO₄ buffer pH 2.6 (see 0) was added to all samples (see Figure 7-3). In one series of sulphide analyses the pH was further lowered to pH 1 with 1 mL 5 M HCl (see Figure 7-3). Afterwards the samples were incubated at room temperature for 24 hours. Then the sulphide and ferrous iron content was analysed. After the sulphide analyses the samples were prepared and analysed for sulphur.

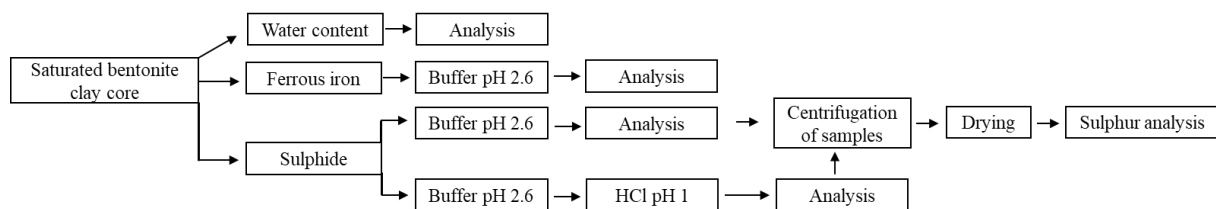


Figure 7-3 Influence of sulphide on bentonite clays during saturation: Schematic overview of samples and analyses.

7.2.4 Influence of bacterial produced sulphide on the swelling pressure capacity of Asha

In this experiment the effect of bacterial produced sulphide on swelling pressure of Asha was examined. Asha was compacted and saturated to a wet density of 1750 kg m⁻³ and 2000 kg m⁻³ under various conditions (see Table 7-2). Identical test cells (TC) were assembled as described in 7.2.2 and the load was registered. The saturation solution was identical to the previous experiment. However, in some test cells lactate was added as a carbon source to induce bacterial activity. The bacterial survival in the bentonite was analysed through the most probable number (MPN) approach. Furthermore, were the sulphate, lactate and acetate concentrations in the saturated bentonite clay cores analysed. Finally, the bentonite clay was analysed for sulphide, ferrous iron and sulphur to investigate the effect of bacterial produced sulphide on the clay chemistry.

Table 7-2. Experimental parameters for each test cell.

Name	Aimed density	Saturation medium	Spiked
TC 17	2000 kg m ⁻³	Salt solution (Table 7-1)	No
TC 18	2000 kg m ⁻³	AGW	No
TC 19	1750 kg m ⁻³	Salt solution + Lactate	Yes
TC 20	2000 kg m ⁻³	Salt solution + Lactate	Yes
TC 21	1750 kg m ⁻³	Salt solution + Lactate	No
TC 22	2000 kg m ⁻³	Salt solution + Lactate	No

Spiking bentonite clay

Desulfovibrio aespoeensis (DSM 10631), *Desulfotomaculum nigrificans* (DSM 574) and *Desulfosporosinus orientis* (DSM 765) were used to spike the bentonite clay Asha with SPB species in this work. *D. aespoeensis* was isolated from deep groundwater (Motamedi and Pedersen 1998), *D. nigrificans* is a mesophilic, spore-forming sulphide-producing bacterium and *D. orientis* is a spore-forming sulphide-producing bacterium with the ability to grow with Hydrogen (H₂) as source of energy. The bacteria were grown in appropriate media and temperatures as specified by the German collection of microorganisms and cell cultures (DSMZ). Bacterial numbers for each of the three bacterial cultures were determined in 1 mL samples using the acridine orange direct count method as devised by Hobbie et al. (1977) and modified by Pedersen and Ekendahl (1990).

The three different bacterial cultures were mixed into one cocktail and poured out on a bed of Asha bentonite powder in a large glass Petri dish. The whole content of the Petri dish was then passed through a mesh. The Asha bentonite had a bacterial content of approximately 1×10^7 SPB g⁻¹. This bentonite clay is referred to as “spiked”. All the work was performed inside of an anaerobic box with an atmosphere consisting of 97 % N₂ and 3 % H₂, O₂ < 1 ppm (COY Laboratory Products, Grass Lake, MI, USA).

Saturation of bentonite

The composition of the salt solution was as described in Table 7-1 but the salt solution for TC19 – 22 additionally contained 0.028 M lactate (Table 7-2).

Sampling of bentonite clay from test cells

The sampling positions were as before. The first position was the bottom of the test cell (water saturation bottom lid), the second and third positions were 7 mm and 14 mm measured from the bottom towards the top of the saturated clay core. Figure 7-3 shows an overview of sampling and analyses handling.

Samples for the water content and pore water

For the estimation of the amount of pore water the test cell without saturation lid was weighed with the saturated bentonite clay and without it.

For the estimation of the water content three 50 mL Falcon tubes were weighed. 1 g from each position was transferred to the three Falcon tubes. Then the Falcon tubes were weighed again with the samples. The estimation of the water content and pore water is described in 7.2.5.

Samples for sulphide, ferrous iron and sulphur

For the estimation of the sulphide, ferrous iron and sulphur content, 1 g of sample was taken from each position. The bentonite clay samples were transferred into 50 mL serum bottles. Afterwards 18 mL deoxygenated AGW was added to each sample to dissolve the bentonite. Then the serum bottles were sealed with blue rubber plugs. The samples were shaken overnight in the anaerobe box. After 24 h the samples were taken out of the anaerobic box and 2 mL of a citric acid/ Na₂HPO₄ buffer pH 2.6 (see Table 7-3) as added to all samples. Then the pH was further decreased to 1 through addition of 1 mL 5 M HCl. The samples were incubated at room temperature for 24 hours. Then the sulphide and ferrous iron content was analysed in the same serum bottle as described in in 7.2.5. After the sulphide analyses the samples were prepared and analysed for sulphur.

Samples for sulphate, lactate and acetate analyses

For the estimation of the sulphate, lactate and acetate content, 1 g from each position was transferred into a 50 mL Falcon tube. The sample was dissolved in 20 mL sterile AGW by shaking for 2 hours. Afterwards the samples were centrifuged for 15 min at $4000 \times g$. The supernatant was transferred into a new 50 mL Falcon tube and analysed for sulphate, lactate and acetate.

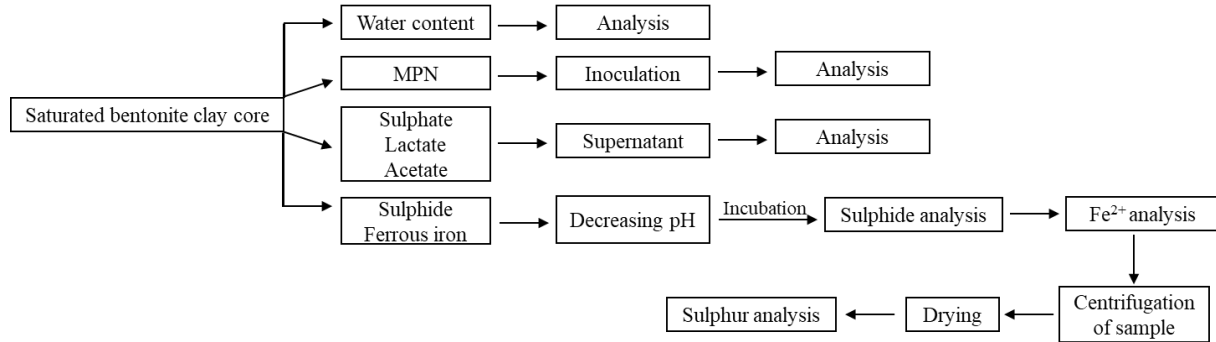


Figure 7-4. Influence of bacterial produced sulphide on the swelling pressure capacity of Asha: Schematic overview of samples and analyses.

7.2.5 Analyses

Estimation of the water content and pore water

The water content samples were dried for 20 hours at 105 °C. The average of the weight difference before and after heating for the three samples was equal to the water content of each saturated bentonite clay core.

$w = \text{water content of the clay (\%)}$

$clay_{wet} = \text{Weight of clay before drying (g)}$

$clay_{dry} = \text{Weight of dried clay (g)}$

$$w = \frac{clay_{wet} - clay_{dry}}{clay_{wet}} \times 100\%$$

The measured pore water was calculated as.

$w_{pore} = \text{pore water (mL)}$

$w = \text{water content of the clay (\%)}$

$gww = \text{Weight of saturated clay core (cm}^3\text{)}$

$$w_{pore} = \frac{w}{100} \times gww$$

pH adjustment

The pH was decreased to move the dissociation of sulphide species to volatile dissolved H₂S which could be purged from the serum bottles. A buffer was used to stabilise the pH because

purging the sulphide continuously consumes protons when $\text{HS}^- + \text{H}^+$ form H_2S and concomitantly increases the pH.

Sulphide that precipitated due to abiotic processes was later possible to analyse through method development. The pH was further decreased (pH \sim 1) with buffer and then additionally HCl to dissolve acid-extractable sulphide from iron sulphide.

Table 7-3 Buffer concentrations for experiment 6-9 and 11.

pH	Citric acid ^a concentration in buffer (M)	Na_2HPO_4 ^b concentration in buffer(M)
2.6	0.446	0.108

a 1 M stock solution

b 2 M stock solution

Sulphide analysis

The samples in the serum bottles were gas-flushed with N_2 for 30 minutes for the analysis of dissolved sulphide and acid-extractable sulphide from iron sulphide. Hydrogen sulphide gas was driven off into serum bottles with 0.02 M Zink acetate (ZnAc) and precipitated as zinc sulphide (ZnS), as shown in Figure 7-5.

The ZnS was analysed using the colorimetric methylene blue method in which samples containing S^{2-} will receive a blue colour (Swedish standard Method SIS 028115). The method uncertainty is $\pm 17\%$. Reducing agents, such as iron, can affect the analysis by decreasing the colour formation or to completely inhibit it.

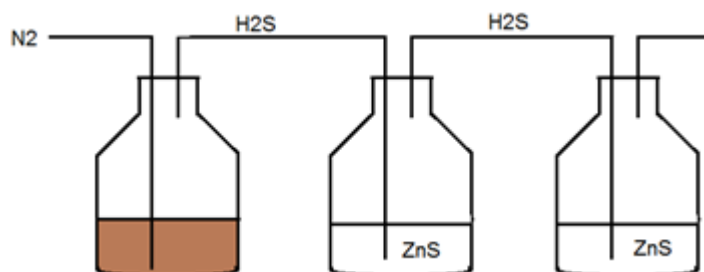


Figure 7-5. Experimental set up to drive off the H_2S gas for the sulphide analysis from bentonite clay samples.

Ferrous iron analysis with 1,10-phenanthroline

The ferrous iron concentration was analysed using the HACH method no. 8146 and measured on a HACH DR/2500 Odyssey (Hach Lange AB, Sköndal, Sweden) spectrophotometer. Samples that contained Fe^{2+} became orange because Fe^{2+} complexed with 1,10-phenanthroline. The method can only measure free Fe^{2+} and will not react with FeS or other minerals.

Sulphur analysis

The dissolved bentonite clay was after the sulphide analysis centrifuged in 50 mL Falcon tubes at 10.000 rpm for 15 minutes. The supernatant was decanted, and the bentonite clay was dried at 60 °C for 24 hours.

The dried bentonite clay was weighed into GC-vials. 500 μL carbon disulphide (CS_2) was added and the GC vial were shaken. Afterwards they were incubated for 24 hours at room temperature.

The liquid phase was transferred into a new GC-vial and again 500 μL were added to the bentonite clay. After sedimentation of the bentonite clay the liquid phase was transferred to the GC-vial of the first extraction. The volume was adjusted to 1 mL by adding CS_2 . The GC-vial were then analysed with GC-MS.

Sulphate, lactate and acetate analysis

The sulphate concentrations were determined using the turbidimetric SulfaVer4 BaSO_4 precipitation method (Method #8051, range 2 – 70 mg L^{-1} , HACH Lange, Sköndal, Sweden). Acetate and lactate concentrations were determined with the enzymatic UV method (kit no. 10148261035 for acetate and kit no. 10139084035, for lactate; Boehringer Mannheim/R-Biopharm AG, Darmstadt, Germany) using a Genesys 10UV spectrophotometer (Thermo Fisher Scientific) for detection. The analyses were tested on two clays with increasing amounts of added lactate or acetate.

Most probable number (MPN)

Samples for MPN-analysis were transferred to the anaerobic box with an atmosphere consisting of 97 % N_2 and 3 % H_2 , $\text{O}_2 < 1$ ppm. The bentonite was dissolved with 20 mL sterile anaerobic 0.9 % NaCl solution and then put on a shaker to disperse the bentonite. After the bentonite was dispersed (>2 hours) the samples were inoculated in five tubes for each of total two 10-time dilutions, resulting in an approximate 95% confidence interval lower limit of 1/3 of the obtained value and an upper limit of three times the value (Greenberg 1992). The cultivation tubes were previously filled with 9 mL anaerobic SPB growth medium, mixed as described by Widdel and Bak (1992) for preparing anoxic media and modified as described elsewhere (Pedersen et al. 2008). The MPN samples were cultured in 30 °C for four weeks before analysis. SPB were detected by measuring sulphide production using the CuSO_4 method according to Widdel and Bak (1992) on a UV visible spectrophotometer (Genesys UV 10, Thermo Electron Corporation).

7.2.6 Data processing, graphics and statistics

Data processing, statistical analyses and data visualizations were performed using Microsoft Office Excel 2016 (Microsoft Corporation, Redmond, USA) and Statsoft Statistica v 13 (Statsoft, Tulsa, USA) software.

7.3 Results

7.3.1 Influence of sulphide on bentonite clays during saturation

Density and swelling pressure

The water content of the saturated bentonite clays was analysed to ensure that the aimed wet density of 2000 kg m^{-3} was reached. The aimed wet densities were reached (data not shown). Figure 7-6 to Figure 7-8 show the swelling pressure registered by force transducers throughout the saturation of the bentonite clays.

Asha control decreased in pressure for 56 days, then stabilised until day 76 and decreased again until it stabilised around 1000 kPa. The test cells with sulphide in the saturation solution decreased until day 33 and then stabilised at different swelling pressure. The lowest concentration of sulphide produced the lowest swelling pressure, the medium concentration of sulphide ($\sim 50 \mu\text{mol g}^{-1}$) produced the highest swelling pressure and the highest concentration of sulphide was in-between. Indicating no direct correlation between sulphide concentration and swelling pressure for Asha. . However, difficulties producing stable swelling pressures with the Asha

bentonite were repeatedly encountered (Bengtsson and Pedersen 2017). The reasons are not clear at present. Other bentonite clays studied with our experimental set-up generally reproduce expected swelling pressure much better.

The Calcigel test cells showed only small variations in swelling pressures. Calcigel control stabilised at 1350 kPa after 36 days, the low sulphide concentration at 1400 kPa after 64 days, the medium sulphide concentration at 1350 kPa after 36 days and the high sulphide concentration at 1250 kPa after 36 days.

The MX-80 control test cell experienced a sudden loss in pressure at start for unclear reasons, it was expected to reach >2000 kPa. MX-80 control swelling pressure increased from ~600 kPa to 1500 kPa after a few days, then it rapidly fell and stabilised at ~900 kPa. Test cells with sulphide in the saturation solution showed an increase in swelling pressure. The lowest concentration of sulphide produced the highest swelling pressure. The highest concentration of sulphide produced the lowest swelling of the three sulphide concentrations.

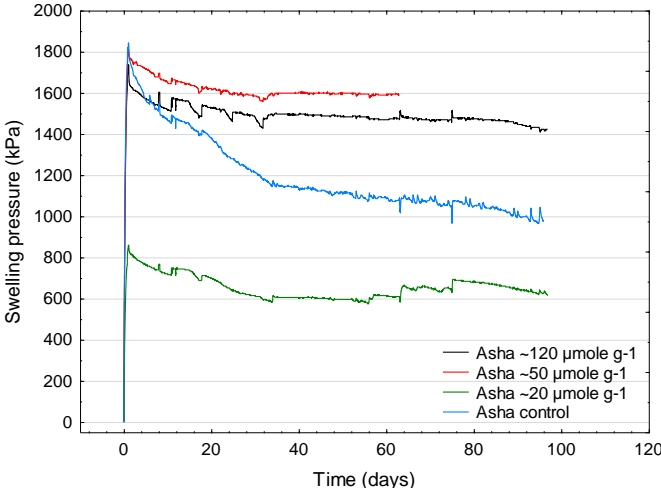


Figure 7-6. Pressure registered by force transducers for compacted Asha bentonite clay with a wet density of 2000 kg m^{-3} , during saturation with different sulphide concentrations.

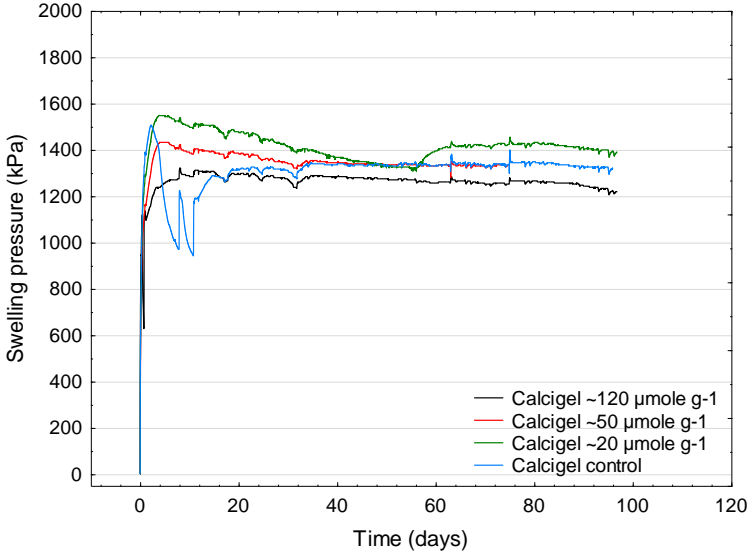


Figure 7-7. Pressure registered by force transducers for compacted Calcigel bentonite clay with a wet density of 2000 kg m^{-3} , during saturation with different sulphide concentrations.

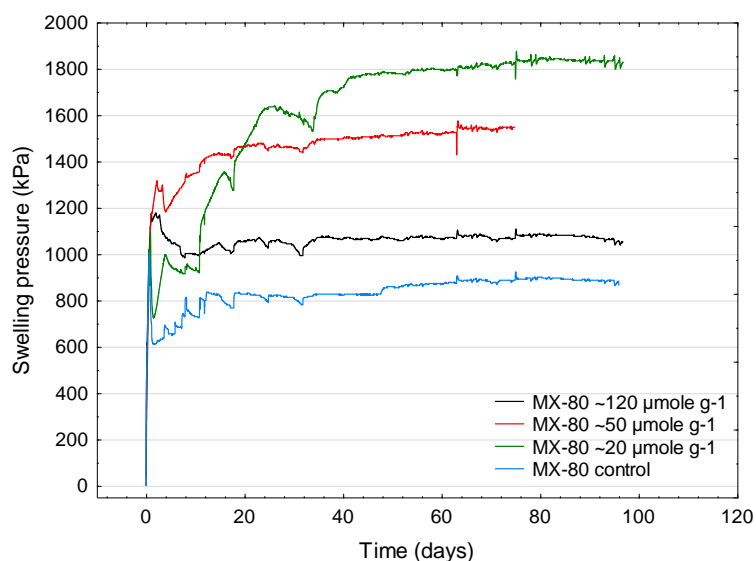


Figure 7-8. Pressure registered by force transducers for compacted MX-80 bentonite clay with a wet density of 2000 kg m^{-3} , during saturation with different sulphide concentrations. The MX-80 control test cell experienced a sudden loss in pressure at start for unclear reasons, it was expected to reach $>2000 \text{ kPa}$.

Analysed sulphide, -sulphur, -ferrous iron and immobilised sulphide

The abiotic immobilisation processes lead to the oxidation of sulphide to sulphur and is referred to as immobilisation of sulphide. Therefore, the difference between added sulphide and analysed sulphide is referred to as H_2S immobilised (Table 7-4). Samples with concentrations $<1 \mu\text{mol g}^{-1}$ were neglected.

Table 7-4 summarizes the results of the analyses of sulphide, ferrous iron and sulphur. The three bentonite clays had different concentrations of added sulphide because the amount of pore water was different in the clays, although the saturation solution had the same Na_2S concentration.

The analyses for Asha showed that sulphide was only detected at position 2 in samples with buffer and HCl treatment (Figure 7-9, left). Sulphur was found at position 1 (pH 2.6) and position 2 (pH1) (Figure 7-10, left).

The analyses for Calcigel showed that sulphide was detected at position 1 at both pH (Figure 7-11, left). Figure 7-12 (left) shows that sulphide was present at the positions 1 and 3 at both pH.

The analyses for MX-80 showed that sulphide was detected at position 1 for pH 2.6 and position 1 and 3 for pH 1 (Figure 7-13, left). Figure 7-14 (left) shows that sulphur was found at position 1 and 3 for both pH.

Over all the ferrous iron concentrations were similar at all three positions in each analysed bentonite clay (Figure 7-10, Figure 7-12 and Figure 7-14, right figures)

A black colouration was noticed in every clay at the bottom and top which increased with increasing sulphide concentration in the saturation solution (Figure 6-1). The rest of the clay cores, showed the ambient coloration of the bentonite clays.

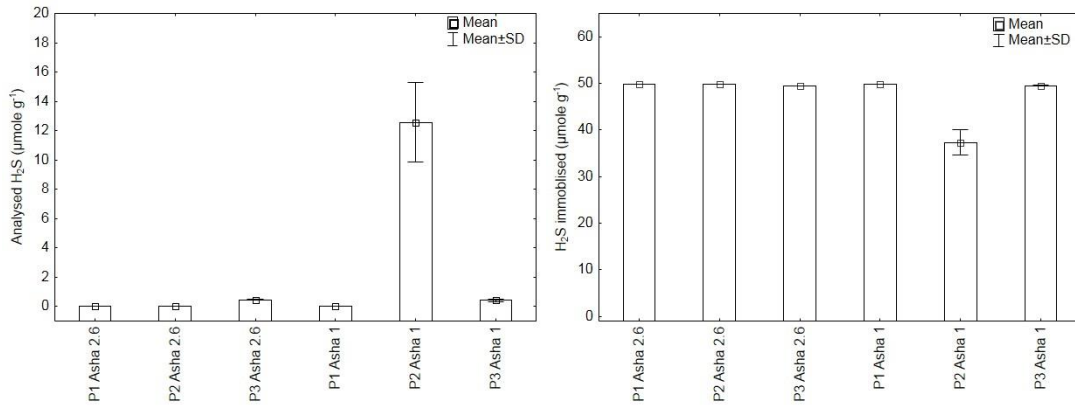


Figure 7-9. The analysed sulphide concentrations (left figure) and the immobilised sulphide concentrations (right figure) for the three analysed positions of the saturated Asha bentonite clay core.

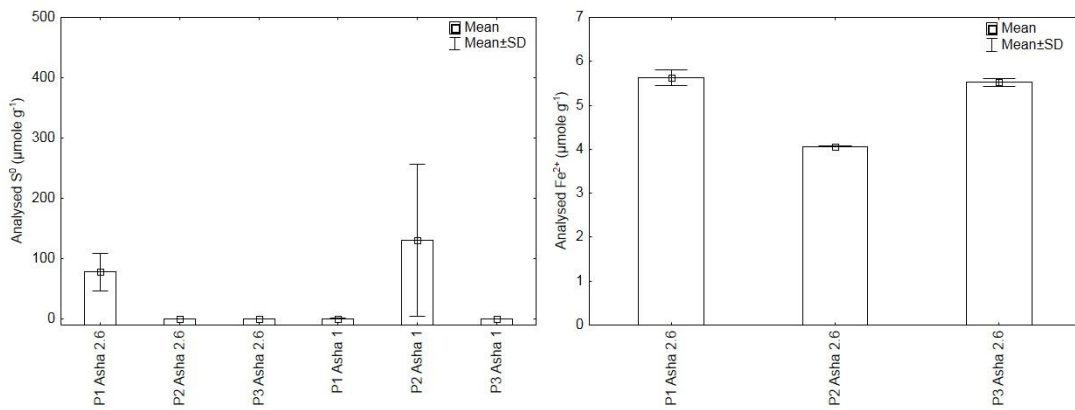


Figure 7-10. The analysed sulphur concentrations (left figure) and the analysed Fe²⁺ concentrations (right figure) for the three analysed positions of the saturated Asha bentonite clay core.

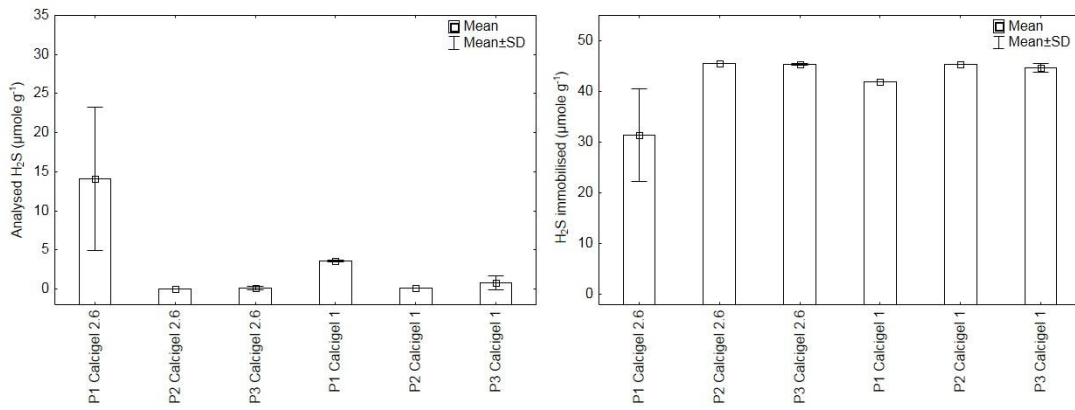


Figure 7-11. The analysed sulphide concentrations (left figure) and the immobilised sulphide concentrations (right figure) for the three analysed positions of the saturated Calcigel bentonite clay core.

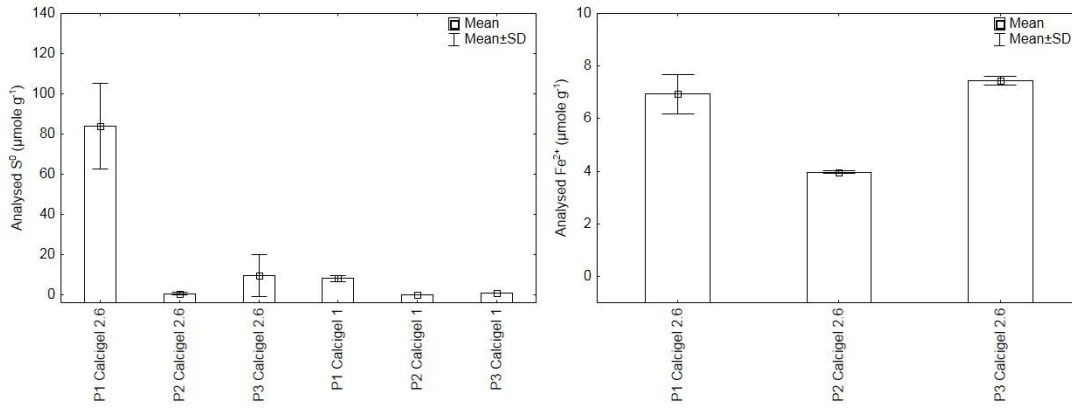


Figure 7-12. The analysed sulphur concentrations (left figure) and the analysed Fe²⁺ concentrations (right figure) for the three analysed positions of the saturated Calcigel bentonite clay core.

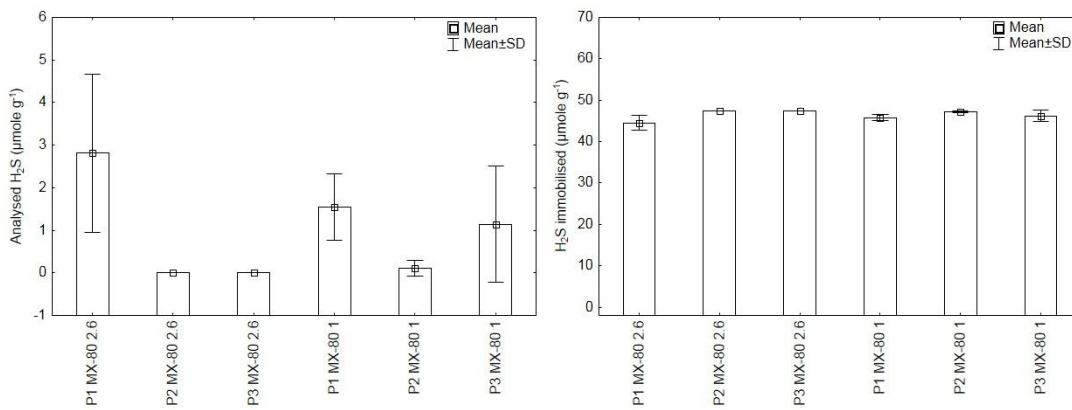


Figure 7-13. The analysed sulphide concentrations (left figure) and the immobilised sulphide concentrations (right figure) for the three analysed positions of the saturated MX-80 bentonite clay core.

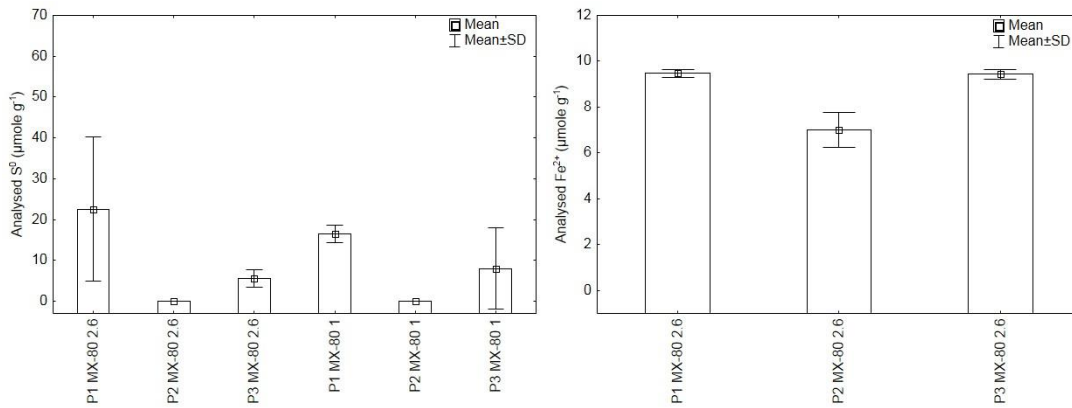


Figure 7-14. The analysed sulphur concentrations (left figure) and the analysed Fe²⁺ concentrations (right figure) for the three analysed positions of the saturated MX-80 bentonite clay core.

7.3.2 Influence of bacterially produced sulphide on the swelling pressure capacity of Asha

Density and swelling pressure

The water contents of the saturated bentonite clays were analysed to ensure that the aimed densities of 1750 kg m⁻³ and 2000 kg m⁻³ were reached. After 250 days of saturation the aimed densities were reached (data not shown).

Figure 7-15 shows that the pressure curves for TC19 and 21 stabilized at around ~300 kPa and for TC17 and 20 at around ~3000 kPa. Further, the pressure curve for TC22 stabilized at around ~4200 kPa. Moreover, the pressure curve of TC18 decreased from ~3000 kPa and stabilized at around ~800 kPa, there might have been a problem with the force transducer in TC18 or it was an effect from the AGW without ionic strength.

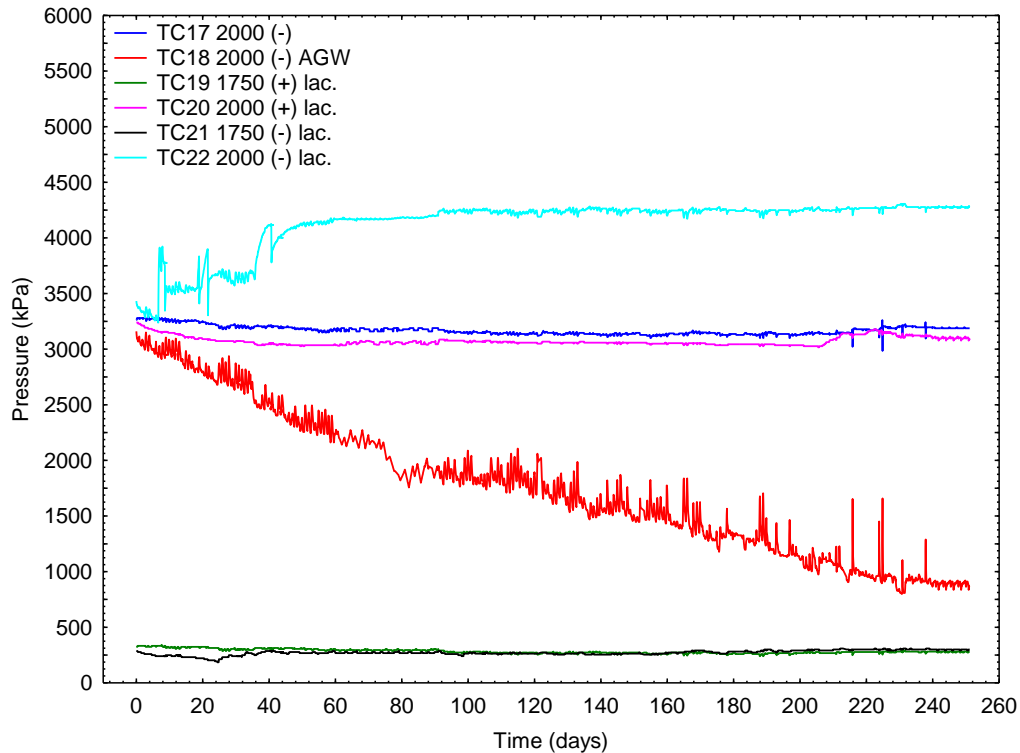


Figure 7-15. Pressure curves for each test cell with Asha bentonite during the saturation time (0 – ~250 days). The key shows test cell number, bentonite density, addition of bacteria (+/-), AGW as saturation medium and addition of lactate (lac.).

MPN-samples

The MPN-samples results showed if added or innate SPB survived in the bentonite clays during incubation. Figure 7-16 shows that viable SPB could be cultivated from all test cells. The TC17 and 18 showed the lowest numbers of viable SPB and the number decreased from position 1 to 3 in both test cells (Figure 7-16 and Table 7-5). Furthermore, TC19 showed overall the highest numbers of viable SPB. In addition, test cells with a density of 2000 kg m⁻³ showed in general lower numbers of viable SPB than test cells with a density of 1750 kg m⁻³. Overall the MPN-analyses showed large deviation between the three sampled positions, except for TC19.

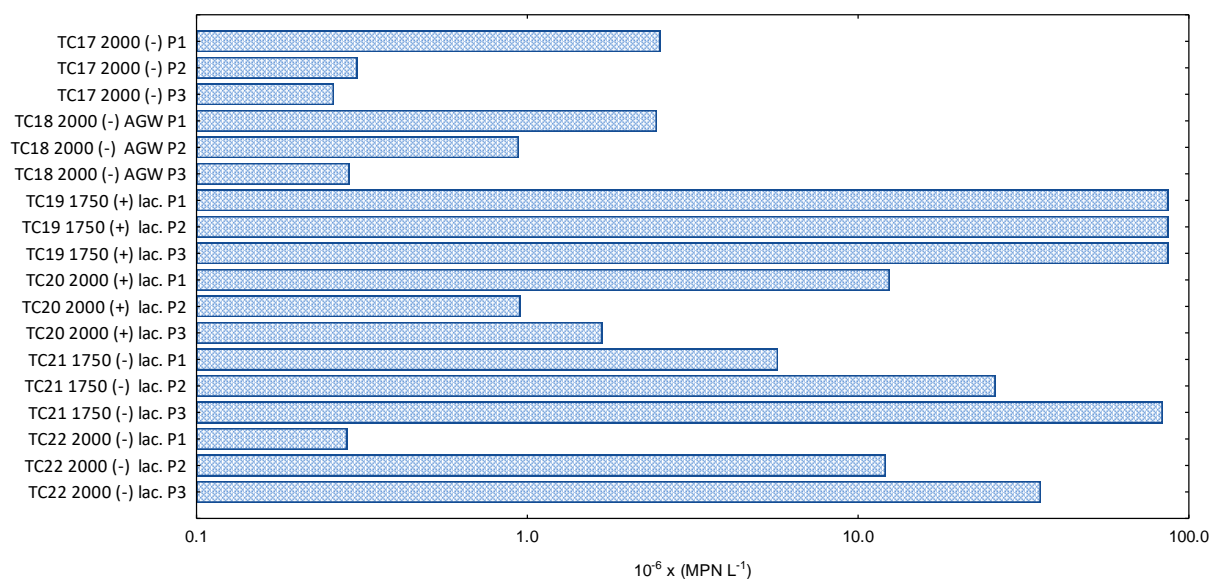


Figure 7-16. Most probable numbers of sulphide producing bacteria in pore water at three positions in bentonite cores of each test cell. The names indicate test cell number, bentonite density, addition of bacteria (+/-), AGW as saturation medium, addition of lactate (lac.) and position (P).

Concentration of sulphate, lactate and acetate

Asha contains naturally leachable sulphate which can be reduced to sulphide by SPB. Table 7-6 shows the average sulphate concentrations ranged from 31 – 58 $\mu\text{mol gdw}^{-1}$ for the analysed position of the test cells. The TC19 to 22 had larger deviations in sulphate concentrations between the sampled positions than TC17 and 18 (Figure 7-17 and Table 7-6).

Table 7-6 shows that lactate was only found at all three sampled positions in TC20. Lactate was detected at one position in TC19 and 22. In TC21 lactate was under the detection limit.

Figure 7-18 shows that acetate was detected in TC19 to 22. TC22 had the highest average with 5.5 $\mu\text{mol gdw}^{-1}$ (Table 7-6). Overall the acetate concentrations were similar between the test cells.

TC17 and 18 were absent of lactate and acetate.

Concentrations of sulphide, ferrous iron and sulphur

Sulphide was not detected in any test cell at any sampling position (data not shown).

Figure 7-19 shows that ferrous iron was found in all test cells. TC19 to TC22 showed similar amounts of ferrous iron while TC18 had only half the amount. TC17 more than 20 times less ferrous iron than TC19.

Table 7-6 shows that sulphur was present in all test cells however with large difference between the test cells and sample positions in the test cells. TC17 and 18 showed the lowest amounts of sulphur and TC22 the highest amount.

Figure 7-20 shows the Asha clay cores after incubation. In TC17, 19 and 21 a black colouration was noticed which is likely due to precipitation of FeS.

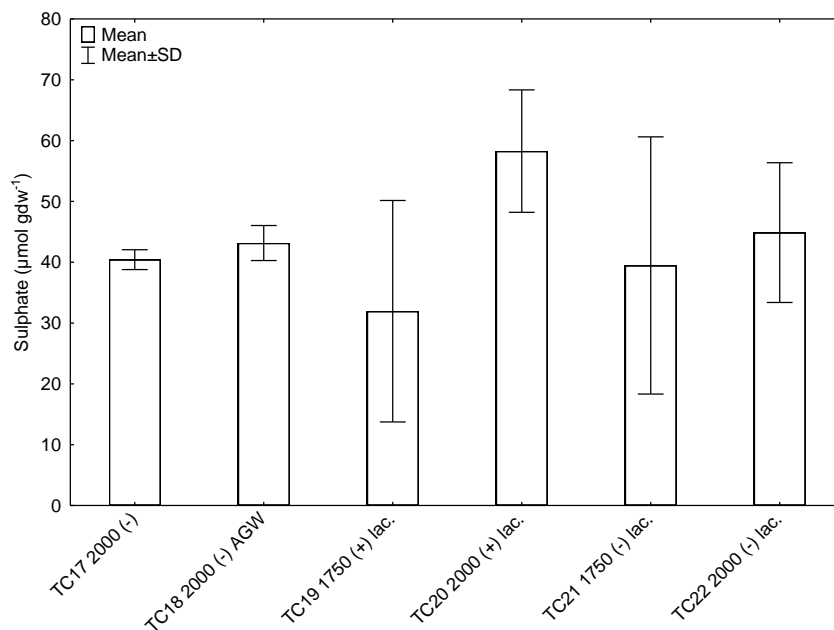


Figure 7-17. Concentration of sulphate in bentonite cores for each test cell. The names indicate test cell number, bentonite density, addition of bacteria (+/-), AGW as saturation medium and addition of lactate (lac.).

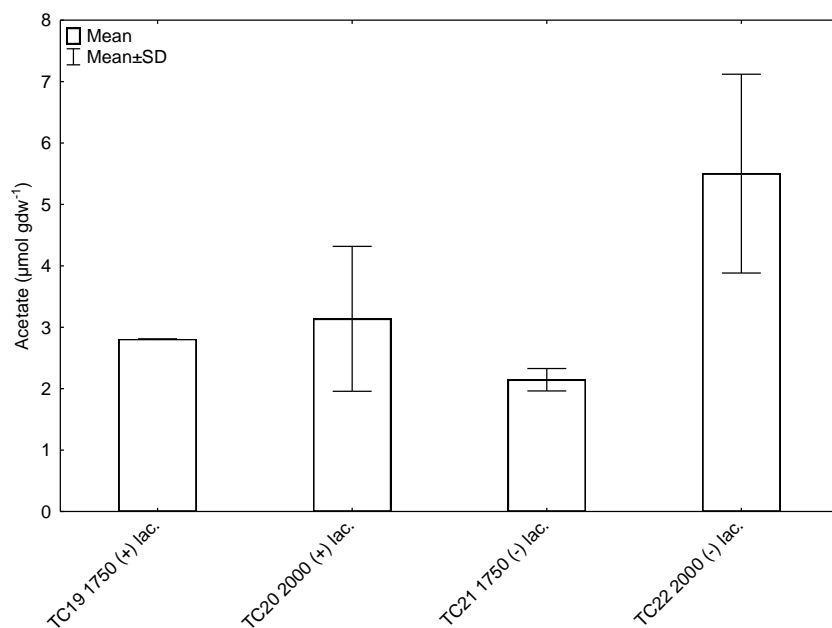


Figure 7-18. Concentration of acetate at three positions in bentonite cores for each test cell. The names indicate test cell number, bentonite density, addition of bacteria (+/-), AGW as saturation medium and addition of lactate (lac.).

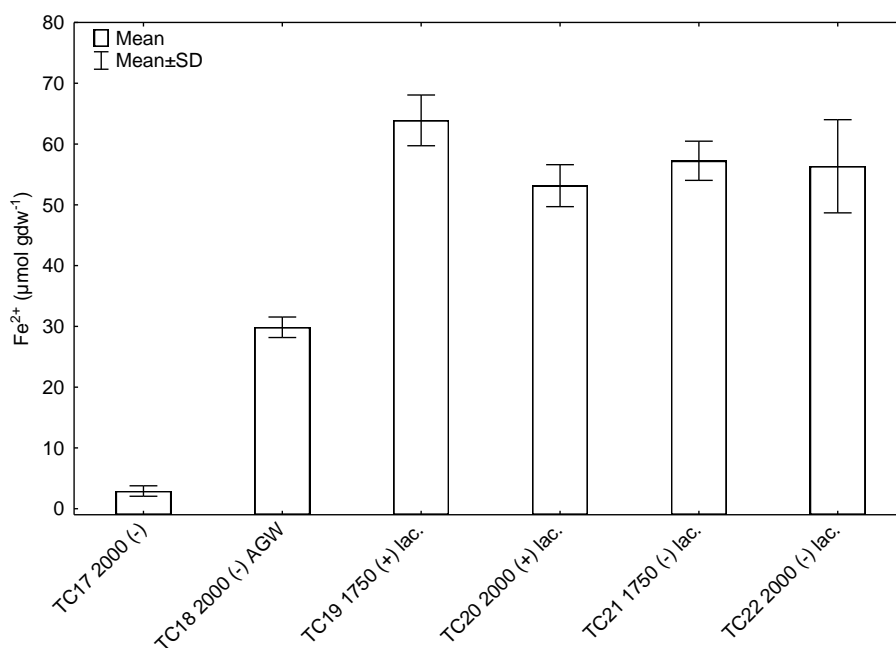


Figure 7-19. Concentration of Fe²⁺ at three positions in bentonite cores for each test cell. The names indicate test cell number, bentonite density, addition of bacteria (+/-), AGW as saturation medium and addition of lactate (lac.).

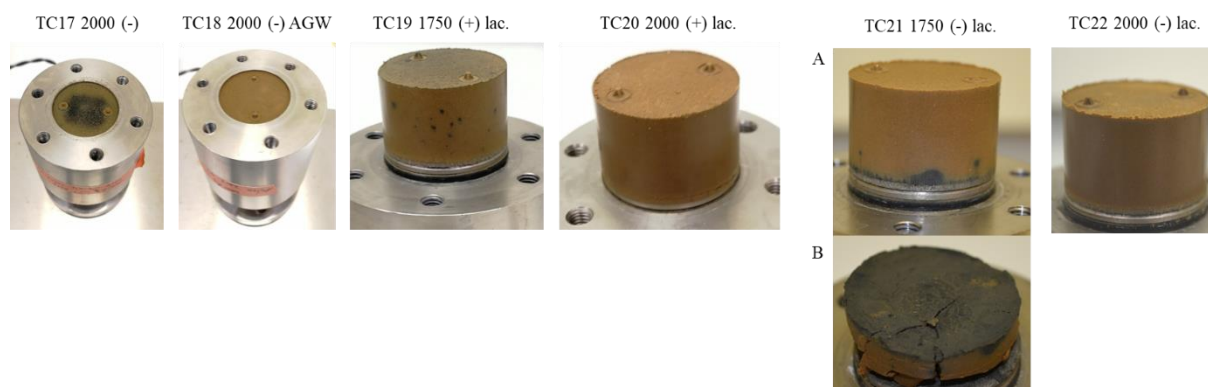


Figure 7-20. Pictures of Asha clay cores from each test during sampling after incubation. The names indicate test cell number, bentonite density, addition of bacteria (+/-), AGW as saturation medium and addition of lactate (lac.).

Acetate and lactate analysis

There was a very good agreement between added and analysed amounts of these compounds when added to Asha and Rokle bentonites (Figure 7-21 and Figure 7-22). The background values for lactate and acetate in clays without addition of lactate or acetate were ~0.1 and ~0.5 µmol gdw⁻¹, respectively. The background for acetate in GMZ was determined to 0.7 µmol gdw⁻¹.

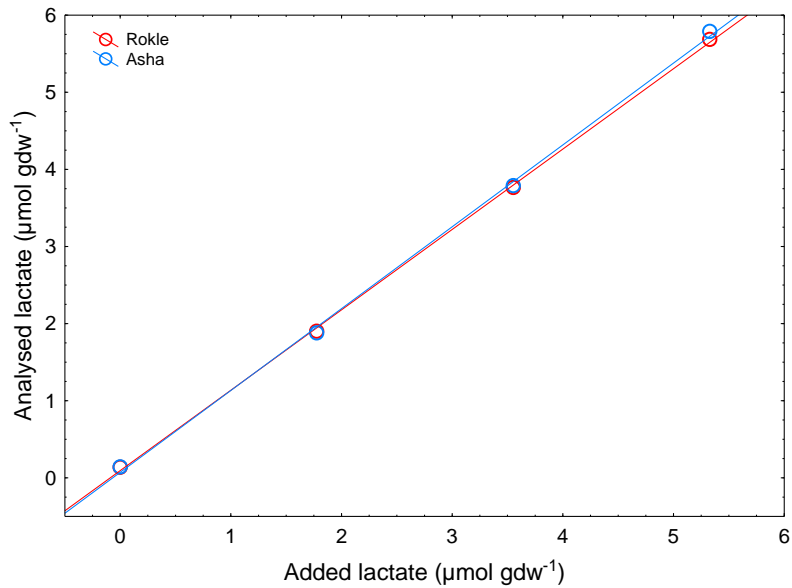


Figure 7-21. Added amounts of lactate to Rokle and Asha bentonite clays and the corresponding analysed amounts (Bengtsson et al. 2017b).

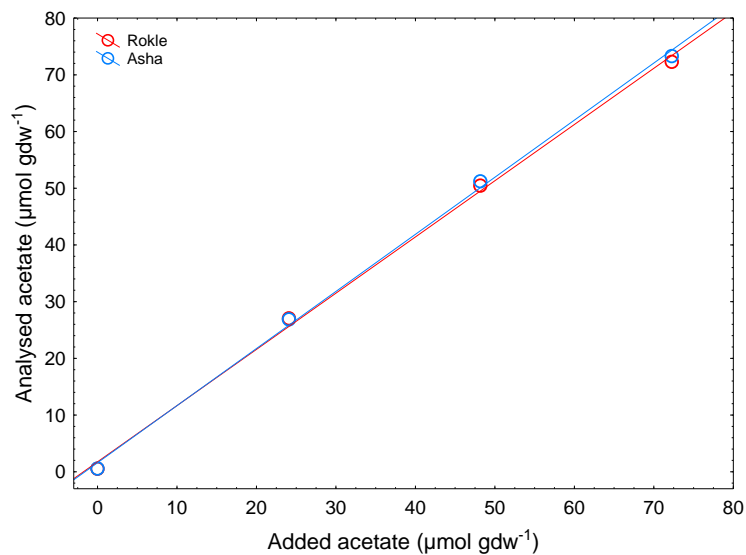


Figure 7-22. Added amounts of acetate to Rokle and Asha bentonite clays and the corresponding analysed amounts (Bengtsson et al. 2017b).

7.4 Discussion

7.4.1 Influence of sulphide on the swelling pressure of bentonite clays

In this experiment it was shown that sulphide can affect the swelling pressure depending on the bentonite clay. In Asha the swelling pressures from test cells with sulphide in the saturation solution differed from the control. However, there was no correlation between sulphide concentration and resulting swelling pressure. In MX-80 the lowest sulphide concentration produced the highest swelling pressure and the highest sulphide concentration the lowest swelling pressure. This indicates that the oxidation of sulphide to sulphur and concomitant with the reduction of a range of different ferric iron minerals to ferrous iron negatively affected the swelling pressure in MX-80. However, the swelling pressure in the control was even lower than in

test cells with sulphide in the saturation solution. In Calcigel the sulphide had little to no effect on the swelling pressure.

All bentonite clay cores showed a black colouration at the top and bottom. The layer increased with increasing amount of sulphide in the saturation solution. This indicates that sulphide formed FeS at these positions and therefore, H₂S and S⁰ were mainly found at P1 (bottom position). Asha was an exception because sulphide was only detected at P2 after the pH was lowered to 1 probably dissolving FeS and releasing sulphide for the analysis. It is to mention that P3 does not correspond with the top of the clay core. P3 was located approximately 7 mm before the top of the clay core. This explains why little to no sulphide was detected at P2. Together with the results from the diffusion experiment it shows that sulphide is immobilised to a certain extend at contact with bentonite clay preventing it from diffusing further into the clay. This effect is presumably advantageous for the repository because the sulphide might not reach the copper canister depending on the location of the sulphide source.

7.4.2 Influence of bacterial produced sulphide on the swelling pressure capacity of Asha

The influence of bacterial produced sulphide on the swelling properties of Asha was analysed with two different sources of SPB and at two densities. The test cell were either spiked with three different species of SPB or carried the inherent populations of SPB (non-spiked). The chosen SPB for spiking the bentonite covered representative of SPB with different capabilities to survive extreme conditions and grow in deep groundwater and bentonite. They have been identified in the buffer-rock interface in full scale experiments at Äspö HRL previously (Arlinger et al. 2013a). They are all incomplete oxidizers of lactate and with acetate as a end product. This allowed to validate bacterial activity by analysing acetate in the bentonite clays. SPB have been cultivated from bentonite which indicates that sporeforming bacetria are present in bentonites. However, little is known about the diversity and metabolic capabilities of the inherent SPB in bentonite clays (Bengtsson et al. 2017a). In the conducted experiments it is not possible to determine which SPB produced the sulphide in the test cells with spiked clay because inherent SPB were probably also present.

The results in this report show, as reported before, that the cultivability of SPB in compacted bentonite correlates negatively with increasing density and swelling pressure (Masurat et al. 2010b; Pedersen 2010; Pedersen et al. 2017a). Yet, the data is based on cultivation and there might be inherent SPB which cannot be cultivated with the used method but might contribute to sulphide production in the bentonite clay.

In addition, it shows that SPB survived in the bentonite clay and that they are naturally present. The MPN approach does not allow a direct conclusion of bacterial activity in the bentonite clay during incubation.

As in the previous experiment precipitated FeS was visible as black colouration in the lower density test cells. Bacterial produced sulphide and ferrous iron from the bentonite clay formed FeS by reduction of structural ferric iron in montmorillonite of Asha by sulphide. This process could be detrimental to the swelling capacity of bentonite clays. The swelling pressure of the test cell saturated with AGW decreased continuously and stabilized far lower than test cells with the same density. An explanation might be the lack of ions in the AGW and the resulting of diffusion of ions from the montmorillonite into the bentonite clay pore water which is detrimental for the swelling capacity.

TC22 showed a higher swelling pressure than other test cells with the same density (2000 kg m^{-3}) but was not spiked. However, the number of MPN was higher than in TC17 and TC20, although TC20 contained spiked Asha. Bengtsson et al. (2017a) also overserved that spiked Asha at 2000 kg m^{-3} has a lower swelling pressure in comparison to non-spiked Asha.

The first experiments with added sulphide showed effects on the swelling pressure depend on the bentonite clay and the sulphide concentrations. The SPB were not able to produce the same amount of sulphide during the incubation time as was used in the addition experiments. However, SPB produced sulphide might be a problem for the integrity of a SNF disposal canister in a long-time span of 100 000 years. The precipitated FeS in the bentonite cores was also an direct indicator of bacterial activity in the bentonite clay. The sulphide that reduced the ferrous iron could have only originated from bacterial metabolism. Another indicator of bacterial activity was acetate in the bentonite clay which stemmed from bacterial oxidation of the added lactate. It was expected that the acetate concentrations were lower and the lactate concentrations higher in test cells with a higher density due to the lower numbers of MPN. However the acetate concentrations were simliar in all test cells and lactate was almost absent in all test cells except TC20. An explanation could be that other microorganism in the clay oxidized the lactate to acetate explaining the discrepancy between MPN and lactate consumption and acetate production.

Furthermore, the sulphate concentration in the bentonite clay could indicate SPB activity. The reported concentration of leachable sulphate from raw, dry Asha is $38 \mu\text{mol g}^{-1}$ (Bengtsson et al. 2017a). Leachable sulphate concentrations ranged from $32 - 58 \mu\text{mol gdw}^{-1}$ and sulphide was absent in all test cells. This would indicate that SPB were not active during the incubation time. However, produced sulphide could have been reduced to sulphur and formed FeS as indicated by the black colouration in the lower density test cells. Sulphur was indeed detected in some test cells, but the concentrations did not correlate with the number of MPN. A reason might be that inherent SPB were active during the incubation but could not be cultivated trough the MPN approach.

7.5 Data

Table 7-4 Results of the sulphide analyses of the bentonite clay samples. P = position.

Sample name	pH control (HCl / Buffer)	H ₂ S _{Added} ($\mu\text{mol g}^{-1}$)	Average H ₂ S _{Analysed} ($\mu\text{mol g}^{-1}$)	SD	Average H ₂ S _{immobilised} ($\mu\text{mol g}^{-1}$)	SD	Average S ⁰ _{analysed} ($\mu\text{mol g}^{-1}$)	SD	Average Fe ²⁺ _{Analysed} ($\mu\text{mol g}^{-1}$)	SD
P1 Asha	Buffer	49.9	0.0	0.0	49.9	0	78	31.1	6	0
P2 Asha	Buffer	49.9	0.0	0.0	49.9	0	0	0	4	0
P3 Asha	Buffer	49.9	0.45	0.07	49.5	0.07	0	0	5.5	0.71
P1 Asha	Buffer and HCl	49.9	0.0	0.0	49.9	0	0.5	0.71	-	-
P2 Asha	Buffer and HCl	49.9	12.6	2.76	37.3	2.69	131	127	-	-
P3 Asha	Buffer and HCl	49.9	0.4	0.1	49.5	0.07	0	0	-	-
P1 Calcigel	Buffer	45.5	14.1	9.19	31.5	9.12	84	21.2	6.5	0.71
P2 Calcigel	Buffer	45.5	0.0	0.0	45.5	0	0.5	0.71	4	0
P3 Calcigel	Buffer	45.5	0.15	0.21	45.4	0.21	9.5	10.6	7.5	0.71
P1 Calcigel	Buffer and HCl	45.5	3.55	0.07	42.0	0.07	8	1.41	-	-
P2 Calcigel	Buffer and HCl	45.5	0.15	0.07	45.4	0	0	0	-	-
P3 Calcigel	Buffer and HCl	45.5	0.80	0.85	44.7	0.85	1	0	-	-
P1 MX-80	Buffer	47.3	2.8	1.84	44.5	1.84	22.5	17.7	9.5	0.71
P2 MX-80	Buffer	47.3	0.0	0.0	47.3	0	0	0	7	1.41
P3 MX-80	Buffer	47.3	0.0	0.0	47.3	0	5.5	2.12	9.5	0.71
P1 MX-80	Buffer and HCl	47.3	1.55	0.78	45.8	0.78	16.5	2.12	-	-
P2 MX-80	Buffer and HCl	47.3	0.10	0.14	47.3	0.21	0	0	-	-
P3 MX-80	Buffer and HCl	47.3	1.15	1.34	46.2	1.41	8	9.90	-	-

Table 7-5 Most probable numbers of SPB in pore water of Asha bentonite cores at three sample positions.

Test cell	P1		P2		P3	
	10 ⁻⁶ x (MPN L ⁻¹)	Lower – upper 95% confidence interval	10 ⁻⁶ x (MPN L ⁻¹)	Lower – upper 95% confidence interval	10 ⁻⁶ x (MPN L ⁻¹)	Lower – upper 95% confidence interval
TC17 2000 (-)	2.5	1.1 – 5.9	0.3	0.08 – 1.3	0.3	0.1 – 0.6
TC18 2000 (-) AGW	2.5	1.2 – 5.8	0.9	0.4 – 2.7	0.3	0.07 – 1.1
TC19 1750 (+) lac.	86	32 – 287	86	32 – 287	86	32 – 287
TC20 2000 (+) lac.	12	5.1 – 35	0.9	0.4 – 2.8	1.7	0.7 – 6.3
TC21 1750 (-) lac.	5.7	2.1 – 16	26	10 – 104	83	31 – 276
TC22 2000 (-) lac.	0.3	0.1 – 1.2	12	4.9 – 34	36	14 – 143

Table 7-6 Analysed concentration of sulphate, Fe²⁺, lactate and acetate at three positions in bentonite cores for each test cell.

Sample name	Sulphate (μmol gdw^{-1})	Average (μmol gdw^{-1})	SD	Lactate (μmol gdw^{-1})	Average (μmol gdw^{-1})	SD	Acetate (μmol gdw^{-1})	Average (μmol gdw^{-1})	SD	Fe ²⁺ (μmol gdw^{-1})	Average (μmol gdw^{-1})	SD	Sulphur (μmol gdw^{-1})	Average (μmol gdw^{-1})	SD
TC17 2000 (-) P1	39	40	1.6	0	0	0	0	0	0	3.3	2.9	0.9	0.05	0.02	0.03
TC17 2000 (-) P2	42			0			0			3.5			0.01		
TC17 2000 (-) P3	39			0			0			1.9			0		
TC18 2000 (-) AGW P1	40	43	2.9	0	0	0	0	0	0	28	30	1.7	0	0.05	0.08
TC18 2000 (-) AGW P2	46			0			0			32			0.1		
TC18 2000 (-) AGW P3	43			0			0			30			0		
TC19 1750 (+) lac. P1	23	32	18	0	0.5	0.8	2.8	2.8	0	59	64	4.2	6.7	4.6	3.4
TC19 1750 (+) lac. P2	53			0			2.8			65			0.7		
TC19 1750 (+) lac. P3	20			1.3			2.8			68			6.3		
TC20 2000 (+) lac. P1	49	58	10	1.9	2	0.4	1.9	3.1	1.2	53	53	3.4	0.8	1.6	0.8
TC20 2000 (+) lac. P2	57			1.7			3.2			50			2.4		
TC20 2000 (+) lac. P3	68			2.5			4.3			57			1.6		
TC21 1750 (-) lac. P1	54	40	21	0	0	0	2.2	2.1	0.2	59	57	3.2	0	1.8	2.4
TC21 1750 (-) lac. P2	49			0			1.9			53			1		
TC21 1750 (-) lac. P3	15			0			2.2			59			4.6		
TC22 2000 (-) lac. P1	49	45	11	0	0.4	0.6	4.8	5.5	1.6	53	56	7.7	49	45	11
TC22 2000 (-) lac. P2	53			1.1			4.3			65			54		
TC22 2000 (-) lac. P3	32			0			7.3			50			32		

8 Summary of factors influencing bacterial life in compacted bentonite

Bacterial life and survival, presence, viability and activity will depend on several different variables in a buffer or backfill that relate to the water saturation and swelling of bentonites compacted to high density. Consequently, it is not density *per se* that controls bacterial activity in compacted clays. Rather, other factors, that to some extent are related to the density and type of clay, control bacterial activity (Figure 8-1).

The pH of most bentonite clays is slightly alkaline but still well within the range of what most bacteria can tolerate. In radioactive waste repository concepts, the maximum surface temperature of canisters may not exceed 90 °C in order to avoid formation of steam when water comes in contact with the canister. It was previously found that heat treatment at 120 °C for 15 h (Masurat et al. 2010b) or 110 °C for 170 h (Bengtsson and Pedersen 2017) did fail to kill inherent bacteria in the bentonite. Heat was expected to be efficient, but that was still not enough to kill off sulphide producing bacteria in the bentonite because intensive sulphide-producing activity and large numbers of cultivable sulphide producing bacteria were observed in heat treated MX-80. Bentonite or rather montmorillonite, has a verified high affinity for water and the cell membrane of bacterial cells is water permeable. If a bacterial cell is surrounded by bentonite, it is possible that the water affinity of montmorillonite will extract water from the cell, leaving it in a desiccated state. The phenomenon of drying cells for prolonged storage is well known and commonly used in microbiology (Gherna 1994). Slow desiccation can yield higher viability, after prolonged storage, than can fast desiccation (Laroche and Gervais 2003; Potts 1994) and also increased heat resistance and viability for both spores and vegetative cells (Fine and Gervais 2005). Bacteria consequently have several mechanisms to survive prolonged periods of exposure to heat and desiccation. When water saturation of the clay starts, spores and desiccated cells can be activated and start to metabolize. Bacteria consequently have several mechanisms to survive prolonged periods of exposure to heat.

Transport of nutrients to, and metabolic products such as sulphide from bacteria will be diffusion limited due to the low porosity of buffers and backfill (See these references for data on sulphide diffusion Pedersen 2010; Pedersen et al. 2017b). Bacterial activity will, consequently, be diffusion limited in backfill and buffers when the bentonite buffer and backfill are fully water saturated. The only position not affected by diffusion barriers will be the interface between rock/aquifers/engineered disturbed zone and buffer and backfill.

The swelling pressure in the bentonite originates from separating flocs in the bentonite. This means that a mechanical pressure arises between the separating flocs, approximately equal to the swelling pressure. Even in low-density bentonites (1500 kg m^{-3}), a pore size in the nm range would theoretically not allow for bacterial existence unless the bacteria could withstand the mechanical pressure from the separating flocs (0.09 MPa at 1500 kg m^{-3}). Prokaryotic cells can compensate for the mechanical pressure in compacted bentonite by turgor pressure. Published data on turgor pressure in prokaryotic cells mention pressures between 0.08 MPa and 2 MPa (Potts 1994). An upper limit of 2 MPa turgor pressure would mean that cell integrity is possible, though limited, at bentonite swelling pressures below 2 MPa . Present results suggest a limit at approximately 1 MPa (Figure 5-5). However, endospores can survive a much higher pressure.

Water is needed for active bacterial life and this water must be present externally because bacteria (except spores) cannot keep water inside their cell membranes that are freely permeable for water.

Low water content in clays, a_w , will inactivate or kill bacteria (Motamedi et al. 1996; Potts 1994). However, as was discussed for temperature above, many bacteria survive desiccation and can be activated again when there is enough water.

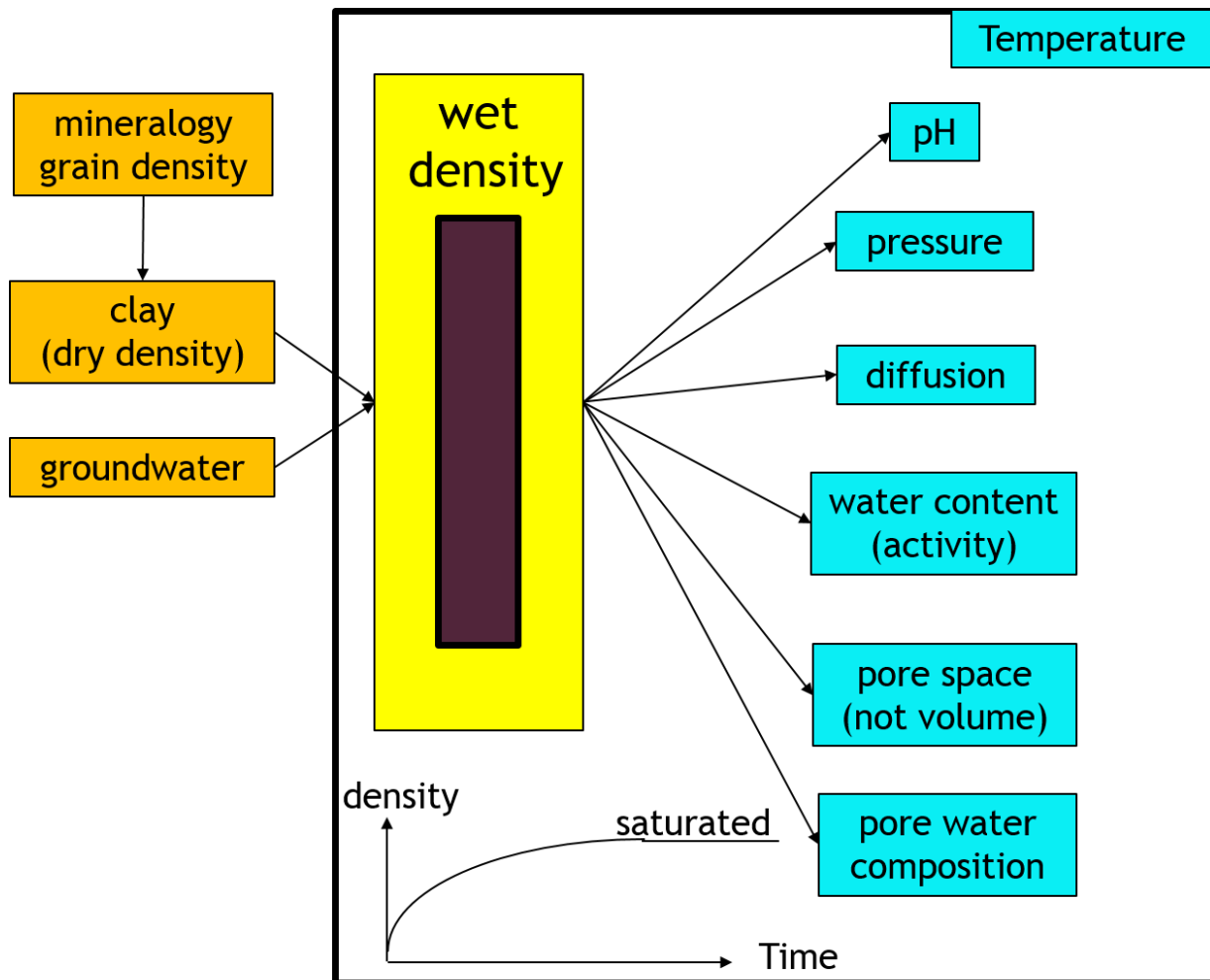


Figure 8-1. Variables influencing wet density, that upon water saturation give rise to suggested factors influencing bacterial viability, cultivability and activity (turquoise) except temperature, not coupled to wet density.

Bacteria are very small and if there are pores or other inhomogeneities in buffer and backfill with lower than planned pressures, local bacterial activity will be possible. In addition, there will be interfaces between rock engineered disturbed zone and bentonite and between bentonite and canisters at which pressures may differ from the bulk of buffer and backfill. Figure 8-2 and Figure 8-3 show that sulphide-producing bacteria can form local colonies in compacted clays, likely in positions where impurities of the clay offer enough large pore space for bacterial life.

The pore water composition will vary with the type of bentonite and the composition of the saturating groundwater. Bentonites vary in composition with respect to elements and minerals and the type and content of natural organic matter (Table 2-2, Table 2-3 and Table 2-4). The conditions for survival and activity of bacteria may, consequently vary significantly between different bentonite types as inferred by the variation in the highest wet density at which sulphide production can be detected in compacted clays (Bengtsson and Pedersen 2017).

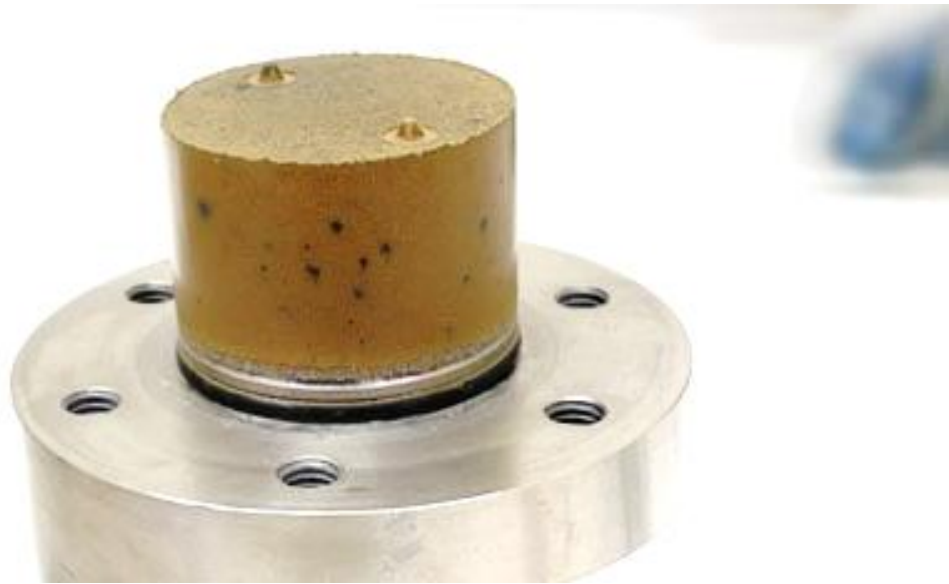


Figure 8-2. Black colonies of iron sulphide produced by sulphide producing bacteria in Asha bentonite at 1750 kg/m³ wet density and with addition of lactate and sulphide producing bacteria (From Figure 7-20).



Figure 8-3. Black colonies of iron sulphide produced by sulphide producing bacteria observed during sampling of test cell with GMZ bentonite (Bengtsson et al. 2017b).

9 Acknowledgements

This project has received funding from the Euroatom research and training program 2014-2018 under grant agreement No. 661880. SKB is acknowledged for providing the bentonite clays, Posiva Oy for access to ONKALO and funding of the SURE project that enabled the metagenome investigation and Nagra for funding and access to the FEBEX experiment. The metagenome and 16S rDNA sequencing data were made possible by the Deep Carbon Observatory's Census of Deep Life program supported by the Alfred P. Sloan Foundation. Sequencing was performed at the Marine Biological Laboratory (Woods Hole, MA, USA). We are grateful to Jill Banfield at Berkely University of California for access to ggkbase and assistance with loading of the sequencing data into ggkbase.

10 References

- Arlinger, J., Bengtsson, A., Edlund, J., Eriksson, L., Johansson, J., Lydmark, S., Rabe, L., Pedersen, K., 2013a. Prototype repository - Microbes in the retrieved outer section. SKB Report P-13-16. 44.
- Arlinger, J., Bengtsson, A., Edlund, J., Eriksson, L., Johansson, J., Lydmark, S., Rabe, L., Pedersen, K., 2013b. Prototype repository - Microbes in the retrieved outer section. SKB Report P-13-16 44.
- Bengtsson, A., Blom, A., Hallbeck, B., Heed, C., Johansson, L., J., S., Pedersen, K., 2016. Microbial sulphide-producing activity in water saturated MX-80, Asha2012 and Calcigel bentonite at wet densities from 1500 to 2000 kg m⁻³. SKB report TR 16-09. Swedish Nuclear Fuel and Waste Management Co, Stockholm Sweden, 1-96.
- Bengtsson, A., Blom, A., Hallbeck, B., Heed, C., Johansson, L., Ståhlén, J., Pedersen, K., 2017a. Microbial Sulphide-producing Activity in Water Saturated MX-80, Asha and Calcigel Bentonite at Wet Densities from 1500 to 2000 Kg M-3. Svensk Kärnbränslehantering AB, Swedish Nuclear Fuel and Waste Management Company.
- Bengtsson, A., Blom, A., Johansson, L., Taborowski, T., Eriksson, L., K., P., 2017b. Bacterial sulphide- and acetate-producing activity in water saturated Rokle and Gaomiaozhi bentonite at wet densities from 1750 to 1950 kg m⁻³. SKB report TR 17-05. Swedish Nuclear Fuel and Waste Management Co, Stockholm, Sweden, 1-38.
- Bengtsson, A., Blom, A., Johansson, L., Taborowski, T., Lena, E., Pedersen, K., 2017c. Bacterial sulphide- and acetate-producing activity in water saturated Calcigel bentonite cores in a wet density gradient from 1 750 to 2 000 kg m⁻³. SKB report 17-18. Swedish Nuclear Fuel and Waste Management Co, Stockholm, Sweden, 1-26.
- Bengtsson, A., Blom, A., Taborowski, T., Schippers, A., Edlund, J., Pedersen, K., 2017d. FEBEX-DP: Microbiological report. NAB 16-015. National Cooperative for the Disposal of Radioactive Waste, Wettingen, Switzerland.
- Bengtsson, A., Pedersen, K., 2016. Microbial sulphate-reducing activity over load pressure and density in water saturated Boom Clay. *Applied Clay Science* 132-133, 542-551.
- Bengtsson, A., Pedersen, K., 2017. Microbial sulphide-producing activity in water saturated Wyoming MX-80, Asha and Calcigel bentonites at wet densities from 1500 to 2000kg m⁻³. *Applied Clay Science* 137, 203-212.
- Bradbury, M.H., Berner, U., Curti, E., Hummel, W., Kosakowski, G., Thoenen, T., 2014. The long term geochemical evolution of the nearfield of the HLW repository. NAGRA report 12-01. National Cooperative for the Disposal of Radioactive Waste (NAGRA), CH-5430 Wettingen, Switzerland.
- Chi Fru, E., Athar, R., 2008. In situ bacterial colonization of compacted bentonite under deep geological high-level radioactive waste repository conditions. *Appl. Microbiol. Biotechnol.* 79, 499-510.
- Edlund, J., Rabe, L., Bengtsson, A., Hallbeck, B., Eriksson, L., Johansson, J., Johansson, L., Pedersen, K., 2016. Understanding microbial reduction of sulphate to sulphide in deep Olkiluoto groundwater. Compilation and interpretation of three consecutive Sulphate Reduction Experiments (SURE) performed during 2010 - 2014. Posiva Working Report 2016-48. Posiva Oy, Olkiluoto, Finland, 1-164.
- Eriksen, T., Jacobsson, A., 1982. Diffusion of hydrogen, hydrogen sulfide and large molecular weight anions in bentonite. *SKBF* 82-17.
- Fine, F., Gervais, P., 2005. Thermal destruction of dried vegetative yeast cells and dried bacterial spores in a convective hot air flow: strong influence of initial water activity. *Environ. Microbiol.* 7, 40-46.
- Gabor, E.M., Vries, E.J., Janssen, D.B., 2003. Efficient recovery of environmental DNA for expression cloning by indirect extraction methods. *FEMS Microbiol. Ecol.* 44, 153-163.

- Gherna, R.L., 1994. Culture preservation, in: Gerhardt, P., Murray, R.G.E., Willis, A.W., Noel, R.K. (Eds.), *Methods for General and Molecular Bacteriology*. Society for Microbiology, Washington, DC, USA, pp. 278–292.
- Greenberg, A.E., Clesceri, L.S., Eaton, A.D., 1992. Estimation of Bacterial Density, Standard methods for the examination of water and wastewater. American Public Health Association 18, 9-49.
- Hallbeck, L., Pedersen, K., 2014. The Family *Gallionellaceae*, in: Rosenberg, E., DeLong, E., Lory, S., Stackebrandt, E., Thompson, F. (Eds.), *The Prokaryotes*. Springer Berlin Heidelberg, pp. 853-858.
- Hansel, C.M., Lentini, C.J., Tang, Y., Johnston, D.T., Wankel, S.D., Jardine, P.M., 2015. Dominance of sulfur-fueled iron oxide reduction in low-sulfate freshwater sediments. *ISME J* 9, 2400-2412.
- Herbert, H.-J., Moog, H.C., 2002. Untersuchungen zur Quellung von Bentoniten in hochsalinaren Lösungen. Abschlussbericht GRS - 179. Gesellschaft für Anlagen und Reaktorsicherheit (GRS) mbH, Schwertnergasse 1, 50667 Köln, Germany.
- Hobbie, J.E., Daley, R.J., Jasper, S., 1977. Use of nucleopore filters for counting bacteria by fluorescence microscopy. *Appl. Environ. Microbiol.* 33, 1225-1228.
- Jacobsen, C.S., Rasmussen, O.F., 1992. Development and application of a new method to extract bacterial DNA from soil based on separation of bacteria from soil with cation-exchange resin. *Appl. Environ. Microbiol.* 58, 2458-2462.
- Jensen, W.B., 2007. The Origin of the Soxhlet Extractor. *J. Chem. Educ.* 84, 1913-1914.
- Johansson, A.J., Lilja, C., Sjögren, L., Gordon, A., Hallbeck, L., Johansson, L., 2017. Insights from post-test examination of three packages from the MiniCan test series of copper-cast iron canisters for geological disposal of spent nuclear fuel: impact of the presence and density of bentonite clay. *Corrosion Engineering, Science and Technology* 52, 54-60.
- Karnland, O., 2010. Chemical and mineralogical characterization of the bentonite buffer for the acceptance control procedure in a KBS-3 repository. SKB Report TR-10-60. Swedish Nuclear Fuel and Waste Management Co, Stockholm, Sweden, 1-29.
- Karnland, O., Olsson, S., Dueck, A., Birgersson, M., Nilsson, U., Hernan-Håkansson, T., Pedersen, K., Nilsson, S., Eriksen, T.E., Rosborg, B., 2009. Long term test of buffer material at the Äspö Hard Rock Laboratory, LOT project. Final report on the A2 test parcel. SKB Technical Report TR-09-29 297.
- Karnland, O., Olsson, S., Nilsson, U., 2006. Mineralogy and sealing properties of various bentonites and smectite-rich clay materials. SKB Technical Report TR-06-30 SKB, 117.
- King, F., Lilja, C., Pedersen, K., Pitkänen, P., Vähänen, M., 2011. An update of the state-of-the-art report on the corrosion of copper under expected conditions in a deep geologic repository. Posiva Report 2011-01. Posiva Oy, Eurajoki, Finland, 1-252.
- Lantenois, B., Lanson, B., Muller, F., Bauer, A., Jullien, M., Plançon, A., 2005. Experimental study of smectite interaction with metal Fe at low temperature: 1. Smectite destabilization. *Clays Clay Miner.* 53, 597-612.
- Laroche, C., Gervais, P., 2003. Unexpected Thermal Destruction of Dried, Glass Bead-Immobilized Microorganisms as a Function of Water Activity. *Appl. Environ. Microbiol.* 69, 3015-3019.
- Lee, S.-W., Chang, C.-T., Lin, C.-C., Wei, T.-Y., Sulfide Corrosion by Sulphate-Reducing Bacteria in MX-80 Bentonites.
- Lindahl, V., Bakken, L.R., 1995. Evaluation of methods for extraction of bacteria from soil. *FEMS Microbiol. Ecol.* 16, 135-142.
- Liu, D., Dong, H., Bishop, M.E., Zhang, J., Wang, H., Xie, S., Wang, S., Huang, L., Eberl, D.D., 2012. Microbial reduction of structural iron in interstratified illite-smectite minerals by a sulfate-reducing bacterium. *Geobiology* 10, 150-162.

- Lopez-Fernandez, M., Cherkouk, A., Vilchez-Vargas, R., Jauregui, R., Pieper, D., Boon, N., Sanchez-Castro, I., Merroun, M.L., 2015. Bacterial Diversity in Bentonites, Engineered Barrier for Deep Geological Disposal of Radioactive Wastes. *Microb. Ecol.* 70, 922-935.
- Lydmark, S., Pedersen, K., 2011. Äspö hard rock laboratory canister retrieval test microorganisms in buffer from the canister retrieval test – numbers and metabolic diversity. SKB Report P-11-06 35.
- Malave-Orengo, J., Borglin, S., Hazen, T., Rios-Velazquez, C., 2010. A modified cell extraction method to access microbial community structure in soil samples by phospholipid fatty acid analysis, *Current Research, Technology and Education Topics in Applied Microbiology and Microbial Biotechnology*.
- Marshall, K.C., 1976. *Interfaces in microbial ecology*. Harvard University Press, Cambridge.
- Marshall, M.H.M., McKelvie, J.R., Simpson, A.J., Simpson, M.J., 2015. Characterization of natural organic matter in bentonite clays for potential use in deep geological repositories for used nuclear fuel. *Appl. Geochem.* 54, 43-53.
- Marshall, M.H.M.S., M J. , 2014. State of science review: Natural organic matter in clays and groundwater. NWMO TR 2014-05. Nuclear Waste Management Organization, Toronto, Canada.
- Masurat, P., Eriksson, S., Pedersen, K., 2010a. Evidence of indigenous sulphate-reducing bacteria in commercial Wyoming bentonite MX-80. *Applied Clay Science* 47, 51-57.
- Masurat, P., Eriksson, S., Pedersen, K., 2010b. Microbial sulphide production in compacted Wyoming bentonite MX-80 under in situ conditions relevant to a repository for high-level radioactive waste. *Applied Clay Science* 47, 58-64.
- Morgan, C.A., Herman, N., White, P.A., Vesey, G., 2006. Preservation of micro-organisms by drying; a review. *J. Microbiol. Methods* 66, 183-193.
- Motamedi, M., Karland, O., Pedersen, K., 1996. Survival of sulfate reducing bacteria at different water activities in compacted bentonite. *FEMS Microbiol. Lett.* 141, 83-87.
- Motamedi, M., Pedersen, K., 1998. *Desulfovibrio aespoensis* sp nov., a mesophilic sulfate-reducing bacterium from deep groundwater at Äspö hard rock laboratory, Sweden. *Int. J. Syst. Bacteriol.* 48, 311-315.
- Pedersen, K., 2010. Analysis of copper corrosion in compacted bentonite clay as a function of clay density and growth conditions for sulfate-reducing bacteria. *J. Appl. Microbiol.* 108, 1094-1104.
- Pedersen, K., Arlinger, J., Eriksson, S., Hallbeck, A., Hallbeck, L., Johansson, J., 2008. Numbers, biomass and cultivable diversity of microbial populations relate to depth and borehole-specific conditions in groundwater from depths of 4-450 m in Olkiluoto, Finland. *ISME J.* 2, 760-775.
- Pedersen, K., Bengtsson, A., Blom, A., Johansson, L., Taborowski, T., 2017a. Mobility and reactivity of sulphide in bentonite clays—implications for engineered bentonite barriers in geological repositories for radioactive wastes. *Applied Clay Science* 146, 495-502.
- Pedersen, K., Bengtsson, A., Blom, A., Johansson, L., Taborowski, T., 2017b. Mobility and reactivity of sulphide in bentonite clays – Implications for engineered bentonite barriers in geological repositories for radioactive wastes. *Applied Clay Science* 146, 495-502.
- Pedersen, K., Bengtsson, A., Edlund, J., Eriksson, L., 2014. Sulphate-controlled diversity of subterranean microbial communities over depth in deep groundwater with opposing gradients of sulphate and methane. *Geomicrobiol. J.* 31, 617-631.
- Pedersen, K., Bengtsson, A., Edlund, J., Eriksson, L., Johansson, L., 2017c. Distribution of planktonic and attached microbial populations in groundwater of Olkiluoto and ONKALO. Posiva working report 2017-49. Olkiluoto, Finland, 1-51.
- Pedersen, K., Ekendahl, S., 1990. Distribution and activity of bacteria in deep granitic groundwaters of southeastern sweden. *Microb. Ecol.* 20, 37-52.

- Pedersen, K., Motamedi, M., Karnland, O., Sandén, T., 2000a. Cultivability of microorganisms introduced into a compacted bentonite clay buffer under high-level radioactive waste repository conditions. *Engineering Geology* 58, 149-161.
- Pedersen, K., Motamedi, M., Karnland, O., Sandén, T., 2000b. Mixing and sulphate-reducing activity of bacteria in swelling, compacted bentonite clay under high-level radioactive waste repository conditions. *J. Appl. Microbiol.* 89, 1038-1047.
- Pedersen, K., Taborowski, T., Johansson, L., Bengtsson, A., Blom, A., 2017d. Mobility and reactivity of sulphide in bentonite clays – implications for engineered bentonite barriers in geological repositories for radioactive wastes. *Applied Clay Science* (in review).
- Potts, M., 1994. Desiccation tolerance of prokaryotes. *Microbiol. Mol. Biol. Rev.* 58, 755-805.
- Preisler, A., de Beer, D., Lichtschlag, A., Lavik, G., Boetius, A., Jorgensen, B.B., 2007. Biological and chemical sulfide oxidation in a Beggiatoa inhabited marine sediment. *ISME J.* 1, 341-353.
- Richard, D., Luther, G.W., 2007. Chemistry of Iron sulfides. *Chem. Rev.* 107, 514-562.
- Sandén, T., Olsson, S., Andersson, L., Dueck, A., Jensen, V., Hansen, E., 2014. Investigation of backfill material. SKB report R-13-08. Swedish Nuclear Fuel and Waste Management Co, Stockholm, Sweden, 1-169.
- Selenska, S., Klingmüller, W., 1991. Direct detection of nif-gene sequences of *Enterobacter agglomerans* in soil. *FEMS Microbiol. Lett.* 80, 243-245.
- Smart, N.R., Rance, A.P., Reddy, B., Hallbeck, L., Pedersen, K., Johansson, A.J., 2014. *In situ* evaluation of model copper-cast iron canisters for spent nuclear fuel: a case of microbiologically influenced corrosion (MIC). *Corrosion Engineering, Science and Technology* 49, 548-553.
- Soltermann, D., 2014. Ferrous iron uptake mechanisms at the montmorillonite-water interface under anoxic and electrochemically reduced conditions, ETH Zurich.
- Stone, W., Kroukamp, O., Moes, A., McKelvie, J., Korber, D.R., Wolfaardt, G.M., 2016. Measuring microbial metabolism in atypical environments: Bentonite in used nuclear fuel storage. *J. Microbiol. Methods* 120, 79-90.
- Svensson, D., Dueck, A., Nilsson, U., Olsson, S., Sandén, T., Lydmark, S., Jägwall, S., Pedersen, K., Hansen, S., 2011. Alternative buffer material. Status of the ongoing laboratory investigation of reference materials and test package 1. SKB Technical Report TR-11-06. Swedish Nuclear Fuel & Waste Management Co, Stockholm, Sweden, 1-146.
- van Elsas, J.D., Trevors, J.T., Jansson, J.K., 2006. *Modern soil microbiology*, 2 ed. CRC Press.
- Widdel, F., Bak, F., 1992. Gram-negative, mesophilic sulphate-reducing bacteria. Springer-Verlag, New York.
- Yang, R., Papparini, A., Monis, P., Ryan, U., 2014. Comparison of next-generation droplet digital PCR (ddPCR) with quantitative PCR (qPCR) for enumeration of *Cryptosporidium* oocysts in faecal samples. *Int. J. Parasitol.* 44, 1105-1113.
- Ye, W.-M., 2016. Investigation on chemical effects on GMZ bentonite used as buffer materials. *E3S Web of Conferences* 9, 02001.

11 Appendix A

Table A-1. The co-occurrence of genes affiliated with Bacteria in both metagenome and 16S rDNA libraries from ONK-PVA6 and ONK-KR15 biofilms presented as the percentage of all genes for Bacteria that also were detected by the 16S rDNA analysis.

Class	Order	Family	Genus	ONK-PV6		ONK-KR15	
				Ggkbase scaffolds	VAMPS hits	Ggkbase scaffolds	VAMPS hits
Actinobacteria	Corynebacteriales	Corynebacteriaceae	Corynebacterium	0.04	1.44	0.05	1.29
Actinobacteria	Propionibacteriales	Propionibacteriaceae	Propionibacterium	0.03	5.81	0.02	5.28
Flavobacteriia	Flavobacteriales	Flavobacteriaceae	Cloacibacterium	0.00	0.77	0.00	0.44
Flavobacteriia	Flavobacteriales	Flavobacteriaceae	Flavobacterium	1.93	1.02	1.59	0.96
Flavobacteriia	Flavobacteriales	Flavobacteriaceae	Lutibacter	0.00	9.76	0.00	13.45
Bacilli	Bacillales	Alicyclobacillaceae	Tumebacillus	0.01	0.31	0.00	0.18
Bacilli	Bacillales	Staphylococcaceae	Staphylococcus	0.02	1.26	0.02	1.14
Bacilli	Lactobacillales	Streptococcaceae	Streptococcus	0.02	0.94	0.03	0.86
Alphaproteobacteria	Rhizobiales	Phyllobacteriaceae	Mesorhizobium	5.41	1.84	1.83	1.97
Alphaproteobacteria	Rhodobacterales	Rhodobacteraceae	Phaeobacter	0.11	0.22	0.25	1.72
Alphaproteobacteria	Rhodobacterales	Rhodobacteraceae	Roseovarius	2.43	0.47	8.38	1.13
Betaproteobacteria	Burkholderiales	Comamonadaceae	Hydrogenophaga	1.68	0.83	4.95	4.09
Betaproteobacteria	Methylophilales	Methylophilaceae	Methylotenera	0.28	0.30	0.86	2.17
Deltaproteobacteria	Desulfobacterales	Desulfobulbaceae	Desulfurivibrio	0.23	3.38	0.05	1.70
Epsilonproteobacteria	Campylobacterales	Campylobacteraceae	Arcobacter	0.03	0.13	0.01	1.12
Gammaproteobacteria	Alteromonadales	Alteromonadaceae	Alteromonas	0.05	1.85	0.01	1.71
Gammaproteobacteria	Alteromonadales	Alteromonadaceae	Marinobacter	0.29	3.10	3.13	2.87
Gammaproteobacteria	Pseudomonadales	Moraxellaceae	Acinetobacter	0.17	3.57	0.22	7.19
Gammaproteobacteria	Pseudomonadales	Pseudomonadaceae	Pseudomonas	22.27	3.24	25.68	5.79
Total				35.01	40.25	47.10	55.07

Table A-2 The co-occurrence of genes affiliated with sulphate reducing bacteria (SRB) in both metagenome and 16S rDNA libraries from ONK-PVA6 and ONK-KR15 biofilms presented as the percentage of all genes for SRB that also were detected by the 16S rDNA analysis.

Order	Family	Genus	Species	ONK-PV6		ONK-KR15	
				Ggkbase scaffolds	VAMPS hits	Ggkbase scaffolds	VAMPS hits
Syntrophobacterales	Syntrophaceae	Desulfobacca	acetoxidans	0.0731	0.1045	0.0083	0.0499
Desulfobacterales	Desulfobacteraceae	Desulfobacterium	-	0.7872	0.2125	0.0744	0.0498
Desulfobacterales	Desulfobulbaceae	Desulfobulbus	-	0.3303	0.0286	0.0923	0.0046
Desulfovibrionales	Desulfomicrobiaceae	Desulfomicrobium	-	0.0587	0.0010	0.0565	0.0009
Clostridiales	Peptococcaceae	Desulfosporosinus	meridiei	0.0078	0.0008	0.0014	0.0020
Desulfuromonadales	Desulfuromonadaceae	Desulfuromonas	-	0.1658	1.3808	0.3252	9.6218
Clostridiales	-	Dethiosulfatibacter	-	0.0000	0.0121	0.0000	0.0024
Hydrogenophilales	Hydrogenophilaceae	Thiobacillus	-	0.8315	0.9753	1.5638	1.3003
Total				2.25	2.72	2.12	11.03

Table A-3. The co-occurrence of genes affiliated with Archaea in both metagenome and 16S rDNA libraries from ONK-PVA6 and ONK-KR15 biofilms presented as the percentage of all genes for Archaea that also were detected by the 16S rDNA analysis.

Phylum	Class	Order	Family	Genus	Species	ONK-PV6		ONK-KR15	
						Ggkbase scaffolds	VAMPS hits	Ggkbase scaffolds	VAMPS hits
Euryarchaeota	Halobacteria	Halobacteriales	Halobacteriaceae	Halococcus	-	0.0065	0.0141	0.0000	0.0199
Euryarchaeota	Methanobacteria	Methanobacteriales	Methanobacteriaceae	Methanobacterium	-	0.0300	0.4170	0.0096	0.8063
Euryarchaeota	Methanobacteria	Methanobacteriales	Methanobacteriaceae	Methanobrevibacter	-	0.0026	0.0025	0.0014	0.0114
Euryarchaeota	Methanobacteria	Methanobacteriales	Methanobacteriaceae	Methanothermobacter	-	0.0013	0.0008	0.0014	0.0043
Euryarchaeota	Methanococci	Methanococcales	Methanocaldococcaceae	Methanocaldococcus	-	0.0078	0.0058	0.0055	0.0000
Euryarchaeota	Methanomicrobia	Methanocellales	Methanocellaceae	Methanocella	-	0.0209	0.0025	0.0083	0.0028
Euryarchaeota	Methanomicrobia	Methanomicrobiales	Methanoregulaceae	Methanoregula	-	0.0091	0.0265	0.0000	1.6779
Euryarchaeota	Methanomicrobia	Methanomicrobiales	Methanospirillaceae	Methanospirillum	-	0.0026	0.0000	0.0000	0.0100
Euryarchaeota	Methanomicrobia	Methanosarcinales	Methanosaetaceae	Methanosaeta	-	0.0483	0.0546	0.0069	2.5667
Euryarchaeota	Methanomicrobia	Methanosarcinales	Methanosarcinaceae	Methanolobus	-	0.0183	1.9386	0.0138	1.0110
Euryarchaeota	Methanomicrobia	Methanosarcinales	Methanosarcinaceae	Methanosarcina	-	0.1110	0.0000	0.0496	0.0242
Euryarchaeota	Methanomicrobia	Methanosarcinales	Methermicoccaceae	Methermicoccus	-	0.0000	0.8440	0.0000	1.4035
Euryarchaeota	Thermoplasmata	-	-	-	-	0.0104	35.5938	0.0096	37.6187
Korarchaeota	-	-	-	-	-	0.0026	0.0207	0.0000	0.0000
Thaumarchaeota	-	-	-	-	-	0.0666	43.5230	0.0716	20.4767
					Total	0.34	82.44	0.18	65.63

12 Appendix B

See next 8 pages



Research paper

Mobility and reactivity of sulphide in bentonite clays – Implications for engineered bentonite barriers in geological repositories for radioactive wastes



Karsten Pedersen*, Andreas Bengtsson, Anders Blom, Linda Johansson, Trevor Taborowski

Microbial Analytics Sweden AB, Mölnlycke, Sweden

ARTICLE INFO

Keywords:

Asha
Bacteria
Calcigel
Diffusion
Montmorillonite
MX-80
Sulphate
Sulphur

ABSTRACT

Bentonite clays will be used as barriers in geological repositories for radioactive wastes. Anoxic conditions will prevail in such repositories, and the presence of sulphide-producing bacteria in commercial bentonites and deep groundwater environments is well established. In this study, sulphide was found to reduce ferric iron in bentonites denoted Asha, MX-80 and Calcigel under the formation of elemental sulphur, ferrous iron and iron sulphide. These reactions rendered an immobilisation capacity of the clays that was $40 \mu\text{mole sulphide (g clay)}^{-1}$ or more, depending on the load of sulphide, and type of clay. In addition, the effective diffusion coefficients for sulphide in Asha bentonite, compacted to saturated wet densities of 1750 kg m^{-3} and 2000 kg m^{-3} , were determined to $2.74 \times 10^{-11} \text{ m}^2 \text{ s}^{-1}$ and $6.60 \times 10^{-12} \text{ m}^2 \text{ s}^{-1}$, respectively. The found immobilisation effect can reduce the mass of sulphide that corrode metal canisters over repository life times, but the concomitant reduction of ferric iron may be problematic due to the destabilizing effect of ferrous iron on dioctahedral smectites such as montmorillonites.

1. Introduction

Bentonites rich in swelling montmorillonite are used to construct engineered barriers in geological repositories for low- intermediate- and soon also high-level radioactive wastes. While there are several low- and intermediate-level repositories in operation around the world, high-level repositories are still in planning or under construction. Various types of metal containers, made of iron or copper will be used to encapsulate the wastes. Sulphide is in general corrosive to these metals, and safety cases for radioactive waste disposal must, therefore, evaluate the risks involved with sulphide corrosion (e.g. King et al., 2011). The inorganic reduction of sulphate to sulphide is kinetically hindered at normal pressure and temperature (Cross et al., 2004). The main source of sulphide in geological repository environments is, therefore, past and present microbial reduction of sulphate to sulphide. Sulphide-producing bacteria (SPB) have been found in most commercially available bentonites (Masurat et al., 2010; Svensson et al., 2011), and they frequently occur in deep geological formations and deep groundwater (e.g. Moser et al., 2005; Pedersen et al., 2014). The dissociation constant for $\text{HS}^-/\text{H}_2\text{S}$ is $10^{-6.98}$ (Richard and Luther, 2007). The pH of groundwater in repository environments, and in clay pore water is buffered above 7, which means that sulphide mainly will be

present as HS^- when pH approaches 8 or higher.

Microbial sulphide-producing activity in compacted clays was recently investigated as a function of clay type, saturated wet density, and geomechanical stress (Bengtsson and Pedersen, 2016; Bengtsson and Pedersen, 2017). The registered sulphide-producing activity generally decreased with increasing stress and density. The sulphide-production was analysed as formation of radioactive Cu_2^{35}S on copper discs, and as decrease in concentration of sulphate in pore water. A discrepancy was observed as the decrease in pore water sulphate concentration was larger than the modelled decrease based on the amount of Cu_2^{35}S on the copper discs. It was proposed that the investigated clays, to some extent, immobilised HS^- (Bengtsson and Pedersen, 2016; Bengtsson and Pedersen, 2017). A similar effect was recently observed elsewhere for Wyoming MX-80 clay (Stone et al., 2016). Such effect was also noticed in diffusion experiments where HS^- break-through was delayed compared to what was expected for monovalent anions (Eriksen and Jacobsson, 1982).

Sulphide produced by SPB has been shown to reduce ferrihydrite to ferrous iron in bioreactors (Hansel et al., 2015). The process of anaerobic reduction of ferric iron with H_2S produced by SPB to ferrous iron and S_8 is known to occur in marine (Richard and Luther, 2007), and subsurface sediments (Kwon et al., 2014). This process has been

* Corresponding author.

E-mail address: kap@micans.se (K. Pedersen).

<http://dx.doi.org/10.1016/j.clay.2017.07.003>

Received 20 February 2017; Received in revised form 5 June 2017; Accepted 5 July 2017

Available online 11 July 2017

0169-1317/ © 2017 The Authors. Published by Elsevier B.V. This is an open access article under the CC BY license (<http://creativecommons.org/licenses/by/4.0/>).

connected to a microbial cryptic sulphur cycle (Holmkvist et al., 2011). In analogy, it can be hypothesized that a similar process can occur in bentonite. That hypothesis was recently tested on illite-smectite minerals, and it could not be falsified (Liu et al., 2012). The results showed that bio-reduction of structural ferric iron to ferrous iron by SPB was positively correlated with the amount of smectite and surface area. Taken together, the above cited literature suggests that sulphide can reduce ferric iron to ferrous iron in bentonites with the concomitant reduction of sulphide to elemental sulphur. It has been demonstrated that dioctahedral smectites are destabilized by ferrous iron (Lantenois et al., 2005). Bentonites to be used in engineered barriers contain ferric iron both in accessory minerals, and to a small extent also in the montmorillonite. If sulphide can reduce ferric iron in bentonite to yield ferrous iron and sulphur, it may explain the observed immobilisation effects described for sulphide in experiments with activity of SPB in compacted bentonites (Bengtsson and Pedersen, 2016; Bengtsson and Pedersen, 2017). Such process may be detrimental to the bentonite due to the destabilizing effect of ferrous iron on montmorillonite (Bradbury et al., 2014; Soltermann, 2014).

In this study, the reactivity of sulphide with ferric iron in suspensions of Wyoming MX-80, Asha and Calcigel bentonite clays in water was studied. The immobilisation of sulphide by the clays, and the formation of ferrous iron and elemental sulphur as a function of sulphide concentration was quantified. In addition, the apparent diffusion coefficients of H^{35}S^- in iron rich Asha bentonite at two saturated wet densities, 1750 and 2000 kg m^{-3} , were determined. Possible implications for engineered barriers in radioactive waste repositories are discussed.

2. Materials and methods

2.1. Bentonites

Three bentonite types were used in the study. They were Wyoming MX-80, Asha and Calcigel which were supplied by Swedish Nuclear Fuel and Waste Management CO. The mineral compositions of these clays were previously characterised in detail (Table 1) (Herbert and Moog, 2002; Karnland, 2010; Sandén et al., 2014). The element composition was analysed with inductively coupled plasma sector field mass spectrometry (ICP-SFMS) after sintering and dissolution in diluted

Table 1

Average results from the XRD analyses of mineral compositions of the MX-80 ($n = 6$), (Karnland, 2010), Asha ($n \geq 5$) (Karnland, 2010; Sandén et al., 2014) and Calcigel ($n = 2$) (Herbert and Moog, 2002) and the element composition of the bentonite materials expressed as weight percent of major element oxides of dry mass after sintering and analysis on ICP-SFMS. LOI denotes the percent mass loss due to ignition. n: number of independent samples.

Component	MX-80	Asha	Calcigel
<i>Minerals</i>			
Montmorillonite	81	82	66
Muscovite	3.4	1.9	14
Plagioclase	3.5	0.82	3
Pyrite	0.6	0.66	0
Quartz	3.0	1.2	8.2
Other	8.5	13.4	8.8
<i>Elements</i>			
SiO_2	61.2	45.5	56.6
Al_2O_3	18.4	16.9	17.8
CaO	1.15	2.85	1.69
Fe_2O_3	4.15	13	6.11
K_2O	0.599	0.128	1.55
MgO	2.02	2.34	2.92
MnO	0.0146	0.112	0.085
Na_2O	1.56	1.3	0.251
P_2O_5	0.0541	0.0954	0.0531
TiO_2	0.148	1.03	0.402
Loss of ignition	5.9	9.5	7

nitric acid (ALS Scandinavia, Luleå, Sweden). MX-80 and Asha are sodium bentonites with five times more Na_2O compared with Calcigel. Asha distinguished from the other clays by a larger amount of iron and Calcigel distinguished from the other clays by a smaller amount of montmorillonite, 66%. MX-80 and Asha bentonites contained approximately 80% montmorillonite.

2.2. Preparation of clay suspensions

The water contents of the clays were determined before the preparation of clay suspensions. Duplicate clay samples were placed in aluminium bowls and heated for 24 h at 105 °C. An average of the weight difference before and after the heating was registered as the water content of each bentonite clay batch and was used to calculate the dry weight in gram of the clays. The water content of the clays were 6.8% for Asha, 8.8% for MX-80 and 8.8% for Calcigel. All clay weights in this paper are dry weights without water.

Clay suspensions were prepared inside an anaerobic box with an atmosphere of 97% N_2 and 3% H_2 , $\text{O}_2 < 1$ ppm (Coy Laboratory Products, Grass Lake, MI, USA). Series of 50 mL glass injection bottles (No 772, Nordic Pack, Nykvarn, Sweden) with 0.5 g of the respective clay were mixed with 17 mL deoxygenated Analytical Grade Water (AGW), sealed with butyl rubber stoppers (Bellco Glass, Inc., Vineland, NJ, US, no. 2048-117800), and crimped with aluminium seals (Bellco, no. 2048-11020). Sealed injection bottles were removed from the anaerobic glove box and immediately evacuated two times down to < 2.0 kPa. The bottles were filled with 120 kPa scientific N_2 between evacuations. Following the second evacuation, bottles were left at 120 kPa.

2.3. Addition of Na_2S

Stock solutions of Na_2S were prepared to give a range of amounts of sulphide per gram clay; from 50 $\mu\text{mol Na}_2\text{S (g clay)}^{-1}$ up to 320 $\mu\text{mol Na}_2\text{S (g clay)}^{-1}$, analysed amounts are given in the results section. The stock solutions were prepared by dissolving $\text{Na}_2\text{S} \times 9\text{H}_2\text{O}$ under N_2 -infusion in 50 mL O_2 -free AGW. When dissolved, the solutions were transferred with N_2 -flushed syringes into O_2 -free 100 mL injection bottles (Nordic Pack, No 1500) that were sealed with butyl rubber stoppers and crimped with aluminium seals. The obtained concentrations of the stock solutions were analysed with CuSO_4 according to Widdel and Bak (1992). Series of injection bottles with clay suspensions and blank injection bottles with only water were added with 1 mL of the respective stock solutions, agitated and left to incubate for 24 h.

2.4. Adjustment of pH with buffer and HCl

The pH of the clay suspensions was adjusted for 24 h after addition of Na_2S with two different methods. A buffer method used a citric acid + Na_2HPO_4 mix to obtain three different pH values in the clay suspensions: pH 7 was obtained by addition of 2 mL buffer with 0.065 M citric acid and 0.872 M Na_2HPO_4 , pH 5 with 2 mL of 0.243 M citric acid and 0.514 M Na_2HPO_4 and pH 2.6 with 2 mL of 0.446 M citric acid and 0.108 M Na_2HPO_4 . A HCl method comprised addition of a 2 M solution of HCl in AGW to reach pH lower than 3 in clay suspensions. However, they were first adjusted to pH 2.6 with the buffer method and then purged for volatile H_2S (see Section 2.5) before further pH adjustment. The injection bottles were agitated after pH adjustment and the pH values were analysed on withdrawn aliquots with a pH meter (Scott, mod. CG 843P, VWR International AB, Stockholm, Sweden) equipped with a Hamilton electrode (Polilyte lab temp DIN, product no 242058/01, Genetec, Sweden).

2.5. Analysis of volatile H_2S

The pH adjusted clay suspensions were left for 24 h before analysis

of volatile H_2S was done. A modification of a purge method for marine sediments (Jorgensen and Fenchel, 1974) was assembled. The stoppers of the bottles with clay suspensions were penetrated with a 2.1×80 mm needle (Cat No 121410, Next2vet, Ystad, Sweden) connected to a 50 mL s^{-1} gas-stream of O_2 -free N_2 Alphagaz 1, $\text{O}_2 < 2$ ppm (Air Liquid, Mölndal, Sweden). Volatile H_2S was purged at room temperature and transferred via a peek tube-needle-system to a series of H_2S traps. These traps consisted of two 50 mL, butyl rubber stoppered, injection bottles filled with 30 mL of a 20 mM zink acetate solution. H_2S in the purge gas stream was precipitated as ZnS which was subsequently analysed. The sum of ZnS in the two traps represented the amounts of volatile H_2S in the clay suspensions and in the blank bottles with water.

2.6. Sulphide and ferrous iron analysis

Sulphide precipitated as ZnS in the traps was analysed using the colorimetric methylene blue method with an uncertainty of $\pm 17\%$ (Swedish Standard Method SIS 028115). The detection limit was $0.018 \mu\text{mole H}_2\text{S (g clay)}^{-1}$. Ferrous iron concentrations in the aqueous phase of the clay suspensions were determined using the 1–10 phenanthroline method (method no. 8146, programme 255, range 0.4–54 mM with 95% confidence limits of distribution of $\pm 11\%$; HACH Lange AB). The detection limit was $0.05 \mu\text{mole Fe}^{2+} \text{ (g clay)}^{-1}$.

2.7. Sulphur analysis

The clay suspensions were, after the volatile H_2S was purged, centrifuged in 50 mL polypropylene tubes at 4400 relative centrifugal force for 15 min (Heraeus Multifug 3SR+, Swing-out rotor 7500 6445, Fisher Scientific, Göteborg, Sweden). The supernatant was decanted and the clay samples were carefully dried in an oven (60°C) or by freeze drying to remove all water. Thereafter, ≤ 0.5 g of dried clay was weighed into a 1.8 mL extraction glass vessel (Short thread vial hydrolytic, No 11 09 0519, Genetec, Gothenburg, Sweden) and 500 μL of carbon disulphide (99.9% for spectroscopy, Acros Organics, Geel, Belgium) were added to the clay. The vessels were sealed with a red rubber septum lined with a PTFE membrane on the inside vessel (Combination seal, No 09 15 1819, Genetec, Gothenburg, Sweden). The samples were shaken for 1 min to enhance wetting of the clay with carbon disulphide. Thereafter, they were left for extraction either using an ultrasonic bath (Sonorex DT 255, Bandelin, Berlin, Germany) for 2×15 min, or for > 12 h at room temperature. The samples were agitated a second time and left for sedimentation of the clay for > 1 h. The carbon disulphide was removed from the extraction vessel using a Pasteur glass pipette and transferred to a second 1.8 mL extraction glass vessel. The extraction procedure was repeated with a second aliquot of 500 μL carbon disulphide and the two extractions were pooled. The sample volume was thereafter adjusted to a total of 1.0 mL by dropwise addition of carbon disulphide.

A stock solution with a concentration of 0.080 g sulphur (325 mesh 99.5%, Alfa Aesar, Karlsruhe, Germany) in 50 mL of carbon disulphide was prepared. Using the extraction procedure outlined above, extracting 0.5 g of clay to 1.0 mL of carbon disulphide, the concentration of this stock solution would equal an amount of $100 \mu\text{mol S (g clay)}^{-1}$. A calibration curve was made by dilution of this solution 1:1 and 1:3 to yield standards corresponding to sulphur amounts of 25 and $50 \mu\text{mol S (g clay)}^{-1}$. The analyses of samples and standards were run on an GC-MS using ion-trap detection (Saturn 2000/CP3800, Varian, Walnut Creek, USA), and splitless programmed temperature vaporisation-injection from 60 to 300°C (1079 inlet, Varian, Walnut Creek, USA). Analysis time for each sample was 20 min, and the peak for sulphur was detected at a retention time of 13 min using a programmed temperature ranging from 35 to 320°C with a steep initial ramp to 160°C . Detection and integration were performed using the ion fragment 256 (S_8). Blank samples of carbon disulphide were analysed as well. The mean area of

the peak for sulphur in blanks was subtracted from the integrated areas for sulphur in samples and standards before further processing. The areas for the samples were interpreted against the standard curve to obtain the amounts of sulphur in the clay.

2.8. Clay suspension experiments

A total of four sets of experiments were performed with Asha, MX-80 and Calcigel clays.

Experiment 1 tested the release of volatile H_2S with and without addition of Na_2S over a range of five pH values. The experiment was divided in two separate trials. The first trial comprised analysed pH values from 7 to 3.7 which were set with the buffer method. The second trial comprised pH values at 3, 2 and 1 which were obtained with a combination of the buffer and HCl method. This experiment also analysed immobilised sulphide as the difference between volatile sulphide in blank bottles without clay, and the amount of volatile sulphide from bottles with clay suspensions. The amount of formed sulphur was analysed as well.

Experiment 2 tested the release of ferrous iron with and without addition of Na_2S over a range of pH adjusted injection bottles. pH was adjusted with the HCl method for all three clays. In addition, pH values were adjusted with the combination of the buffer and HCl method for the Asha clay suspensions.

Experiment 3 tested immobilised sulphide, release of ferrous iron and produced sulphur with and without addition of Na_2S over a range of 3.4 pH units (7 to 2.6) adjusted with buffer.

Experiment 4 tested immobilised sulphide and release of ferrous iron over a larger range of added amounts of Na_2S than in the previous experiments at adjusted pH values between 3.7 and 3.2.

2.9. Diffusion experiments

All parts of the experiments were performed under O_2 -free conditions (< 1 ppm O_2). The diffusion experiments followed the methodology for determining the sulphate diffusion coefficient in Boom Clay as described in the supplementary data of Bengtsson and Pedersen (2016) with the following modifications. Asha bentonite was compacted to obtain two wet densities, 1750 and 2000 kg m^{-3} , and water saturated with AGW. The sulphate-reducing bacterium *Desulfovibrio aespoensis* (Motamedi and Pedersen, 1998) was used to produce a H^{35}S^- solution from $^{35}\text{SO}_4^{2-}$. A medium for sulphate-reducing bacteria with 1 mM MgSO_4 was produced as described elsewhere (Hallbeck and Pedersen, 2008). A 1 mL aliquot of $\text{Na}_2^{35}\text{SO}_4$ in water (PerkinElmer, cat. no. NEX041H005MC, 5 mCi (185 MBq), specific activity: 1050–1600 Ci (38.8–59.2 TBq mmol^{-1} sodium sulphate)) was added to the medium that was inoculated with *D. aespoensis* (Deutsche Sammlung von Mikroorganismen und Zellkulturen GmbH, no. DSM10631). Additional control cultures without addition of $\text{Na}_2^{35}\text{SO}_4$ were inoculated as well. The sulphide and sulphate concentrations of these control cultures were analysed to determine when all sulphate was reduced to sulphide. Furthermore, the pH in the cultures was adjusted with 1 M NaOH to pH 8.5, so that sulphide was $> 95\%$ dissociated as HS^- . This was done to avoid radioactive H_2S gas in the anaerobic box (Coy Laboratory Products, Grass Lake, MI, USA) during experiment preparation. The bacteria were sterile filter (0.22 μm pore size) separated from the produced H^{35}S^- solution when all sulphate was reduced in the control cultures and used to determine the diffusion coefficients of H^{35}S^- at the two selected wet densities. Any remaining sulphate was precipitated with barium nitrate before filtration. There were 10 mL of AGW on the donor side with a total amount of $10 \mu\text{mole HS}^-$. The 1750 kg m^{-3} and 2000 kg m^{-3} clay cores had dry weights of 22.1 and 29.4 g which give a max load of 0.45 $\mu\text{mole HS}^- \text{ (g clay)}^{-1}$ and 0.34 $\mu\text{mole HS}^- \text{ (g clay)}^{-1}$, respectively.

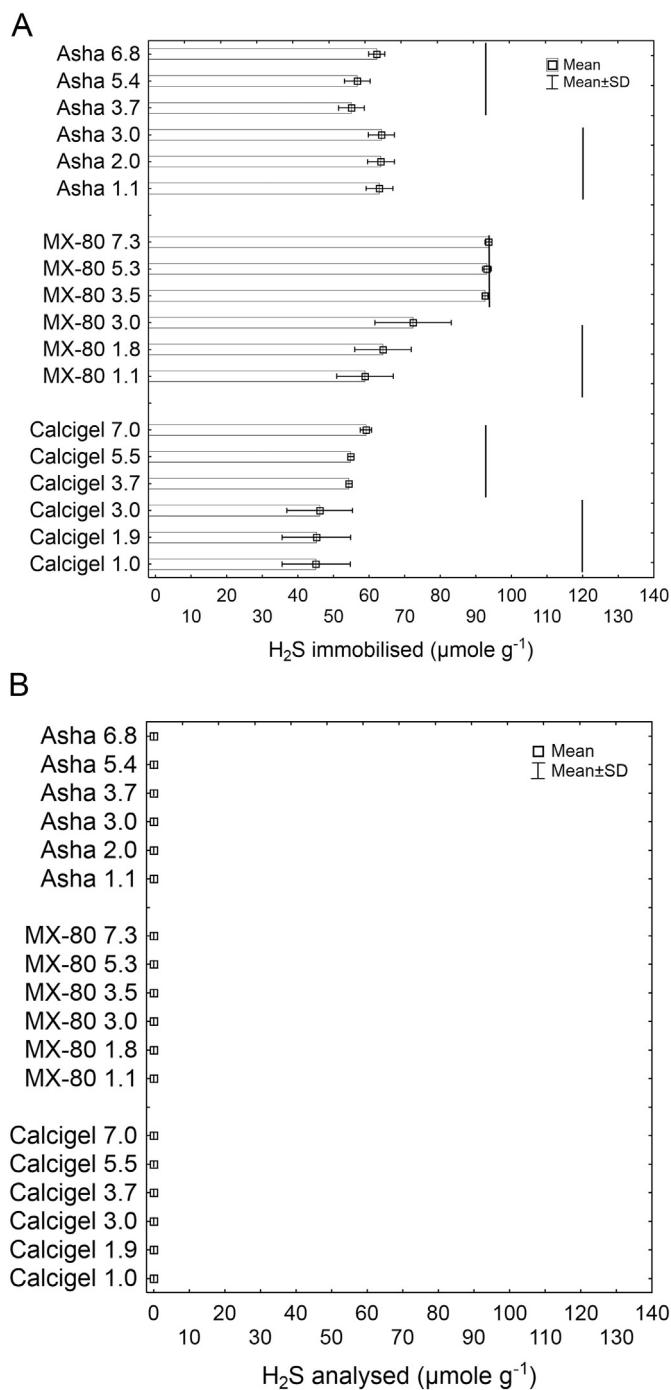


Fig. 1. A. Immobilised, non-volatile H_2S in three different bentonite clays over a range of adjusted pH values. Data are from two independent trials. The vertical lines indicate the added amount of Na_2S in each trial. Numbers after the respective clay name shows analysed pH. Bars indicate standard deviation (SD) of three parallel samples. B. Analysed volatile H_2S in three different bentonite clay suspensions over a range of adjusted pH values without addition of Na_2S . Data are from two independent trials as in Fig. 1A. Numbers after the respective clay name show analysed pH. Bars indicate standard deviation (SD) of three parallel samples.

3. Results

3.1. Experiment 1 - analysed and immobilised sulphide with and without Na_2S addition

The Asha clay immobilised approximately $60 \mu\text{mole } H_2S \text{ g}^{-1}$ irrespectively of the adjusted pH value (Fig. 1). MX-80 immobilised all added sulphide in the first trial with addition of $90 \mu\text{mole } Na_2S \text{ (g clay)}^{-1}$

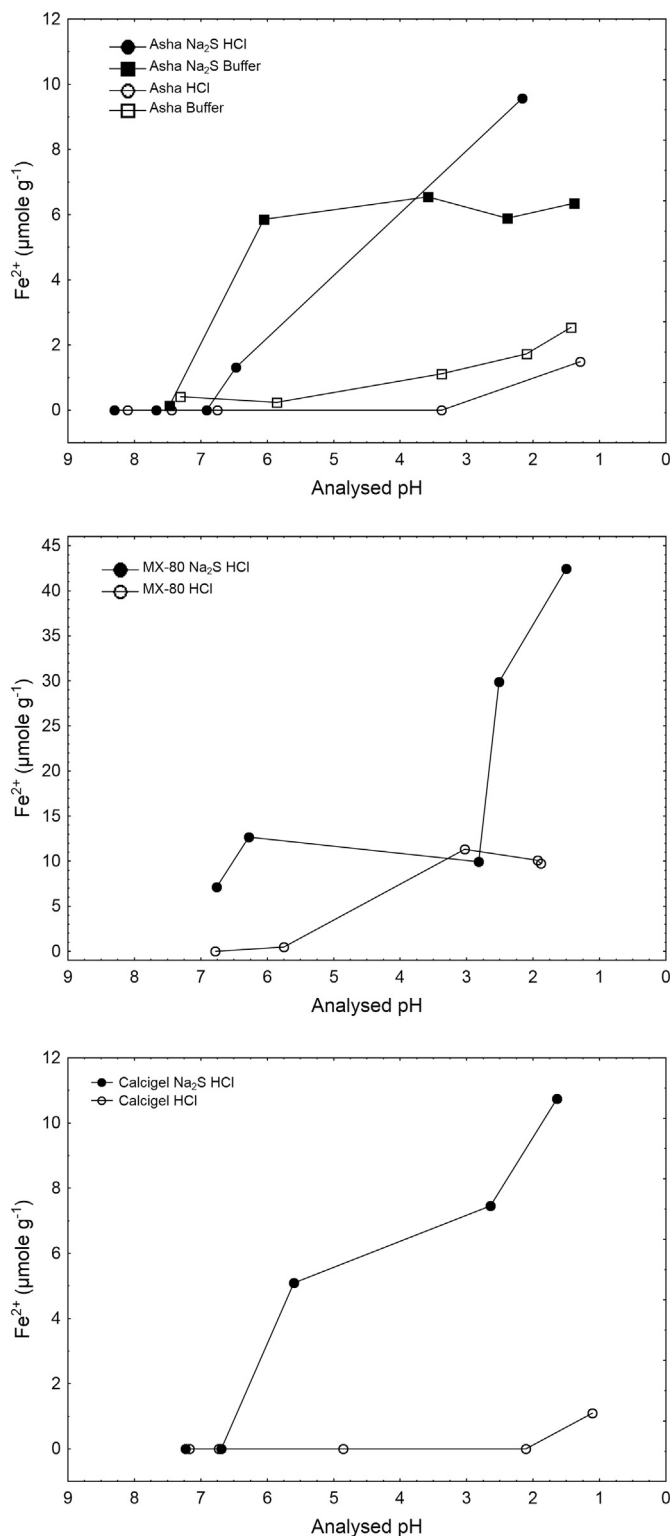


Fig. 2. Released ferrous iron from three different bentonite clay suspensions with and without addition of $100 \mu\text{mole } Na_2S \text{ (g clay)}^{-1}$.

g clay)^{-1} down to pH 3.5. In the second trial with addition of $120 \mu\text{mole } Na_2S \text{ g}^{-1}$, MX-80 immobilised approximately $60 \mu\text{mole } H_2S \text{ g}^{-1}$ at pH 1. Calcigel immobilised on average $45 \mu\text{mole } H_2S \text{ g}^{-1}$ at pH 3 or lower. Volatile H_2S could not be detected in any of the clay suspensions without added Na_2S at any pH (Fig. 1B).

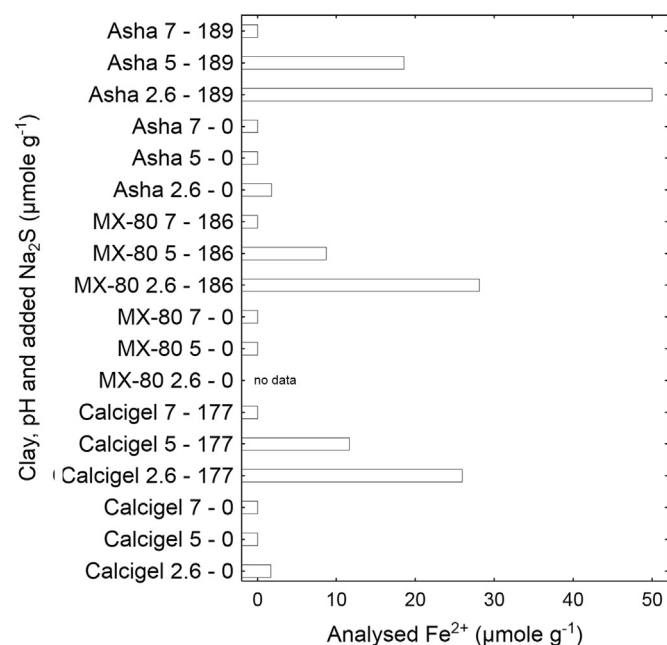
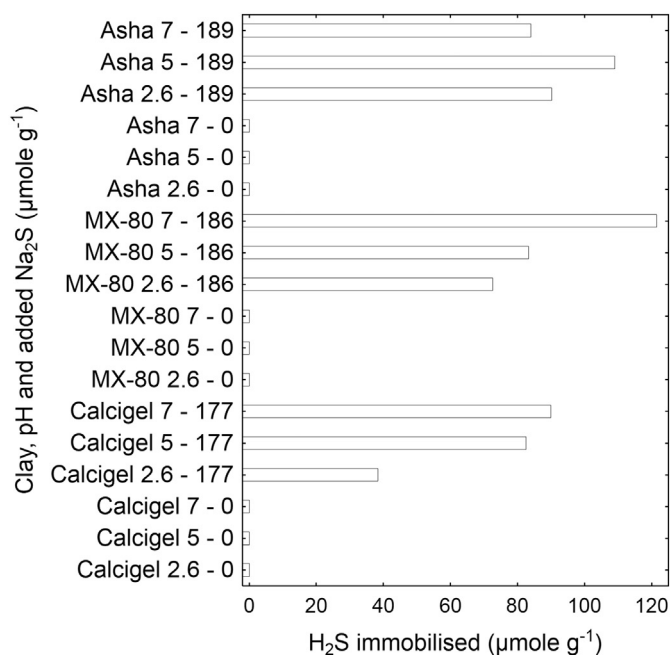


Fig. 3. Immobilised, non-volatile H₂S and released ferrous iron in three different bentonite clay suspensions over a range of three adjusted pH values with and without addition of Na₂S. Numbers after the respective clay name show pH and amount of added Na₂S in µmole (g clay)⁻¹.

3.2. Experiment 2 - released ferrous iron with and without Na₂S addition

There was a clear difference in the amount of released ferrous iron between clay suspensions added with 100 µmole Na₂S (g clay)⁻¹ compared to suspensions without added Na₂S (Fig. 2). Ferrous iron was detected in increasing amounts with decreasing pH below 7 for all three clays added with Na₂S. A small amount of ferrous iron was detected in the non-added suspensions when pH approached 3 or lower. The difference between Asha suspensions that were pH adjusted with buffer compared to HCl adjusted suspensions was small (Fig. 2). The pH adjustments with HCl were very time consuming and difficult to do, because of the low buffer capacity of the clay suspensions. However, the results clearly showed that suspensions added with Na₂S released at

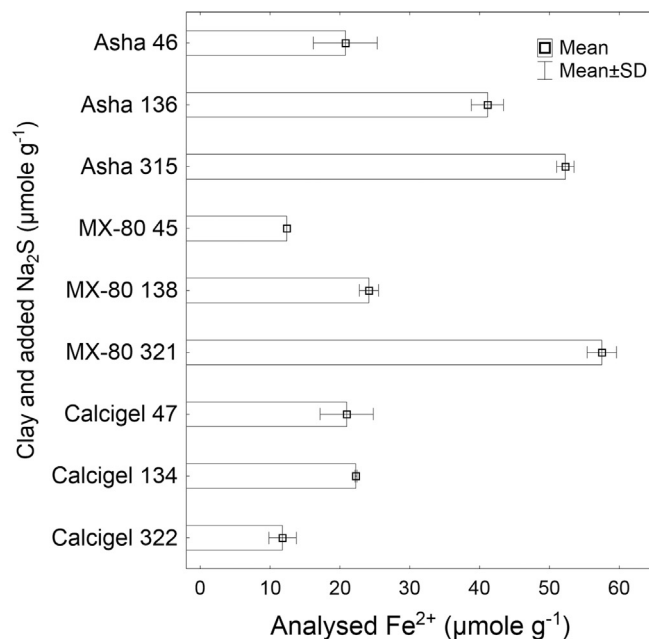
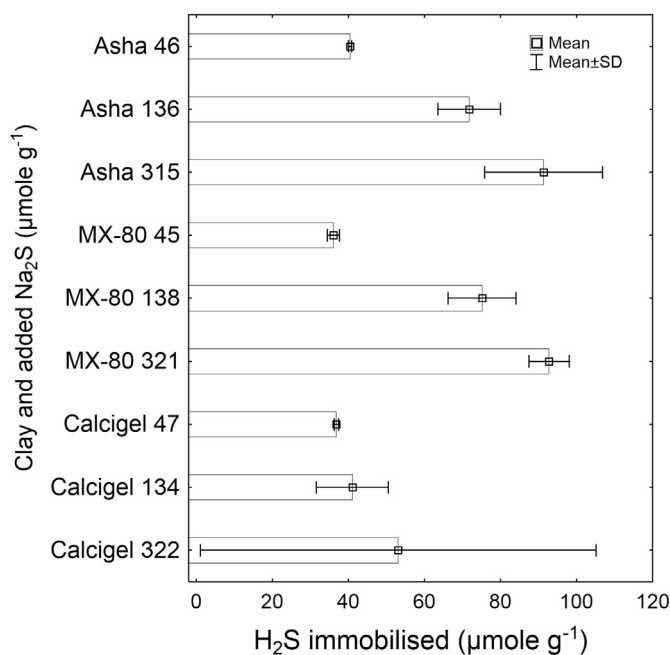


Fig. 4. Immobilised, non-volatile H₂S and released ferrous iron in three different bentonite clays from clay suspensions with and without addition of Na₂S at pH values between 3.7 and 3.2 over a range of amounts of added Na₂S. Numbers after the respective clay name show the amount of added Na₂S in µmole (g clay)⁻¹. Bars indicate standard deviation (SD) of three parallel samples.

least 5 times more ferrous iron than what was found in suspensions without Na₂S.

3.3. Experiment 3 - immobilised sulphide and released ferrous iron

The concomitant analysis of immobilised H₂S and released ferrous iron showed a general inversed relation (Fig. 3). The amount of released ferrous iron increased with decreasing pH while the amount of immobilised sulphide decreased. The added amount of Na₂S was almost twice the amount added in experiment 1 but the amount of immobilised H₂S only increased approximately 25% compared to the values obtained in experiment 1. Suspensions with added Na₂S released much more ferrous iron at all three pH values than did non-added

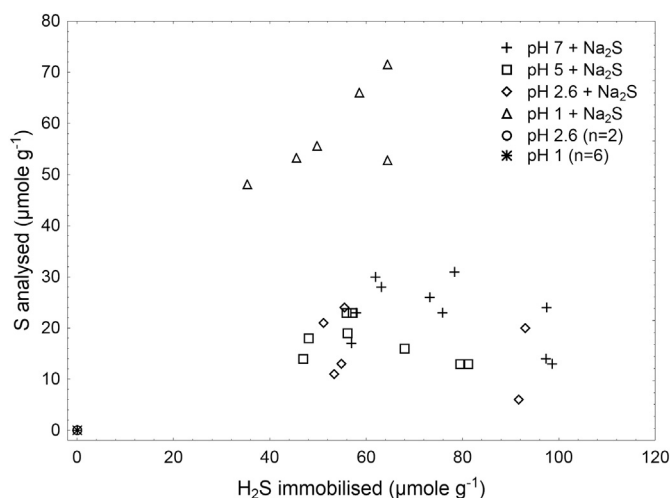


Fig. 5. Amount of elemental sulphur produced at different pH values and the corresponding amounts of immobilised, non-volatile sulphide in clay suspensions with and without added Na_2S . n: number of independent samples.

suspensions.

3.4. Experiment 4 - effect of Na_2S concentration

The increase in amount of added Na_2S was 7 times, from 46 to $320 \mu\text{mole Na}_2\text{S} (\text{g clay})^{-1}$ and it corresponded to an increase in immobilised H_2S from approximately 40 to at most $90 \mu\text{mole H}_2\text{S} (\text{g clay})^{-1}$ (Fig. 4). The increase in released ferrous iron over increasing amount of added Na_2S agreed with the increase in immobilised H_2S , except for Calcigel with addition of $322 \mu\text{mole Na}_2\text{S} (\text{g clay})^{-1}$.

3.5. Produced sulphur

Sulphur was detected in all samples with added Na_2S but not in non-added samples (Fig. 5). The amounts of sulphur corresponded to from 10% to 50% of the immobilised H_2S values except for suspensions at pH 1 where the amount of sulphur corresponded to approximately 90% of the immobilised H_2S values.

3.6. Diffusion of sulphide in compacted Asha bentonite

The ^{35}S concentration on the receiving side for the wet density of 1750 kg m^{-3} began to increase after 3 days but this increase halted after 6 days and was indifferent until day 14 when the increase in concentration recovered and was linear until the end of the experiment after 45 days (Fig. 6A). A similar pattern was observed for the clay with a wet density of 2000 kg m^{-3} . The concentration increased after 4 days, stopped at day 10 and increased linearly after 20 days for the rest of the experimental time (Fig. 6B). Linear regressions of the measurements of activity yield rates of increase of ^{35}S activity in the receiving reservoir gave 0.1292 Bq s^{-1} and 0.0311 Bq s^{-1} for the wet densities 1750 kg m^{-3} and 2000 kg m^{-3} , respectively. Assuming this corresponds to the (quasi)-steady-state flux m' of ^{35}S activity through the clay cores, the effective diffusion coefficients can be calculated from Fick's law (Eq. 2)

$$m' = D_e \cdot A \cdot (C_1 - C_0) / d \quad (1)$$

with D_e the effective diffusion coefficient ($\text{m}^2 \text{ s}^{-1}$),

$A = 0.0175^2 \cdot \pi = 9.62 \times 10^{-4} \text{ m}^2$, the cross-sectional area of the clay core, $C_1 = 9.79 \times 10^{10} \text{ Bq m}^{-3}$, the concentration of H^{35}S^- in the donor reservoir, which can be considered as (quasi)-constant as the flux that leaves this reservoir was very small compared to the inventory in the reservoir,

$C_0 \cong 0 \text{ Bq m}^{-3}$, the concentration in the receiving reservoir, which

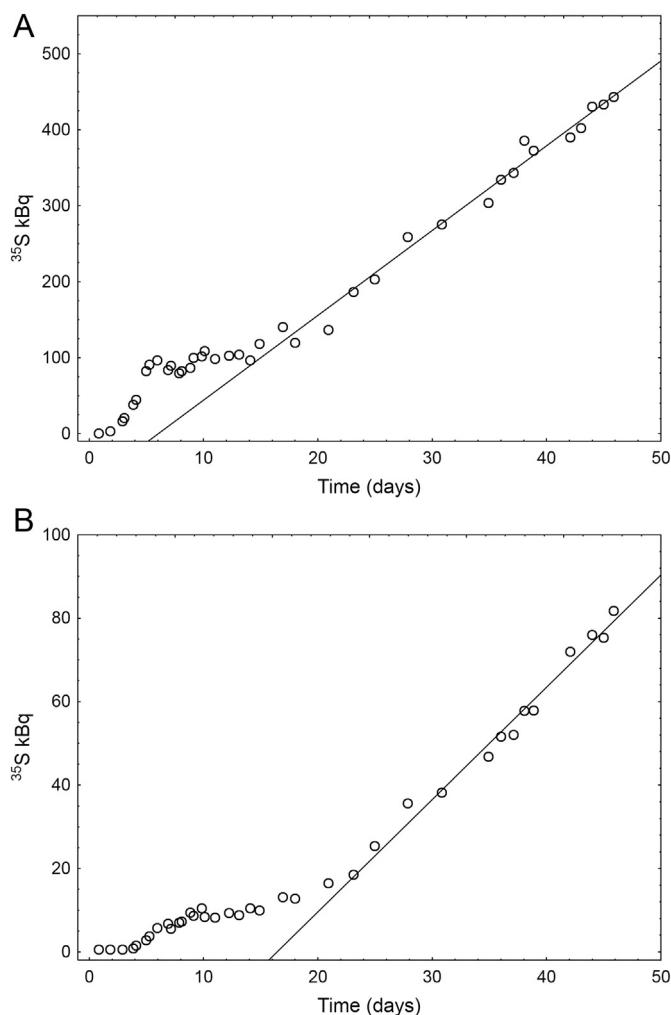


Fig. 6. A. Asha 1750 kg m^{-3} diffusion plot with measured radioactivity over time. The linear fit is based on x-values in the day range 14–45: $^{35}\text{S} = -67.5 + 11.2 (\text{time})$. B. Asha 2000 kg m^{-3} diffusion plot with measured radioactivity over time. The linear fit is based on x-values in the day range from 23 to 45: $^{35}\text{S} = -44.2 + 2.69 (\text{time})$.

can be considered approximately equal to zero as it remained very small compared to C_1 .

and $d = 0.02 \text{ m}$ the thickness of the clay core.

This calculation yielded the effective HS^- diffusion coefficients $2.74 \times 10^{-11} \text{ m}^2 \text{ s}^{-1}$ for the 1750 kg m^{-3} wet density and $6.60 \times 10^{-12} \text{ m}^2 \text{ s}^{-1}$ for the 2000 kg m^{-3} wet density.

4. Discussion

4.1. Mobility of sulphide in compacted bentonite

There are only a few experimentally generated data available in the literature for diffusion of sulphide in compacted, water saturated bentonites. King et al. (2011) estimated D_e for sulphide in 1750 kg m^{-3} wet density bentonite to be in the order of $7 \times 10^{-12} \text{ m}^2 \text{ s}^{-1}$. Eriksen and Jacobsson (1982) determined D_e of H^{35}S^- to be in the order of $9 \times 10^{-12} \text{ m}^2 \text{ s}^{-1}$ in MX-80 at 2100 kg m^{-3} wet density. In this work, we found D_e for H^{35}S^- in Asha to be $2.74 \times 10^{-11} \text{ m}^2 \text{ s}^{-1}$ at 1750 kg m^{-3} wet density and $6.60 \times 10^{-12} \text{ m}^2 \text{ s}^{-1}$ at 2000 kg m^{-3} wet density. Previously, D_e for H^{35}S^- in compacted Wyoming MX-80 bentonite was calculated from experiments studying the activity of sulphate-reducing bacteria in bentonite (Pedersen, 2010). The D_e in Wyoming MX-80 at a wet density of 2000 kg m^{-3} was calculated to be $2 \times 10^{-12} \text{ m}^2 \text{ s}^{-1}$ and $1.2 \times 10^{-11} \text{ m}^2 \text{ s}^{-1}$ at 1750 kg m^{-3} wet

density. The calculated values may vary due to type of bentonite and experimental conditions but they are still consistent. The average value for D_e of sulphide in water saturated bentonite with a density between 2000 and 2100 kg m⁻³ becomes $5.9 (\pm 3.6) \times 10^{-12} \text{ m}^2 \text{ s}^{-1}$ and $1.54 (\pm 1.1) \times 10^{-11} \text{ m}^2 \text{ s}^{-1}$ for the 1750 kg m⁻³ bentonite. The D_e consequently decreased with increasing degree of compaction with $0.19 (\pm 0.11) \times 10^{-11} \text{ m}^2 \text{ s}^{-1}$ per 50 kg m⁻³ water saturated clay.

There was a delay in the break-through of sulphide in the diffusion experiment. After a first small increase in concentration of H^{35}S^- on the receiver side, the flux halted for approximately 10 days before a steady increase in concentration of H^{35}S^- appeared (Fig. 6). A similar effect was observed by Eriksen and Jacobsson (1982) with an 8 mm thick bentonite core where the flux halted soon after an initial break-through of H^{35}S^- for approximately 5 days before a steady increase appeared. The diffusion experiment suggests that sulphide is partly immobilised in bentonite clays and previous experiments with activity of sulphide producing bacteria in compacted clay similarly indicated an immobilisation effect from the clay on the transport of sulphide (Bengtsson and Pedersen, 2016; Bengtsson and Pedersen, 2017). It was deemed important to understand the process behind the observed immobilisation and the suspension experiments were, consequently, designed to investigate this effect in more detail.

4.2. Experimental clay suspension procedures

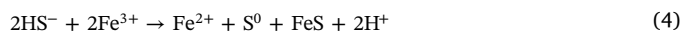
The addition of Na_2S to an unbuffered anaerobic salt solution increases the pH significantly. A high pH will move the 50/50% dissociation of $\text{HS}^-/\text{H}_2\text{S}$ at pH 7 to HS^- at pH above 9 which cannot be purged for analysis of volatile H_2S . The pH adjustment of the experiments was, therefore, necessary. HCl was used in pilot experiments but it was very difficult to obtain stable pH values because the purging of volatile H_2S continuously consumes protons when $\text{HS}^- + \text{H}^+$ form H_2S . The pH concomitantly increases continuously which required continuous addition of HCl which was not possible with the experimental bottle-stopper configuration. The use of the buffer solved this difficulty and pH values did not change more than a few tenths of a pH unit during the purging. HCl was used to obtain pH values lower than 3 in suspensions buffered to pH 2.6. At these pH values, there was very little volatile H_2S left and pH control with HCl, therefore, performed well. The amount of volatile H_2S increased with decreasing pH in most suspensions down to pH below 3 where the amounts approached nil. Suspensions with addition of Na_2S were, between pH 7 and 5, coloured dark or black by FeS. They turned back to the original clay colour when pH was 5 or lower. Soluble FeS dissociates at pH below 7 and the dissociated sulphide and ferrous iron added to the total amounts of volatile H_2S and dissolved ferrous iron. Consequently, it was deemed important to lower pH enough to ensure that the amounts of immobilised volatile H_2S did not include soluble FeS.

There was a small increase in the amounts of dissolved ferrous iron in suspensions not added with Na_2S when pH was lowered to values below 3 but the difference compared to suspensions added with Na_2S was still large (Fig. 2). The majority of the observed amounts of dissolved ferrous iron increased with decreasing pH in relation to the amount of added Na_2S . Likewise, volatile H_2S was below the limit of detection $0.018 \mu\text{mole H}_2\text{S (g clay}^{-1})$ down to pH 1 in suspensions without added Na_2S (Fig. 1B) which demonstrated the absence of sulphide minerals that can be dissociated with HCl to volatile H_2S .

4.3. Reactivity of sulphide with bentonite

Bentonite clays have a significant capacity for adsorption of H_2S gas. This fact is utilised to produce industrial filters for removal of low concentrations of H_2S in gas streams. The absorbance capacity can be increased by the addition of iron to bentonite (Nguyen-Thanh et al., 2005; Stepova et al., 2009). The sulphide scrubbing mechanism is explained by reactions between sulphide and ferric iron. The reduction of

ferric iron by sulphide produced by SPB was recently demonstrated for freshwater sediments (Hansel et al., 2015). The authors showed that sulphide was oxidised to sulphur concomitant with the reduction of a range of different ferric iron minerals to ferrous iron. They suggested that this was an abiotic oxidation-reduction process. A similar process was found to occur in the experiments reported here. Sulphide reduced ferric iron to ferrous iron concomitant with the oxidation of sulphide to elemental sulphur Eq. (2). The ferrous iron could react with free sulphide and form FeS Eq. (3). The generalised sum of these processes is given in Eq. (4).



In this work, the analysis method was designed for the analysis of S_8 which dissolves well in carbon disulphide. In addition to the mass number 256, we also observed lower multiples of the mass number 32 indicating that all produced S was not polymerised to S_8 in the suspensions. It was out of the scope of this work to analyse all sulphur species in the suspensions. The finding of S (polymerised as S_8) in amounts that corresponded from 20% up to 90% of the immobilised H_2S (Fig. 5) attests that Eq. (2) did occur in the suspensions. The blackening of suspensions between pH 7 to 5 indicated the presence of FeS (Eq. 3) as did the increase in volatile H_2S and ferrous iron with decreasing pH (Fig. 2, 3 and 4).

The immobilisation capacities of the clay suspensions were limited between 40 and 90 $\mu\text{mole H}_2\text{S (g clay)}^{-1}$ for MX-80 and Asha, and between 40 and 50 $\mu\text{mole H}_2\text{S (g clay)}^{-1}$ for Calcigel. Asha contains more iron than the other two clays, and MX-80 and Asha contain approximately 80% montmorillonite while Calcigel contains 66% (Table 1). Consequently, the immobilisation capacity correlates with the amount of montmorillonite rather than with the total amount of iron in the clays. The structural ferric iron is charge bound in the dioctahedral clay while ferric iron in minerals are bound in various types of minerals. Structural ferric iron does react easily with sulphur containing reductants such a dithionite that can be used to prepare ferrous iron bentonites (Svensson and Hansen, 2013). This work demonstrates that exposure of bentonite to sulphide can make ferrous iron type bentonites as well. However, while dithionite is absent from radioactive waste repositories, SPB and sulphide are generally found in geological environments intended for waste repositories (King et al., 2011) and, as cited in the introduction, commercial bentonites often harbour dormant SPB that will be part of engineered barrier systems. The presence of sulphide from SPB and the Eq. (4) reaction in repository environments will have some important implications for the engineered barriers in low- intermediate- and high-level repositories for radioactive wastes.

4.4. Implications for engineered barriers

Sulphide may originate from metabolic activity of SPB in the geosphere, buffers, backfill and in organic wastes. All three clays immobilised significant amounts of the added Na_2S up to at most 90 $\mu\text{mole volatile H}_2\text{S (g clay)}^{-1}$ at the highest load of Na_2S . This immobilisation effect can reduce the mass of sulphide that reacts with metal canisters over repository life times which may influence the longevity of metal canisters. There was a clear effect on the transport of sulphide also at a low load of $\leq 0.45 \text{ H}_2\text{S (g clay)}^{-1}$ in the diffusion experiment which suggests that the immobilisation capacity of the clays spans over a large range of sulphide amounts. This immobilisation capacity does not include the immobilisation of sulphide as FeS. The immobilisation capacity may, therefore, be larger than indicated above, in buffers with pH above 7. Sulphide will, consequently, not initially migrate as a non-reactive monovalent anion in engineered clay barriers. The transport of sulphide in bentonite buffers should be modelled as reactive until all

ferric iron available to react with sulphide is reduced to ferrous iron. Further, the oxidation of sulphide to sulphur in bentonite engineered barrier systems will create a concentration gradient of sulphide in groundwater adjacent to the barrier. This gradient will induce a diffusive transport of sulphide towards the clay until reactive ferric iron is depleted and available ferrous iron has formed FeS. Thereafter, the bentonite will act only as a diffusion barrier and the metal canisters will be the only sink for sulphide.

The immobilisation of sulphide by bentonites in engineered barrier systems will reduce the transport of sulphide towards metal canisters, but reduction of structural ferric iron may be problematic due to the destabilizing effect of ferrous iron on dioctahedral smectites (Bradbury et al., 2014; Lantenois et al., 2005; Soltermann, 2014). The sulphide concentrations applied in this work were higher than what is generally found in geological environments intended for radioactive waste repositories and is, therefore, not fully realistic. The incorporation of SPB in experiments with clays as done elsewhere (Bengtsson and Pedersen, 2016; Bengtsson and Pedersen, 2017; Liu et al., 2012; Stone et al., 2016), can provide more realistic experimental conditions for detailed analysis of the influence of sulphide from SPB on the stability of bentonite in engineered barriers.

Acknowledgements

This work received funding from the Euratom Research and Training Program denoted microbiology in nuclear waste disposal (MIND), 2014–2018, under grant agreement No. 661880. The Swedish Nuclear Fuel and Waste Management CO is acknowledged for providing clay for the experiments via Äspö Hard Rock Laboratory.

References

- Bengtsson, A., Pedersen, K., 2016. Microbial sulphate-reducing activity over load pressure and density in water saturated Boom Clay. *Appl. Clay Sci.* 132–133, 542–551.
- Bengtsson, A., Pedersen, K., 2017. Microbial sulphide-producing activity in water saturated Wyoming MX-80, Asha and Calcigel bentonites at wet densities from 1500 to 2000 kg m⁻³. *Appl. Clay Sci.* 137, 203–212.
- Bradbury, M.H., Berner, U., Curti, E., Hummel, W., Kosakowski, G., Thoenen, T., 2014. The long term geochemical evolution of the nearfield of the HLW repository. In: NAGRA Report. National Cooperative for the Disposal of Radioactive Waste (NAGRA).
- Cross, M.M., Manning, D.A.C., Bottrell, S.H., Worden, R.H., 2004. Thermochemical sulphate reduction (TSR): experimental determination of reaction kinetics and implications of the observed reaction rates for petroleum reservoirs. *Org. Geochem.* 35, 393–404.
- Eriksen, T., Jacobsson, A., 1982. Diffusion of hydrogen, hydrogen sulfide and large molecular weight anions in bentonite. *SKBF* 17–82.
- Hallbeck, L., Pedersen, K., 2008. Characterization of microbial processes in deep aquifers of the Fennoscandian Shield. *Appl. Geochem.* 23, 1796–1819.
- Hansel, C.M., Lentini, C.J., Tang, Y., Johnston, D.T., Wankel, S.D., Jardine, P.M., 2015. Dominance of sulfur-fueled iron oxide reduction in low-sulfate freshwater sediments. *ISME J* 9, 2400–2412.
- Herbert, H.-J., Moog, H.C., 2002. Untersuchungen Zur Quellung Von Bentoniten in Hochsalinaren Lösungen, Abschlussbericht. Gesellschaft für Anlagen und Reaktorsicherheit (GRS) mbH, Schwertnergasse 1, 50667 Köln, Germany.
- Holmkvist, L., Ferdelman, T.G., Jørgensen, B.B., 2011. A cryptic sulfur cycle driven by iron in the methane zone of marine sediment (Aarhus Bay, Denmark). *Geochim. Cosmochim. Acta* 75, 3581–3599.
- Jørgensen, B.B., Fenchel, T., 1974. The sulfur cycle of a marine sediment model system. *Mar. Biol.* 24, 189–201.
- Karlund, O., 2010. Chemical and mineralogical characterization of the bentonite buffer for the acceptance control procedure in a KBS-3 repository. In: SKB Report. Swedish Nuclear Fuel and Waste Management Co, Stockholm, Sweden, pp. 1–29.
- King, F., Lilja, C., Pedersen, K., Pitkänen, P., Vähänen, M., 2011. An Update of the State-of-the-art Report on the Corrosion of Copper under Expected Conditions in a Deep Geologic Repository. Posiva Report Posiva Oy, Eurajoki, Finland, pp. 1–252.
- Kwon, M.J., Boyanov, M.I., Antonopoulos, D.A., Brulc, J.M., Johnston, E.R., Skinner, K.A., Kemner, K.M., O'Loughlin, E.J., 2014. Effects of dissimilatory sulfate reduction on Fe(II) (hydr)oxide reduction and microbial community development. *Geochim. Cosmochim. Acta* 129, 177–190.
- Lantenois, B., Lanson, B., Muller, F., Bauer, A., Jullien, M., Plançon, A., 2005. Experimental study of smectite interaction with metal Fe at low temperature: 1. Smectite destabilization. *Clay Clay Miner.* 53, 597–612.
- Liu, D., Dong, H., Bishop, M.E., Zhang, J., Wang, H., Xie, S., Wang, S., Huang, L., Eberl, D.D., 2012. Microbial reduction of structural iron in interstratified illite-smectite minerals by a sulfate-reducing bacterium. *Geobiology* 10, 150–162.
- Masurat, P., Eriksson, S., Pedersen, K., 2010. Evidence of indigenous sulphate-reducing bacteria in commercial Wyoming bentonite MX-80. *Appl. Clay Sci.* 47, 51–57.
- Moser, D.P., Gihring, T.M., Brockman, F.J., Fredrickson, J.K., Balkwill, D.L., Dollhopf, M.E., Lollar, B.S., Pratt, L.M., Boice, E., Southam, G., Wanger, G., Baker, B.J., Pffiffer, S.M., Lin, L.H., Onstott, T.C., 2005. *Desulfotomaculum* and *Methanobacterium* spp. dominate a 4- to 5-kilometer-deep fault. *Appl. Environ. Microbiol.* 71, 8773–8783.
- Motamedi, M., Pedersen, K., 1998. *Desulfovibrio aespoensis* sp. nov., a mesophilic sulfate-reducing bacterium from deep groundwater at Äspö hard rock laboratory, Sweden. *Int. J. Syst. Bacteriol.* 48, 311–315.
- Nguyen-Thanh, D., Block, K., Bandosz, T.J., 2005. Adsorption of hydrogen sulfide on montmorillonites modified with iron. *Chemosphere* 59, 343–353.
- Pedersen, K., 2010. Analysis of copper corrosion in compacted bentonite clay as a function of clay density and growth conditions for sulfate-reducing bacteria. *J. Appl. Microbiol.* 108, 1094–1104.
- Pedersen, K., Bengtsson, A., Edlund, J., Eriksson, L., 2014. Sulphate-controlled diversity of subterranean microbial communities over depth in deep groundwater with opposing gradients of sulphate and methane. *Geomicrobiol J.* 31, 617–631.
- Richard, D., Luther, G.W., 2007. Chemistry of iron sulfides. *Chem. Rev.* 107, 514–562.
- Sandén, T., Olsson, S., Andersson, L., Dueck, A., Jensen, V., Hansen, E., 2014. Investigation of backfill material. In: SKB Report. Swedish Nuclear Fuel and Waste Management Co, Stockholm, Sweden, pp. 1–169.
- Soltermann, D., 2014. Ferrous Iron Uptake Mechanisms at the Montmorillonite-Water Interface under Anoxic and Electrochemically Reduced Conditions. ETH Zurich.
- Stepova, K., Maquarrie, D., Krip, I., 2009. Modified bentonites as adsorbents of hydrogen sulfide gases. *Appl. Clay Sci.* 42, 625–628.
- Stone, W., Kroukamp, O., Moes, A., McKelvie, J., Korber, D.R., Wolfaardt, G.M., 2016. Measuring microbial metabolism in atypical environments: bentonite in used nuclear fuel storage. *J. Microbiol. Methods* 120, 79–90.
- Svensson, P.D., Hansen, S., 2013. Redox chemistry in two iron-bentonite field experiments at Äspö hard rock laboratory, Sweden: an XRD and Fe K-edge XANES study. *Clay Clay Miner.* 61, 566–579.
- Svensson, D., Dueck, A., Nilsson, U., Olsson, S., Sandén, T., Lydmark, S., Jägerwall, S., Pedersen, K., Hansen, S., 2011. Alternative buffer material. Status of the ongoing laboratory investigation of reference materials and test package 1. In: SKB Technical Report. Swedish Nuclear Fuel & Waste Management Co, Stockholm, Sweden, pp. 1–146.
- Widdel, F., Bak, F., 1992. Gram-Negative, Mesophilic Sulphate-Reducing Bacteria. Springer-Verlag, New York.